FRACTOGRAPHY OF POLYETHERIMIDE

by

Doris Zimmerman

Submitted in Partial Fulfillment of the Requirement

for the Degree of

Master of Engineering

in the

Materials Engineering

Program

Richard W. Jones March 10, 1992

Advisor Date

Sally M. Hotchkiss March 16, 1992

Dean of the Graduate School Date

YOUNGSTOWN STATE UNIVERSITY

March, 1992

ABSTRACT

FRACTOGRAPHY OF POLYETHERIMIDE

Doris Zimmerman

Master of Engineering

Youngstown State University, 1992

Different modes of fracture, which consisted of tension, bending, impact, biaxial flexure, torsion, fatigue, and cutting, were selected to determine fracture surface characteristics of polyetherimide under controlled conditions. Fractography, examination of fracture surfaces, was performed using a stereomicroscope and scanning electron microscope (SEM) to characterize and compare modes of failure. The stressed samples exhibited ductility, deformation, and finally brittle fracture shown by a primary fracture surface: mirror, transition region with mists and hackles, and a rough region with Wallner lines. The impacted samples exhibited stress cracking from the point of impact. The cut sample exhibited tear characteristics. Stress corrosion cracking was exhibited by dissolving polyetherimide in a partially halogenated hydrocarbon, trichloroethane.

ACKNOWLEDGEMENTS

The author wishes to thank Dr. Richard W. Jones for being my advisor and Dr. Robert A. McCoy for creating the interest in the subject of failure analysis. The author also wishes to thank Cary Yelin and Gary Casterline of Packard Electric, Warren, Ohio, and Hyung-Kook Yang of Youngstown State University for the stereomicroscope photography, supplying the materials, and the SEM photography of the fatigue samples, respectively. The author wishes to express her grateful thanks for permission to reproduce figures from *An Atlas of Polymer Damage* by Engel, L.; Klingele, H.; Ehrenstein, G. W.; Schaper, H. copyright 1981, Carl Hanser Verlag, Munich, Germany.

TABLE OF CONTENTS

LIST OF FIGURES

CHAPTER I

INTRODUCTION

Statement of Problem

Different modes of fracture were selected to determine fracture surface characteristics of polyetherimide under controlled conditions. The modes of fracture were tension, bending, impact, biaxial flexure, torsion, fatigue, and cutting. Fractography, examination of fracture surfaces, was performed using a stereomicroscope and scanning electron microscope (SEM) to characterize and compare modes of failure. Solubility of polyetherimide in a partially halogenated hydrocarbon, trichloroethane, was also tested.

Composition and Properties of Polyetherimide

Polyetherimide is an amorphous high performance thermoplastic introduced in 1982 by GE Plastics under the trademark of Ultem. Ultem 1000, a low viscosity, unmodified, and unreinforced polyetherimide, was the material studied. This amorphous thermoplastic is characterized by its high strength and rigidity at elevated temperatures, long-term heat resistance, and highly stable dimensional and electrical properties combined with broad chemical resistance (most hydrocarbons, alcohols, and fully halogenated solvents and mineral acids), UV and gamma radiation resistance, and processability. Partially halogenated solvents can be good solvents for polyetherimides. Unmodified polyetherimide, Ultem 1000, is amber transparent in color with opaque colors also being available. It exhibits inherent flame resistance and low smoke generation without the use of additives, and is used in automotive and electronics parts, composites, and wire and cable insulation.

Polyetherimide has a chemical structure based on repeating aromatic imide and ether units as shown in Figure 1.

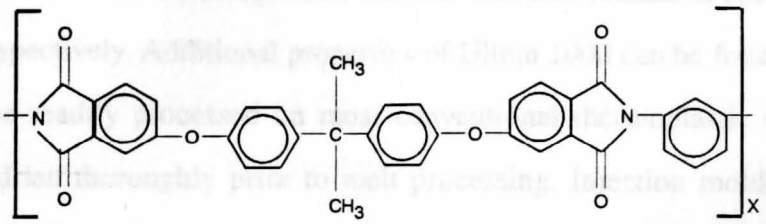

FIGURE 1. Structure of Polyetherimide

This commercial engineering plastics is prepared by nucleophilic aromatic substitution with the leaving group being activated by an electron-withdrawing substituent. This polymer uses the two functionalities of the ether and the imide. The displacement of the nitro group is caused by the electron-withdrawing imide. The rigid imide groups provide the high-performance strength characteristics at elevated temperatures. The ether linkages give the chain flexibility that is necessary for good melt processability and flow. The formation reaction of polyetherimide is shown in Figure 2.[1]

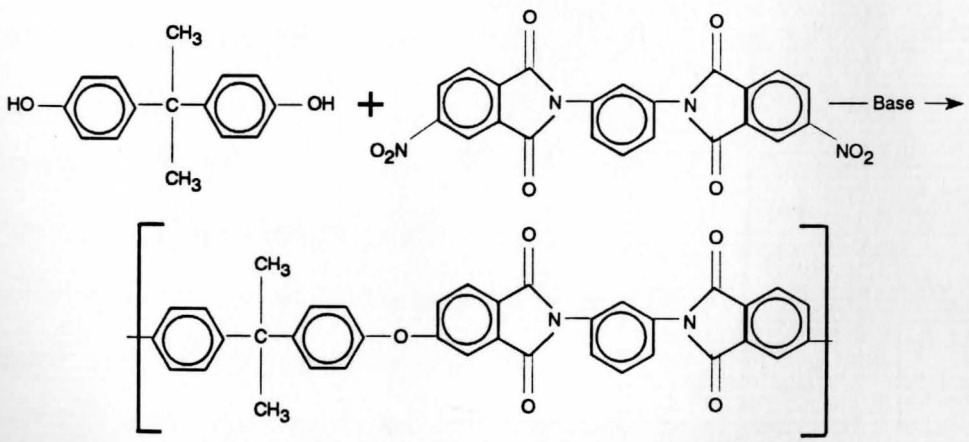

FIGURE 2. Formation Reaction of Polyetherimide

Some physical and mechanical properties are a specific gravity of 1.27, continuous-use temperature rating of 338° F to 356° F, and a glass transition temperature of 419° F. At 356° F, the tensile strength and flexural modulus remain in excess of 6000 and 300,000 psi, respectively. Additional properties of Ultem 1000 can be found in the Appendix 2. It can be readily processed on most conventional thermoplastic equipment. The resin must be dried thoroughly prior to melt processing. Injection molding uses a melt temperature of 600° to 800° F and a mold temperature of 150° to 350° F. Extrusion, thermoforming, and compression molding are also used for producing components.[2,3]

CHAPTER II

GENERALITIES OF FAILURE IN POLYMERS

If external forces are made to act upon polymers, the polymer will first deform elastically or visco-elastically. If the load is removed, the deformation disappears. If the force exceeds a certain threshold, permanent, plastic, irreversible deformation occurs which is called yielding. Polymer chains tend to wander in many directions and become raveled and matted. When a stress is applied these chains have the mobility to rearrange; thus, most polymers continue to deform for a long time after stress application while the chains untangle themselves. The mechanical properties of polymers are dependent on the flexibility of the bonds in the chains and the ease with which the chains can slide over one another during deformation.[4,5]

Polymers can have ductile or brittle fracture. Ductile fracture usually requires more energy than brittle fracture. Before rupture in a ductile fracture, there is considerable plastic deformation that is not recovered. In ductile fracture, the pieces usually are impossible to refit. Macroscopically, ductile fractures show a fibrous surface; while under the SEM, these fractures show uniform fiber pullout. Peaks and fibrils are characteristic features of ductile failure with the minimum fibril diameter at 0.1 μm as shown in Figure 3 (Ref. 4 p. 164).

Tear fractures are characterized by V-or U-shaped ramps parallel to the crack propagation direction. The tips of the ramps point in the direction opposite to that of crack propagation as shown in Figure 4 (Ref. 4 p. 152).

Brittle fracture requires less energy than ductile fracture. In brittle fracture the broken parts can usually be refitted together to the original dimensions; there has been elastic behavior, not permanent deformation. Macroscopically, brittle fractures appear smooth;

while under the SEM, these fractures display shorter isolated fiber structure characteristics.[5,6] Microscopically, brittle failures have sometimes two fracture surfaces after separation, forming oval lids or torn-open blisters, steps and striped patterns. The rims of the microstructures are edged with fine beads and sometimes short fibrils. Brittle fractures have level brittle failure bands and sometimes splintering chips so that the direction of propagation can be determined as shown in Figure 5 (Ref. 4 p. 177). Very flat peaks and dimple structures are also observed as shown in Figure 6 (Ref. 4 p. 181). The main characteristic of embrittlement is smooth fracture surfaces divided into bands by steps, as shown in Figure 7 (Ref. 4 p. 183).

Cyclic stresses result in fatigue fracture and sample heating. This heat increases the mobility or stretching of the molecular chains and may cause many of the molecules to melt or soften. This softening or melting causes the surface characteristics of fracture to be rounded thus resembling continous creep fracture. This change in state would also camouflage striations, crazing, and crack propagations. The softening of the surface's features shown as dimples and small indentations or voids are characteristic of creep fracture as shown in Figure 8, top (Ref. 4, p. 204). When the crack propagation is not camouflaged the surface appears crease-like and rounded with flap-like features, striations, between the propagating cracks as shown in Figure 8, bottom (Ref. 4, p. 214). The roundness of features is again caused by the inherent heating due to fatigue testing of the sample.

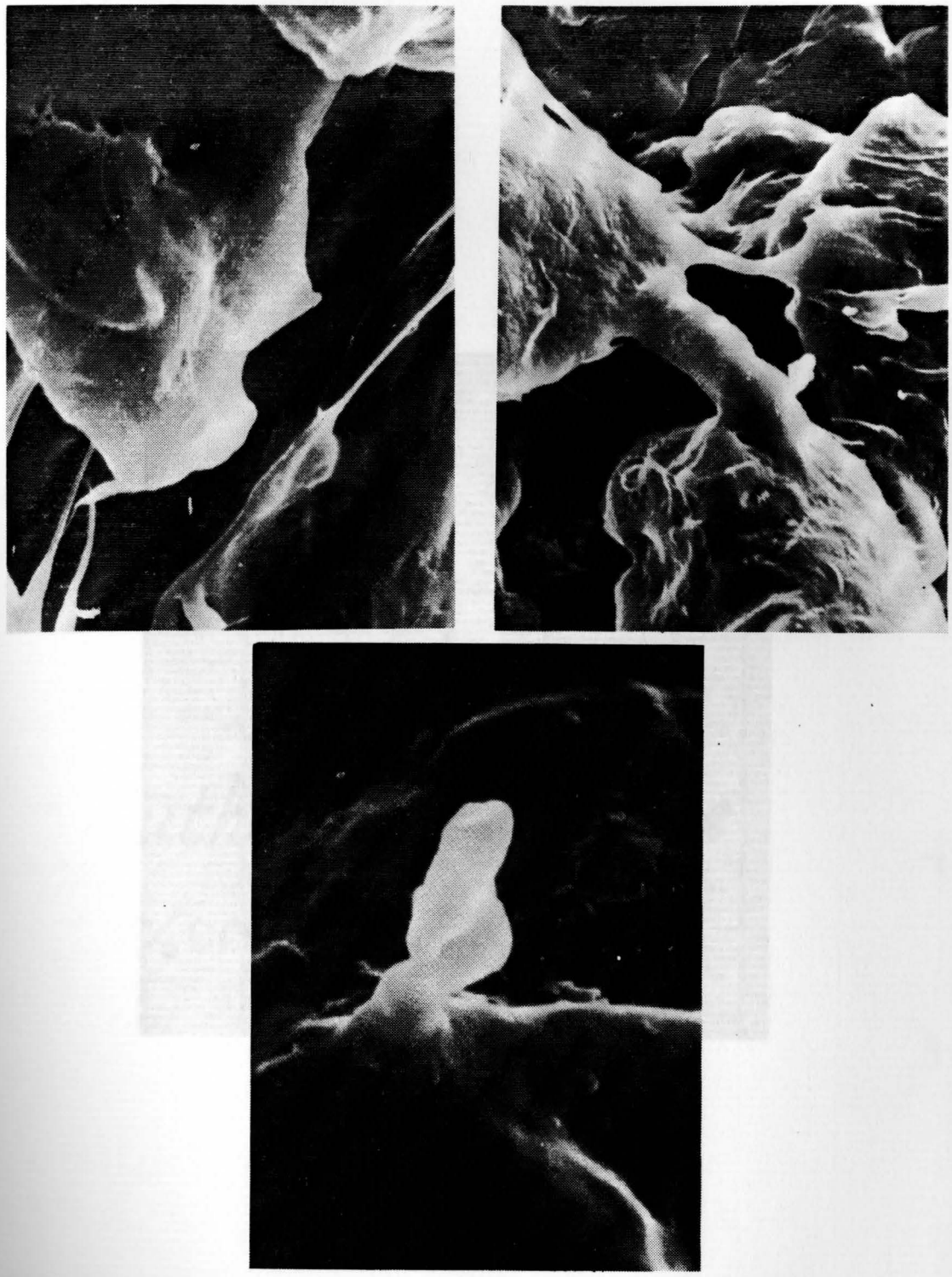

FIGURE 3. Ductile fractures, from Ref. 4. p, 164. Peaks and fibrils are characteristic features (top) with minimum fibril diameter at 0.3 um (bottom).

FIGURE 4. Tear fracture, from Ref. 4, p. 164. V - or U - shaped ramps parallel to the crack propagation direction are characteristic features. The tips of the ramps point in the direction opposite to that of crack propagation.
Reprinted with permission from Engel, L; Klingele, H.; Ehrenstein, G. W.; Schaper, H. *An Atlas of Polmer Damage*; Carl Hanser Verlag: Munich, Vienna, 1981.

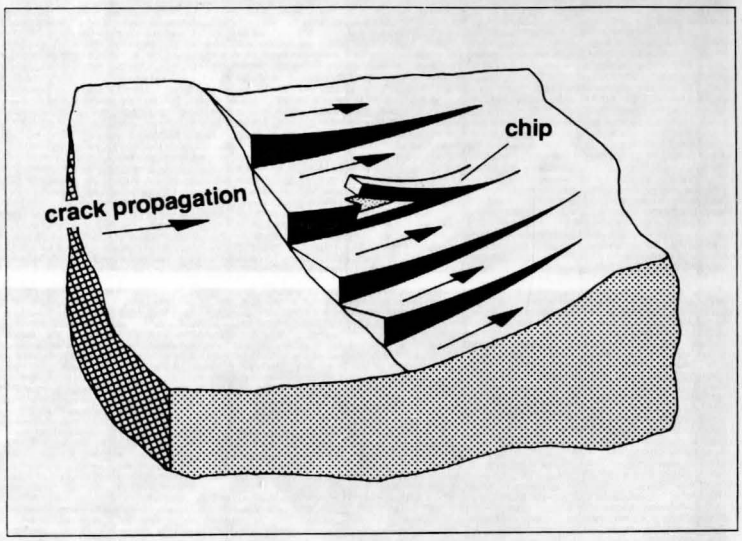

FIGRURE 5. Brittle fracture, from Ref. 4, p. 177. Brittle fractures have level brittle failure bands and sometimes splintering chips so that the direction of propagation can be determined.

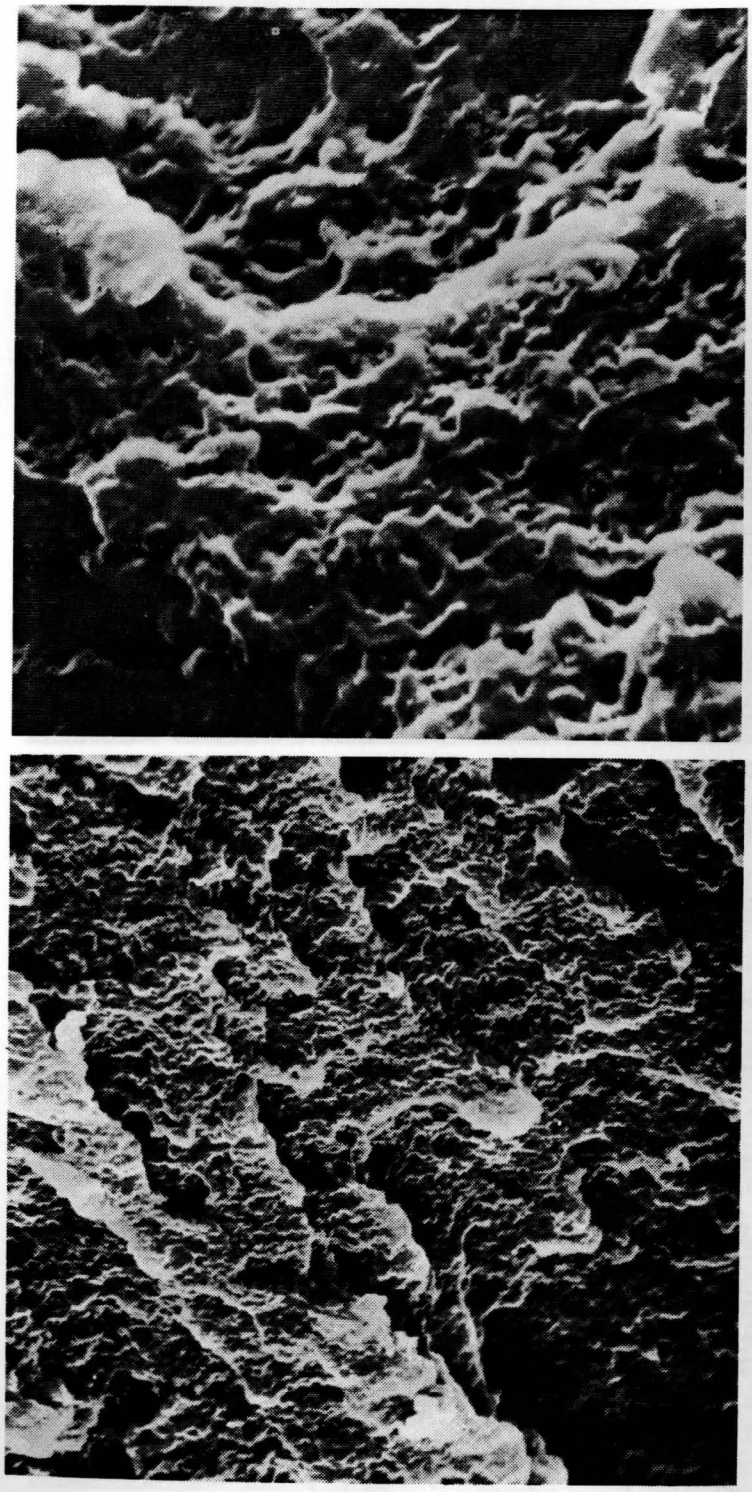

FIGURE 6. Britttle fracture from Ref. 4, p. 181. Bery flat peaks and dimple structures are characteristic features.

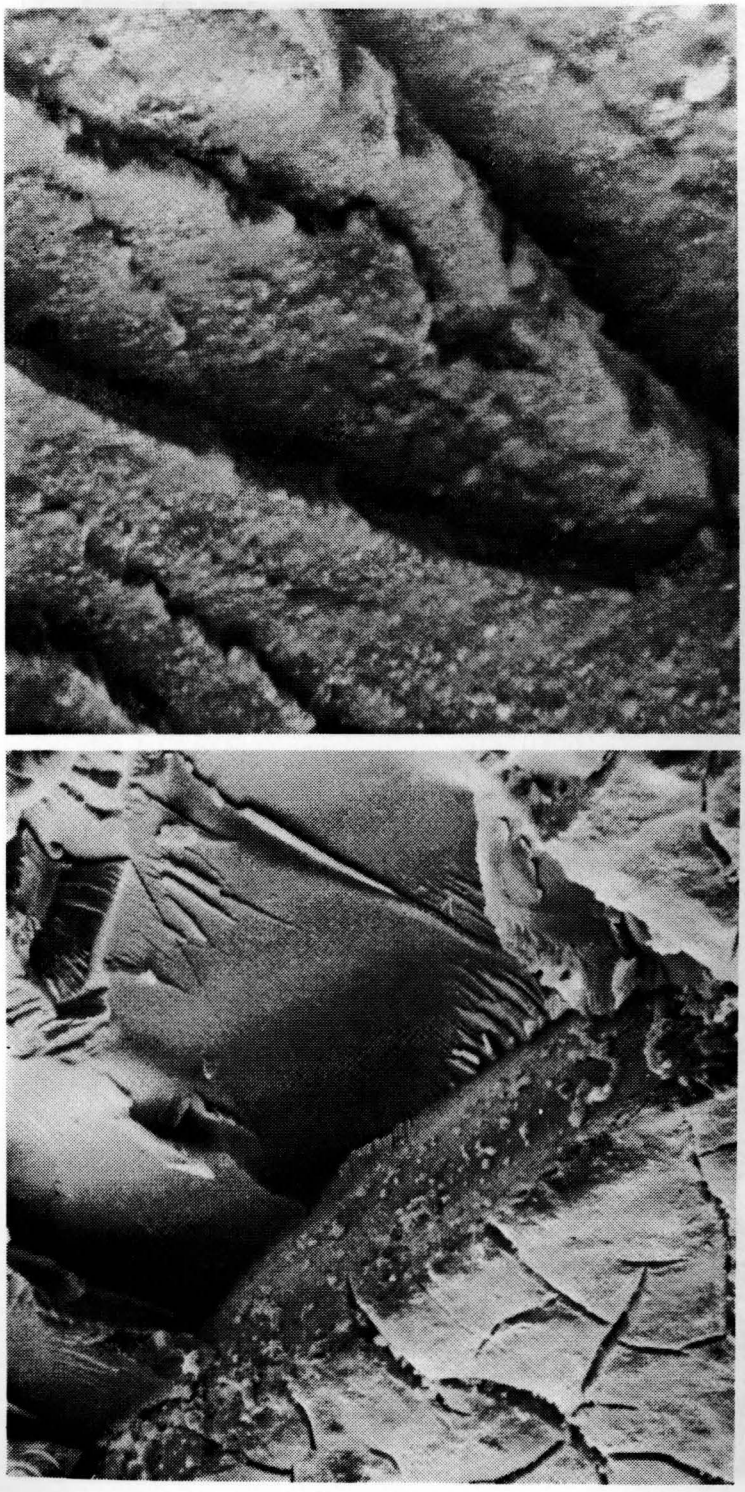

FIGURE 7. Brittle fracture from Ref. 4, P. 183. Smooth fracture surfaces divided into bands by steps are characteristic features.

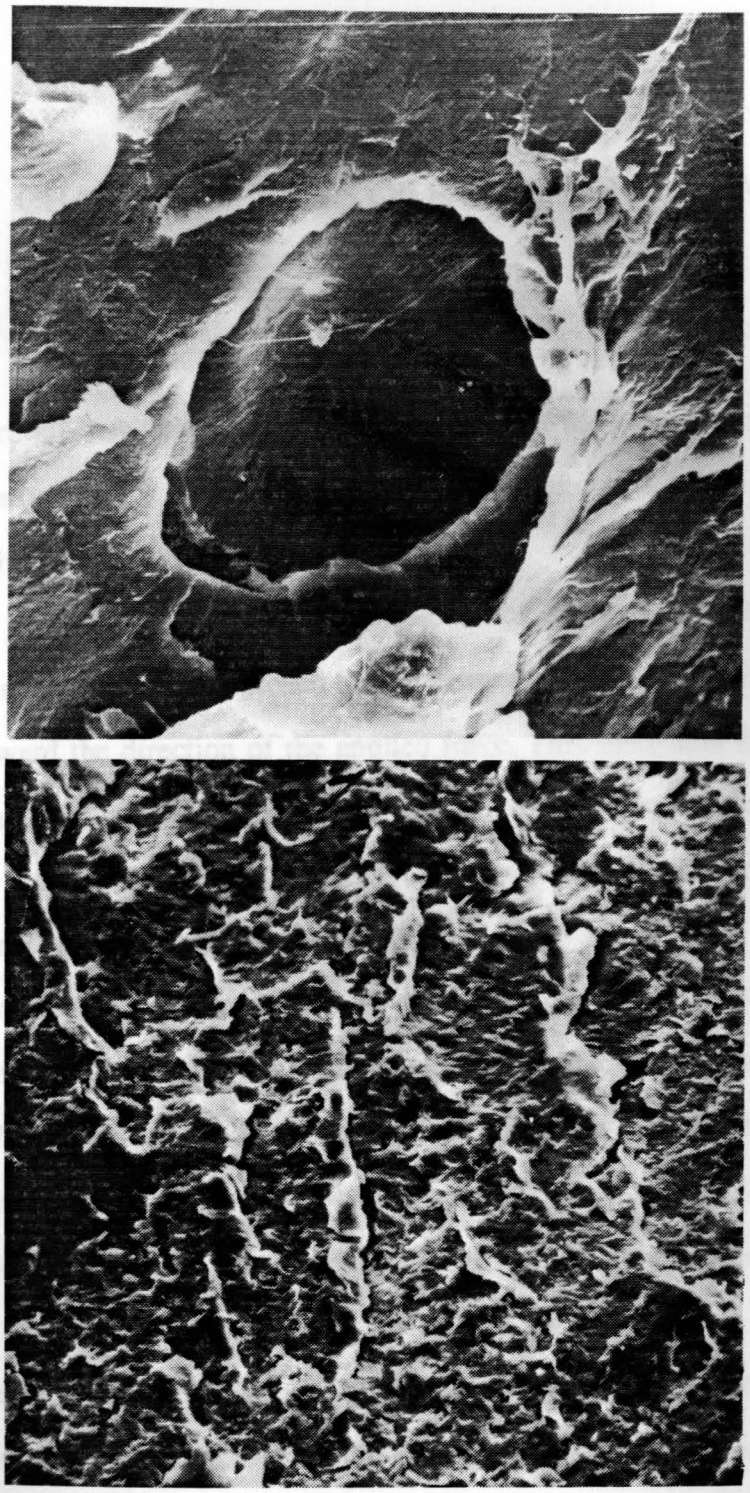

FIGURE 8. Fatigure fracture, from Ref. 4, pp. 204, 214. Top. When striations are camouflaged, the softening of the surface's features are shown as dimples and voids as in continuous creep fracture. Bottom. Without camouflage, characteristics are crease-like, rounded, and flap-like features.

CHAPTER III

CHARACTERISTICS OF FAILURE IN POLYMERS

Tension

There are five principal types of behavior in the simple tensile test as follows: 1. uniform extension, 2. cold drawing, 3. necking rupture, 4. brittle fracture, 5. necking rupture of the second kind.

The uniform extension is a consequence of the high extension of the molecules which occurs as the chains approach their maximum extension and the molecules become oriented toward the direction of the applied force. This molecular orientation makes the specimen harder to extend. In polymers this is referred to as "orientation hardening" as opposed to "strain hardening" or "work hardening" in metals, since the polymers only become harder in the direction of the applied tension.[5,7,8]

"Necking rupture" is defined when the specimen necks and then breaks without restabilization of the neck. It has been noted that specimens which fail by necking rupture occasionally whiten in the neck. This white coloration is usually attributed to the occurrence of very small voids, presumably as a consequence of the triaxial tensile component of the applied tension. This occurrence of voids is understood by considering the stresses on the surface. The material tries to maintain a constant volume under extension, but because neighboring material which has not extended prevents contraction, tensile stresses appear in all directions. These triaxial tensile stresses naturally cause cavitation or microvoiding,[7]

Similarities exist between necking rupture and brittle fracture by four important features: 1) The yield strain has been exceeded in part of the specimen in both cases, 2) The fracture surface in both cases consists partly of oriented polymer materials, 3) The material on both fracture surfaces is partially void, 4) Because of the restraining influence of the neighboring material, the stress system in both modes of fracture have a high triaxial tensile component. The main difference between these two forms of fracture is the depth of material in which the strain exceeds the yield strain. It is much smaller in brittle fracture than in necking rupture. Therefore, brittle fracture can be considered to be an extremely localized form of necking rupture and involve deformation instabilities. Both instability of deformation and fracture toughness are dependent on the rate of orientation hardening beyond the yield point.[7]

As the primary crack advances, secondary cracks may originate. The interactions of these primary and secondary cracks create hyperbolic or parabolic fracture traces, known as Wallner lines. As the crack progresses further, its velocity increases and the surface becomes rougher. The mirror region indicates the primary fracture source.[5,8] In necking rupture of the second kind, the sample becomes very thin at higher temperatures and lower stresses.

The fracture surface is normal to the applied tensile stress. When a tensile specimen fractures in a brittle manner, four characteristic different regions exist as follows: a) primary fracture surface, b) mirror, c) transition region with mists and hackles, and d) rough region with Wallner lines.[5,8]

Bending and Torsion

The characteristics of failure are similar for samples fractured by bending and torsion to those of tension. These samples should exhibit ductility, deformation, and finally brittle fracture shown by a primary fracture surface, mirror, transition region with mists and hackles, and a rough region with Wallner lines.

Impact and Biaxial Flexure

The notched samples used in impact testing should show the natural crack (notch) increasing in length. The energy needed to create this new surface comes from the strain energy of the sample. The notch represents a point of stress concentration. These samples should exhibit crazing and cracking.

Fatigue

Fatigue fracture results from a large number of cyclic stresses. The stress is far below that needed for yielding. The repetitive nature of fatigue causes fracture since a number of the macromolecules are ruptured during each cycle. As with other modes of fracture, the fatigue sample will show diffusion of the molecules, disentanglement, fibrillation, and chain scission, which appear under microscopic observation as crazes, shear bands, and voids respectively.

Fatigue fracture is dependent on time. The first phenomenon observed is crazing or localized yielding which appears as white lines. The second phenomenon is whitening or microvoiding, and the third is necking, followed by fracture. The three principal mechanisms that contribute to fatigue failure are as follows: 1) thermal softening, 2) excessive

creep or flow, and 3) initiation and propagation of cracks. Thermal softening is caused by the dissipation of mechanical energy as heat. The temperature of the sample rises because of high internal friction and the characteristic low thermal conductivity of polymers. Creep or plastic deformation is caused by the disentanglement and rearrangement of the macromolecules. The crack growth is parallel to the load direction and proceeds across crazes. Characteristics of brittle fracture should be observed in fatigue failure as mirror, mists, stress whitening, striations, and crazing.[6,7,9,10,11]

Cutting

A cut sample should exhibit characteristics of a tear fracture. These characteristics are ramps showing direction opposite to the crack propagation with walls that have been pulled and strained.

Stress Corrosion Cracking

Stress Corrosion Cracking from dissolving the sample in a solvent should exhibit a crack on a highly dimpled surface.

CHAPTER IV

EXPERIMENTAL PROCEDURE

The tensile sample had dimensions of 100.59 mm length, 3.17 mm thickness, and 12.66 mm width. The length from the start to the end of the neck was 31.50 mm. The tensile bar of amber Ultem was tested under tension by a standard Instron test. The specimen was extended at a constant speed of 0.1 inch/min for one trial and a constant speed of 10 inch/min for another trial.

The sample used for bending or flexure had dimensions of 126.73 mm length, 3.18 mm thickness, and 12.68 mm width. The specimen was placed in a vise and bent by holding the sample with a crescent wrench close to the clamped section and bending until fracture. This was three point loading.

The Charpy Impact Test stresses a specimen in flexure by means of a swinging pendulum. Samples are notched to have stress concentrations for fracture. The test piece, a rectangular bar similar to the one used for bending fracture, was mounted on a span support and struck in the center on the opposite side of the notch by a swinging pendulum.[7]

For testing biaxial flexure, a black sheet of Ultem 1000 specimen was supported on a hollow steel cylinder with an internal diameter of 2 in (50.8 mm) and impacted by a striker with a hemispherical striking surface 0.5 in (12.7 mm) in diameter. The striker assembly slides freely in vertical guides and is released from a predetermined height to strike centrally on a specimen which is supported on the base of the equipment.[6]

For torsion testing, a test piece, a rectangular bar, similar to the one used for bending fracture, was placed in a vise and twisted by rotation with a crescent wrench.

Fatigue testing involves the application of cyclic stresses. The sample used for the fatigue test was a tensile bar of amber Ultem. The cyclic stresses applied were tensive (tending to pull the molecules apart) and compressive (tending to push the molecules close together).

A sample of the material was cut.

For solubility and possible stress corrosion cracking, a sample was placed in a beaker of trichloroethane for a few hours and then remained in the solution for an additional twenty-four hours.

CHAPTER V

RESULTS

Tension

The sample displayed uniform extension until a load of 189.5 psi was applied. At this loading of 189.5 psi cold drawing was observed. The deformation of the polymer was localized near the narrowest section and a neck formed. The neck length was 85 mm at a constant speed of 0.1 inch/min. When the constant speed was increased to 10 inch/min, the neck was 40 mm. At a loading of 199.7 psi the polyetherimide fractured. An increase in speed demonstrated a decrease in the length of the neck, which is to be expected since the molecules do not have as much time to untangle.

The characteristic behaviors of a polymer in tensile test were observed in the sample: The polyetherimide first uniformly extended, then experienced cold drawing with the formation of a neck, and then fractured. A small whitened area indicating voids of necking rupture was observed. The mirror area covered 3/16 of the fracture surface, while the mists and hackles found in the transition region along with the hyperbolic or parabolic fracture traces known as Wallner lines covered 4/16 of the fracture surface. The rough region covered 9/16 of the fracture surface. The experimental conditions did not permit the observation of necking rupture of the second kind. A stereomicroscope picture of the fracture surface is shown in Figure 9 (page A-1). Using a SEM, the mirror surface, the transition region, and the rough region, were distinguishable as shown in Figures 10, 11, 12 (pages A-2, A-3, A-4).

White spheres were observed throughout the samples under SEM investigations as shown in Figure 10. (p. A-2). These white spheres had their highest concentration near the fracture origination. A possible explanation for these minute particles can be related to entropy. It is possible that the polymer chains under stress break away from one another and form what may be referred to as "strings" or long microfibrils. These microfibrils want to have the lowest possible energy under stress so they form spheres. This process would be the most obvious nearest the fracture origination since the stresses are concentrated at this point and more microfibrils would be formed; thus, the formation of many spheres.[12]

The white threads that appear on the surface are crazes as shown in Figure 10 (p. A-2). Crazes are minute surface cracks with enhanced localized deformation or yielding. These crazes constitute expanded material containing oriented fibrils interspersed with small (100 to 200 A) interconnected voids.[7,12] Crazing is a precursor of crack formation and represents a large sink for strain energy release. The differences in the appearance of the specimen in the rough region can be attributed to this crazing where the fibrils have become oriented or aligned as shown in Figure 12 (p. A-4). Since the craze is weaker, it is an ideal path for crack propagation which is displayed in the fracture on this surface. In the photograph, the raised area and the matching valley where the fracture occurred can be observed in Figure 13 (p. A-5). The darker areas on either side of the lighter craze area represent dimples, voids, and unoriented chains.[12]

Bending or Flexure

The sample showed uniform extension and deformation until fracture. The deformation was permanent since the fractured parts still had curvature after rupture. The fracture surface was very simple, mostly a mirror with a small rough region. A stereomicroscope photograph of the fracture surface is shown in Figure 14 (page A-6).

The characteristics of brittle fracture are also observed for rupture by bending. There is a large mirror region surrounding the origin. Figure 15 (p. A-7) is a SEM photograph of a part of the sample near an edge which shows the mirror, mist, hackles, and rough region. A craze can be noted running from upper right to lower middle. Level brittle failure bands can be observed in the rough region. These parallel fracture paths combine in the direction of crack propagation. Concentric beach marks can also be observed in the rough region. These marks lie at right angles to the fracture bands. (Ref. 8, p. 301 Ref. 4, p. 178, 182-5, 189, 193). White spheres are again present throughout the sample, and they are concentrated at the fracture origin in the mirror region as shown in Figure 16 (p. A-8).

A pronounced void was revealed in the sample at the lower left side of the slightly mirrored fracture surface. Crazing and fracture bands can be observed at the edge of the mirror. A wavy formation of a tear fracture can also be noted in the SEM photograph shown in Figure 17 (p. A-9).

Impact (Charpy)

Brittle fracture again was exhibited. In this mode of fracture, the natural crack (the notch) increases in length; and the energy needed to create the new surfaces comes from the strain energy of the specimen. A stereomicroscope photograph of the fracture surface is shown in Figure 18 (p. A-10). The notch is between the two fracture surfaces. Characteristic fine, knot-like structures and short peaks of brittle fracture can be observed in the SEM photographs. These structures and peaks radiate out from the crack origin at the notched edge as shown in Figure 19 (p. A-11) (Ref. 6 p. 197, Ref. 4 p. 192-193). Under the

SEM, brittle impact failures display a "flaky" fracture surface morphology over the entire surface. Additional SEM photographs of the fracture surface by Charpy impact are shown in Figures 20 and 21 (pp. A-12 and A-13). These photographs show the feathery texture of the concave areas within the fracture paths. (Ref. 4, pp. 188, 192, 193).

Biaxial Flexure or "Dart-Drop

The black sheet of Ultem 1000 was extremely difficult to fracture. The striker showed impact on the surface with some crazing, but no cracking. The presence of white spheres and a similar surface to Charpy Impact specimen were observed as shown in Figure 22 (p. A-14). Upon notching this same sample, crack propagation was noted because of stress concentration at the notch as shown in Figure 23 (p. A-15).

Torsion, Torsion with bending

The specimen twisted through 360° before fracture. The material remained permanently deformed and experienced brittle fracture. When another test specimen was used under the same experimental conditions with both torsion and bending, the sample fracture was at 135°. The fracture from torsion with bending was also brittle, and the material was permanently deformed. With two modes of fracture, failure occurred sooner. Stereomicroscope photograph of the fracture surface of the specimen subjected to only torsion exhibited the surface features similar to the surface features of the specimen fractured by impact, i.e., knot-like structures and short peaks as shown in Figure 24 (p. A-16). Stereomicroscope photograph of the fracture surface of the specimen subjected to both torsion and bending displayed surface features similar to the surface features of the specimen fractured by bending, i.e., mirror and rough region as shown in Figure 25 (p. A-17).

Fatigue

The sample was subjected to cyclic stresses at 6 cycles/second for approximately 6 hours before failure. This amounted to 1.3×10^5 cycles, which is considered to be a low value for fatigue failure.

Fracture did not occur in the center of the sample, as predicted. The failure occurred near the ends with a rounded, not straight, surface which is characteristic of fatigue failure.

Disentanglement and chain scission appear under microscopic observation as crazes, shear bands, and voids. The fatigue fracture surface displayed the crack propagation by white lines, crazes, parallel to the direction of the growth of the crack, with smaller parallel lines perpendicular to the crack propagation. These smaller parallel lines are referred to as fatigue striations. Within these striations, secondary cracks can also be observed. Each striation represented the incremental advance of the crack front as a result of one loading cycle.[12] Crazes and fatigue striations are shown in Figure 26 (p. A-18).

Thermal softening which gives rise to very rounded surfaces is usually observed in fatigue failure. This polymer is heat resistant; therefore, the features were not very rounded. The fatigue striations appeared crease-like and rounded with flap-like features as shown in Figure 27 (p. A-19). Dimples and small indentations or voids were also noted under microscopic investigation as polymer chains were pulled apart.

The final stage of failure occurred at the edge of the sample. Since this fracture occurred quickly a rough region occurs and crazes are located closer together. The rough region shows the formation of white spheres. These spheres result from microfibrils being separated and obtaining a form of lower energy or entropy. The rough region is shown in Figure 28 (p. A-20).

Cutting

SEM investigation of the cut surface showed characteristics of a tear fracture: the U - or V - shaped ramps, whose tips point in the direction opposite to crack propagation and walls which have been pulled up forming beads with wavy crests (Ref. 4, p. 138). The presence of white spheres over the sample surface can be observed as shown in Figure 29 (p. A-21).

Solubility

Ultem 1000 polyetherimide also shows stress corrosion cracking with trichloroethane. The definite formation of a crack on a highly dimpled surface was observed as shown in Figure 30 (p. A-22) (Ref. 4, p. 229). If the sample was allowed to remain in solution for a long period of time, dissolving of the sample occurred as shown in Figure 31 (p. A-23).

CHAPTER VI

SUMMARY

As an engineering plastics, polyetherimide exhibited characteristic fracture surfaces under all the modes of fracture tested: tension, bending, impact, biaxial flexure, torsion, fatigue, and cutting.

Ultem 1000 is an amorphous thermoplastic and as such processes no crystalline areas and much entanglement and flexibility of its molecules. These polymeric characteristics lead to a conclusion of a great deal of inherent deformation and lack of crack propagation due to imperfections or changes in structure. The smooth fracture surface divided into bands by steps with short fiber structures could be refitted, thus indicating brittle fracture.

In non-impact modes of fracture, the same characteristic behavior of brittle fracture was observed. Ultem deformed elastically or visco-elastically at the beginning of stress application due to disentanglement and diffusion. This appeared as necking or a decrease in dimension perpendicular to the applied stress. Whitening was noted at the point of fracture because of the occurrence of very small voids created by triaxial tensile stresses. Four characteristic regions were observed under SEM investigation: primary fracture surface, mirror transition with mists and/or hackles, and rough with Wallner lines (the interaction of primary and secondary cracks). Crazes, minute surface cracks, and white spheres, the lowest entropy form of individual molecular chains, were also observed. Cracks formed along crazes because of the inherent weakness of these minute cracks or oriented or aligned molecular chains.

The impacted samples had the same characteristics of brittle fracture. Since failure was sudden, the surface characteristics were smaller than in the non-impacted samples. The surface is called "flaky and feathery" with short peaks. The concentration of stresses at the notch led to extension of the notch with crazing and cracking. Again white spheres were noted.

The fatigue samples exhibited crazes, fatigue striations, and a rough region with white spheres. The fatigue striations showed microscopic features that were crease-like, rounded, and flap-like. Dimples and voids were also noted due to separation of the polymer chains. Heating of the sample during fatigue testing was not noted.

Under SEM investigation U - or V - shaped ramps were observed in the cut sample. Stress corrosion cracking was observed upon solution in trichloroethane, a partially halogenated hydrocarbon.

Polyetherimide was an excellent amorphous polymeric material for fractography. It was difficult to fracture, but gave characteristic macromolecular surfaces for identification of brittle fracture.

REFERENCES

1 Stevens, M. P. *Polymer Chemistry.* Oxford University Press: New York, 1990; pp 353, 368-369.

2 *Modern Plastics Mid-October Encyclopedia Issue*. p 49,50,66,67 (1989).

3 *Ultem Design Guide*. GE Plastics.

4 Engel, L; Klingele, H.; Ehrenstein, G. W.; Schaper, H. *An Atlas of Polymer Damage*. Carl Hanser Verlag: Munich, Germany, 1981; pp 7-49, 136-243.

5 Felbeck, D. K.; Atkins, A. G. *Strength and Fracture of Engineering Solids.* Prentice-Hall: Englewood Cliffs, N.J., 1984; pp 40-43, 68, 276-280, 324-329, 355.

6 *Failure of Plastics*; Brostow, W; Corneliussen, R. D., Ed; Hanser Publishers: New York, 1986; pp 197-207, 312-329, 430-441.

7 *Mechanical Properties of Polymers*; Bikales, N. M., Ed; Wiley-Interscience: New York, 1971; pp 105-169, 175-195. (Vol 7. pp 292-361 of *Ency. of Poly. Sci. & Tech.*)

8 Andrews, E. H. *Fracture in Polymers*. American Elsevier: New York, 1968; pp 16-20, 54-58, 184-193.

9 Kausch, H. H. *Polymer Fracture*. Springer-Verlag: New York, 1978; pp 204-230, 293-312.

10 Hertzberg, R. W.; Manson, J. A. *Fatigue of Engineering Plastics*. Academic Press: New York, 1980; pp 34-36, 74-82, 146-181.

11 Williams, J. G. *Fracture Mechanics of Polymers*. Halsted Press: New York, 1984; pp 123-124, 170-174, 175-184, 210-226.

12 Hertzberg, R. W. *Deformation and Fracture Mechanics of Engineering Materials*. John Wiley and Sons: New York, 1976; pp 211-223, 474-480, 528-537.

Appendix 1

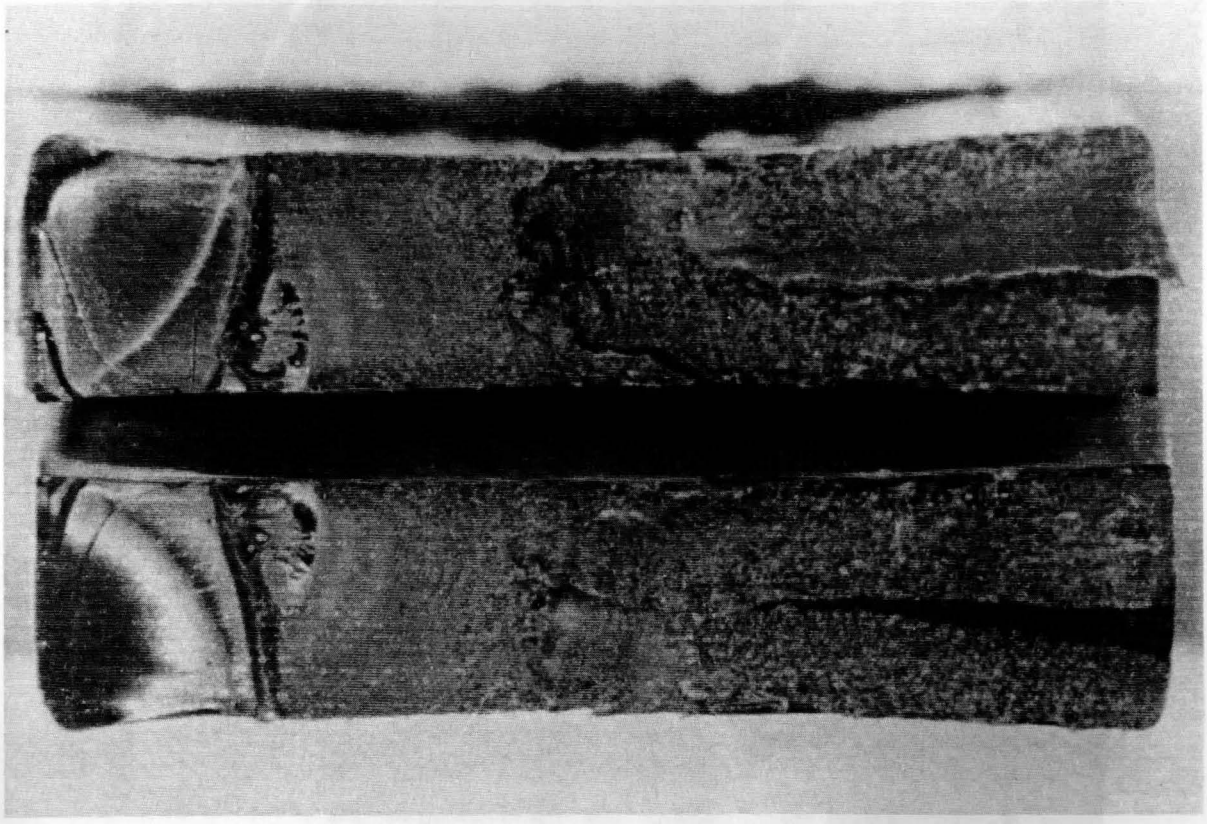

FIGURE 9. Stereomicroscope photograph of specimen in tensile test. There are four regions prominently noted as follows:

1) mirror (far left)
2) transition region (middle) showing mist, hackles, and Wallner lines
3) rough region (far right)
4) crazing fracture, raised area and valley. (right)

The corresponding SEM photographs are on pages A-2 to A-5.

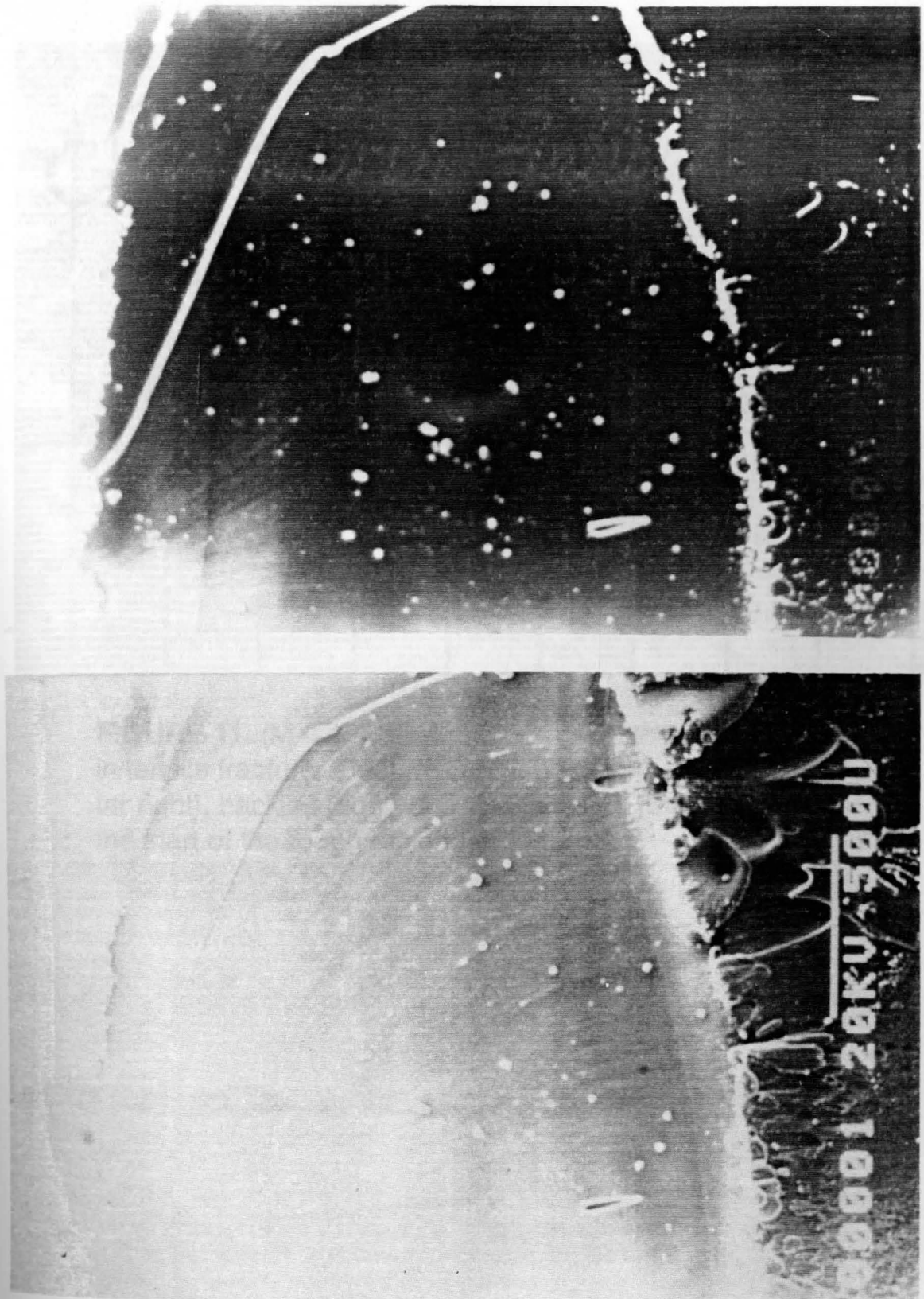

FIGURE 10. (M = 48) SEM photographs of mirror region of tensile fracture. Features to be observed are the white spheres throughout the sample with concentration at the crack initiation point (far right, top); the white thread running from right to bottom which is crazing; and mist and hackles (far left, bottom).

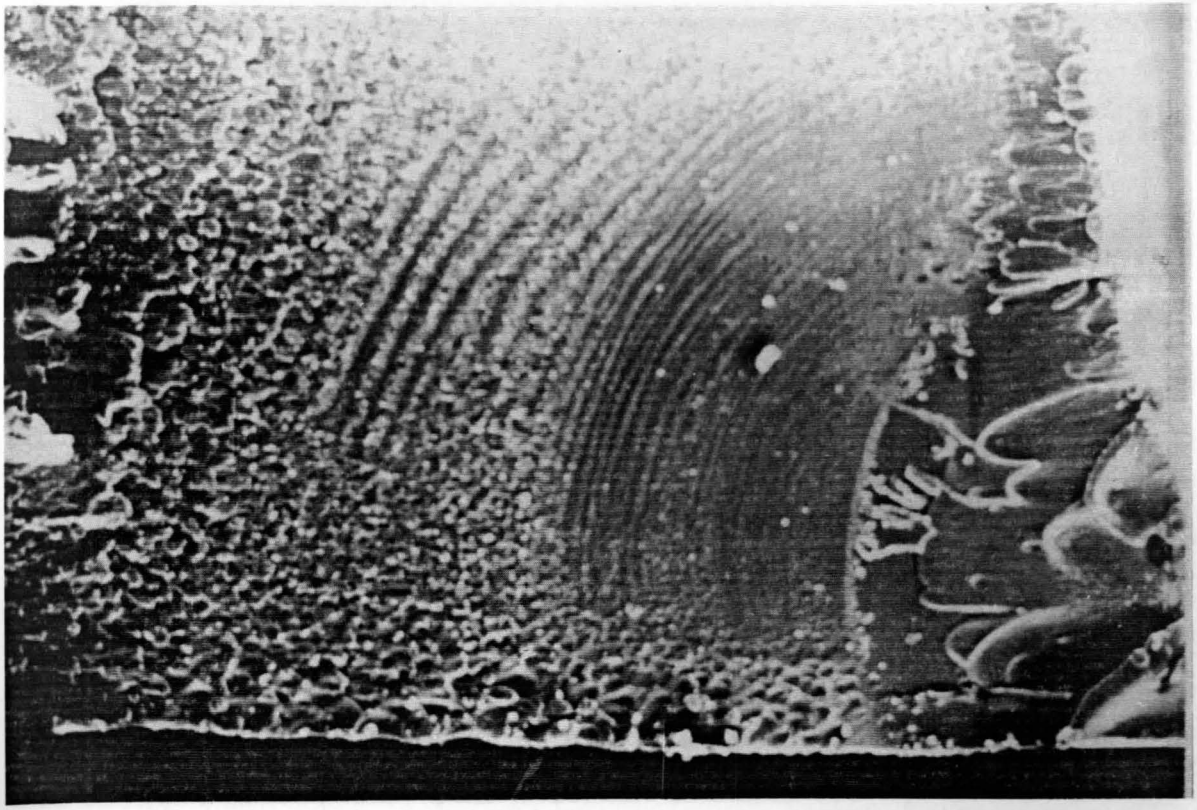

FIGURE 11. (M = 48) SEM photograph of the transition region in tensile fracture. Features to be observed are the mist far right), hackles (right) and Wallner lines (middle), and the start of the rough region (far left).

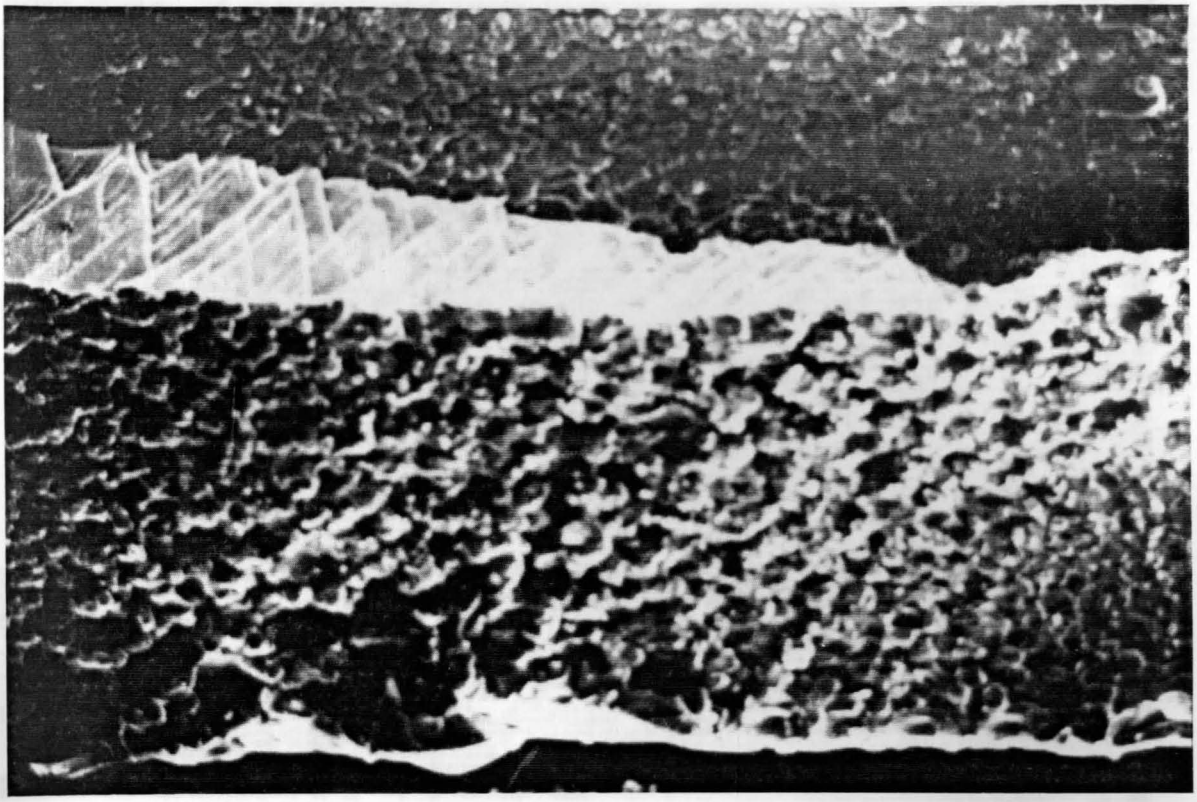

FIGURE 12. (M = 48) SEM photograph of the rough region in tensile fracture. Features to be observed are the differences in appearance of the surface. The oriented chains (light) and the unoriented chains or dimples and voids (dark areas on either side of the light area).

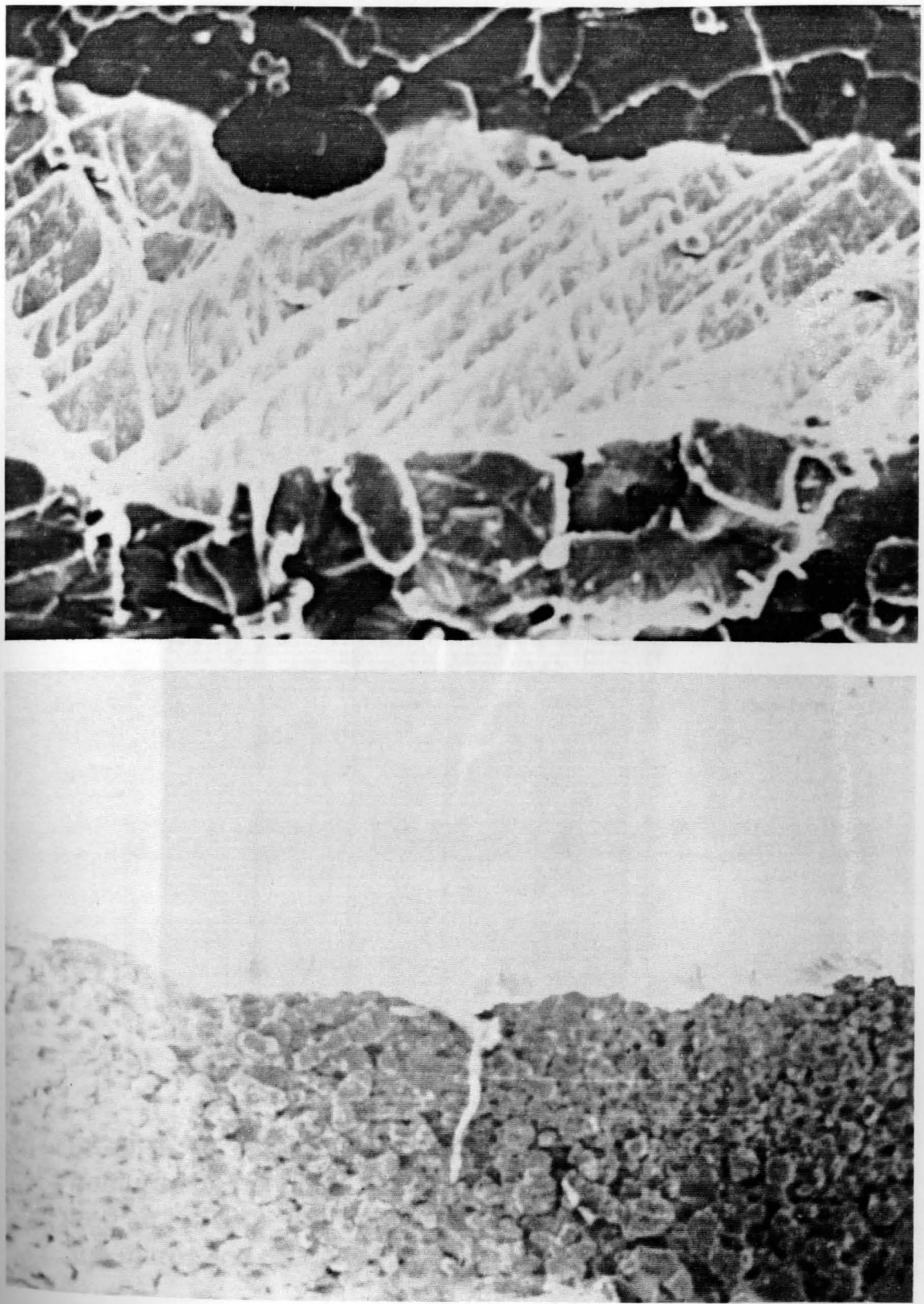

FIGURE 13. (M = 250 top and M = 48 bottom) SEM photographs of the rough region in tensile fracture showing raised area and matching valley of oriented fibrils.

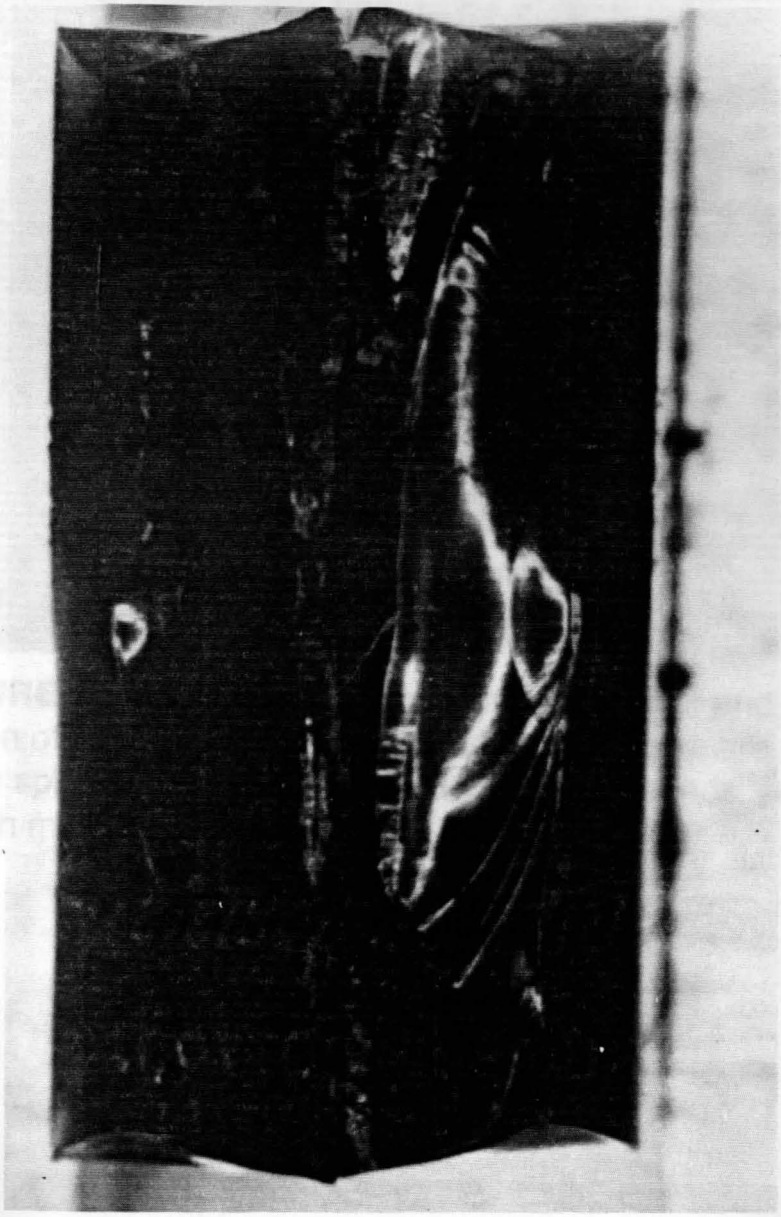

FIGURE 14. Stereomicroscope photograph of specimen fractured by bending. The point of fracture is on far right and far left as a very light area. Features to be noted are the mirror and rough region.

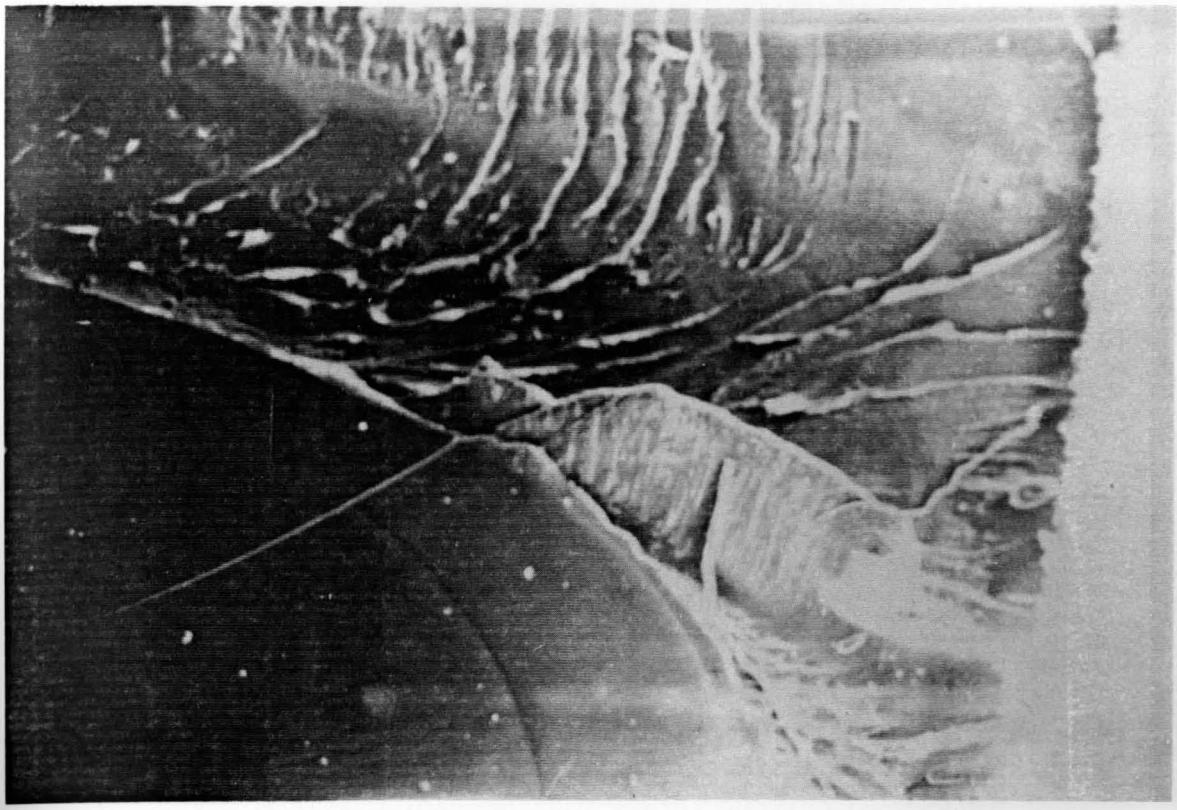

FIGURE 15. (M = 50) SEM photograph of mirror and rough region of bending fracture. Features to be noted are craze, white spheres, mirror, mist, hackles, fracture bands, and beach marks.

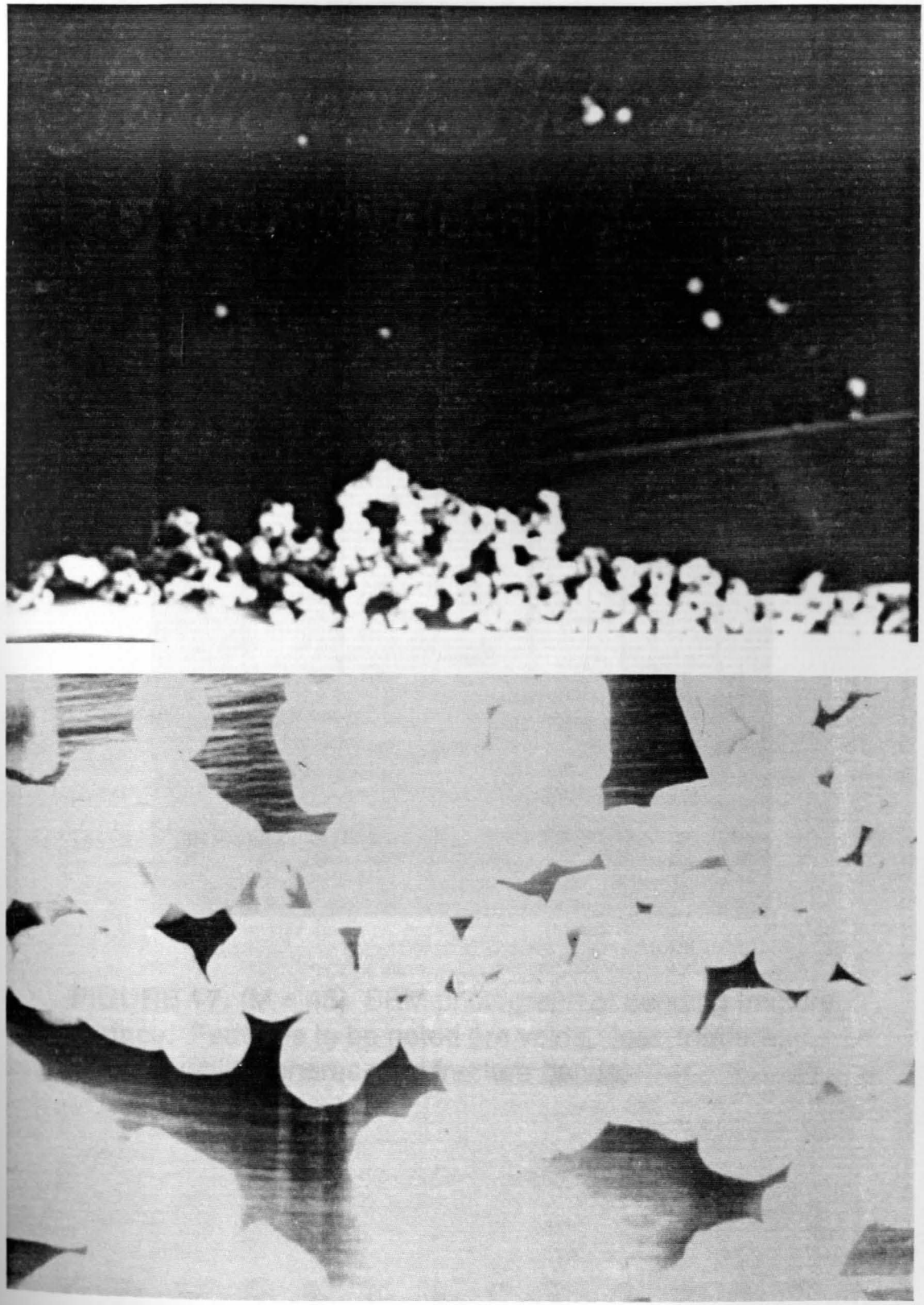

FIGURE 16. (M = 140 top and M = 1000 bottom) SEM photographs of white spheres concentrated at fracture origin in the mirror region of bending fracture.

FIGURE 17. (M = 45) SEM photograph of bending fracture surface. Features to be noted are voids, tear fracture, crazing, white spheres, and fracture bands.

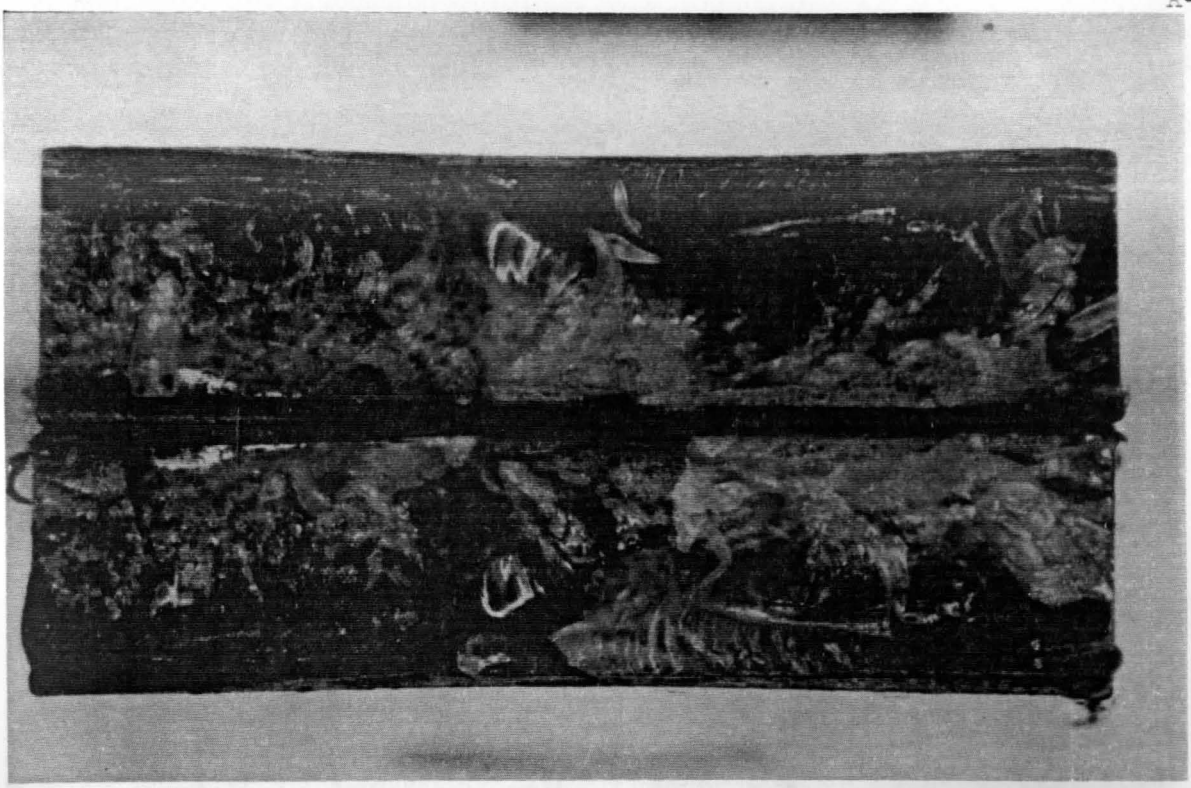

FIGURE 18. Stereomicroscope photograph of specimen fractured by Charpy impact test. The notched edges are in the center of photograph horizontally. Features to be noted are the flakes which cover most of the fracture surface.

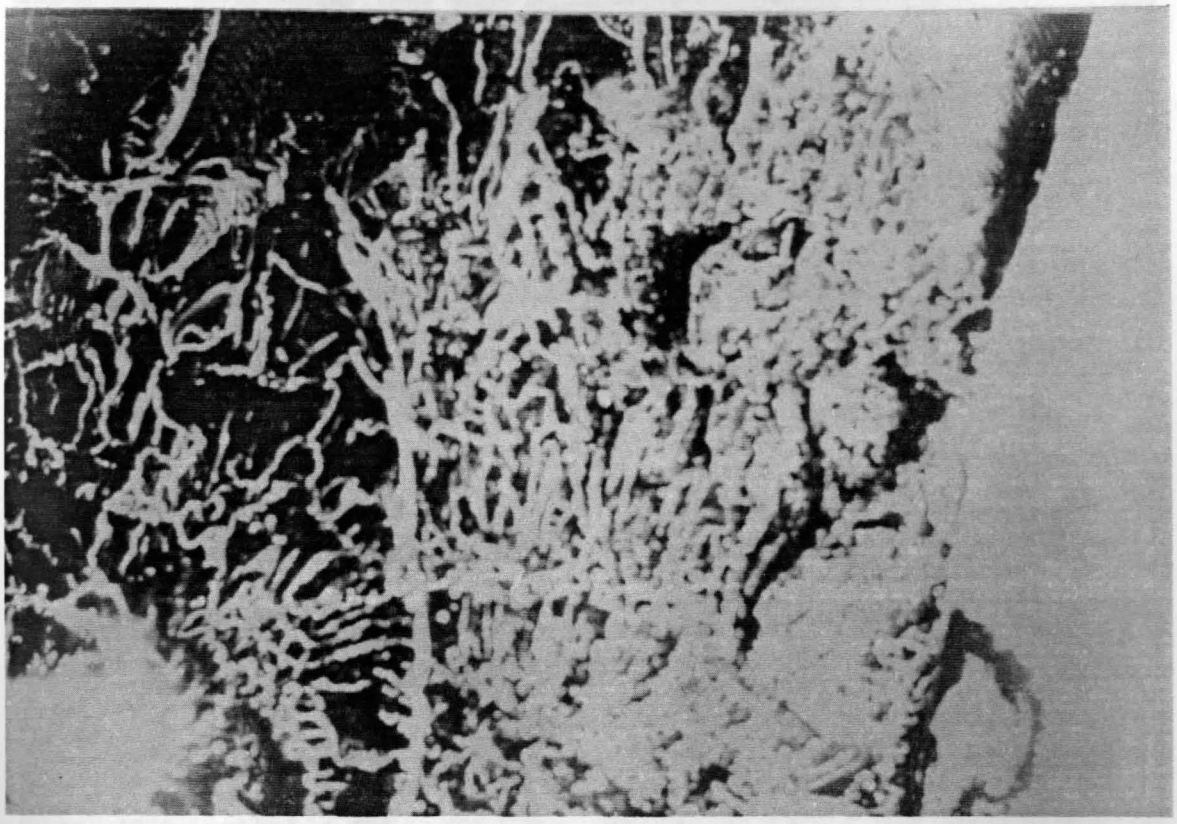

FIGURE 19. (M = 49) SEM photograph of notched edge of Charpy impact fracture surface. Notched surface is at bottom of the photograph. Features to be noted are characteristic of brittle fracture: fine, knot-like structures and short peaks showing the propagation of the crack from the notched surface.

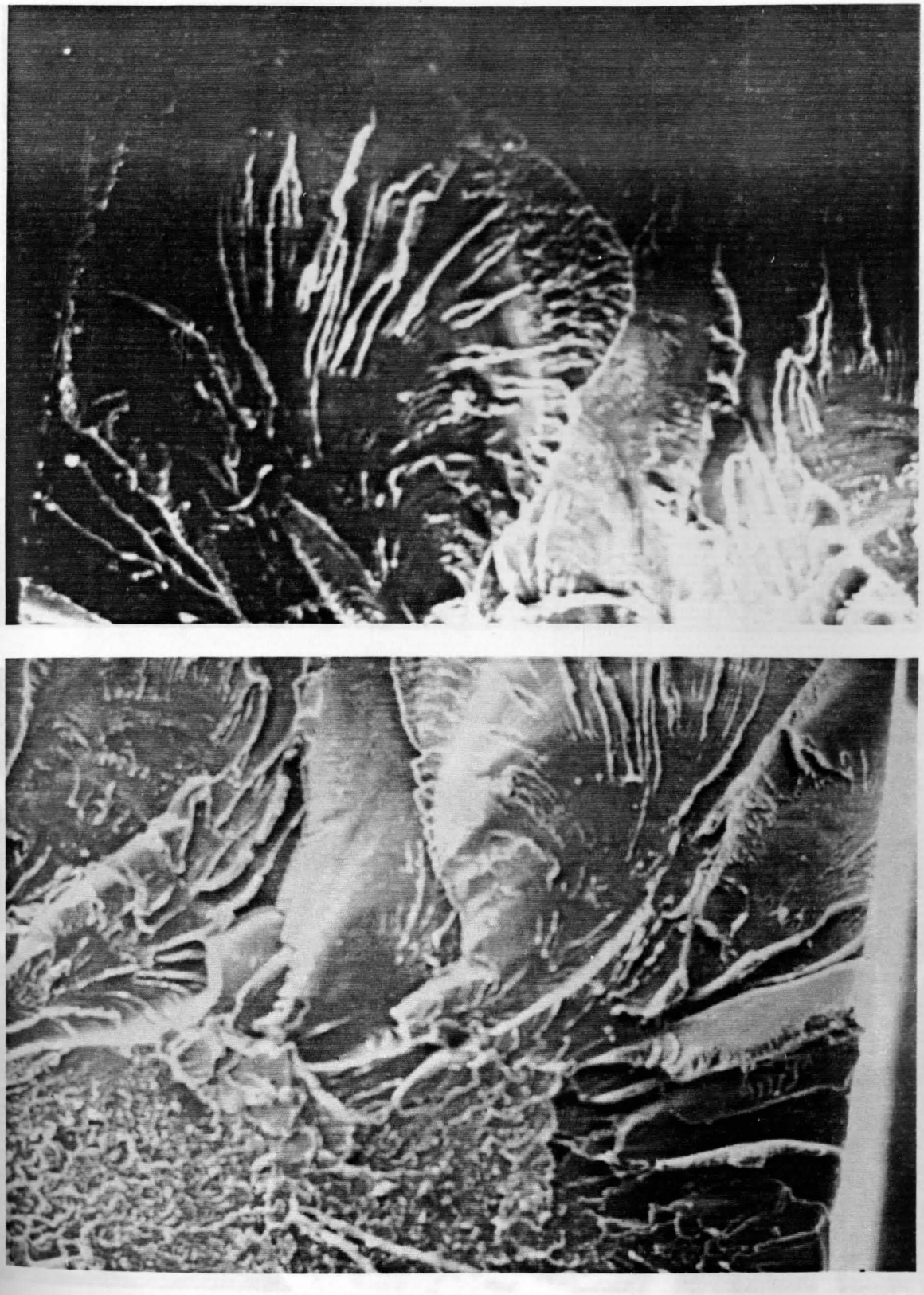

FIGURE 20. (M = 142) Top - SEM photograph of edge opposite notched edge in Charpy impact fracture. Bottom - SEM photograph of notched edge (at bottom of photograph). Features to be noted are concave areas within the fracture paths characterized as feathery or flaky.

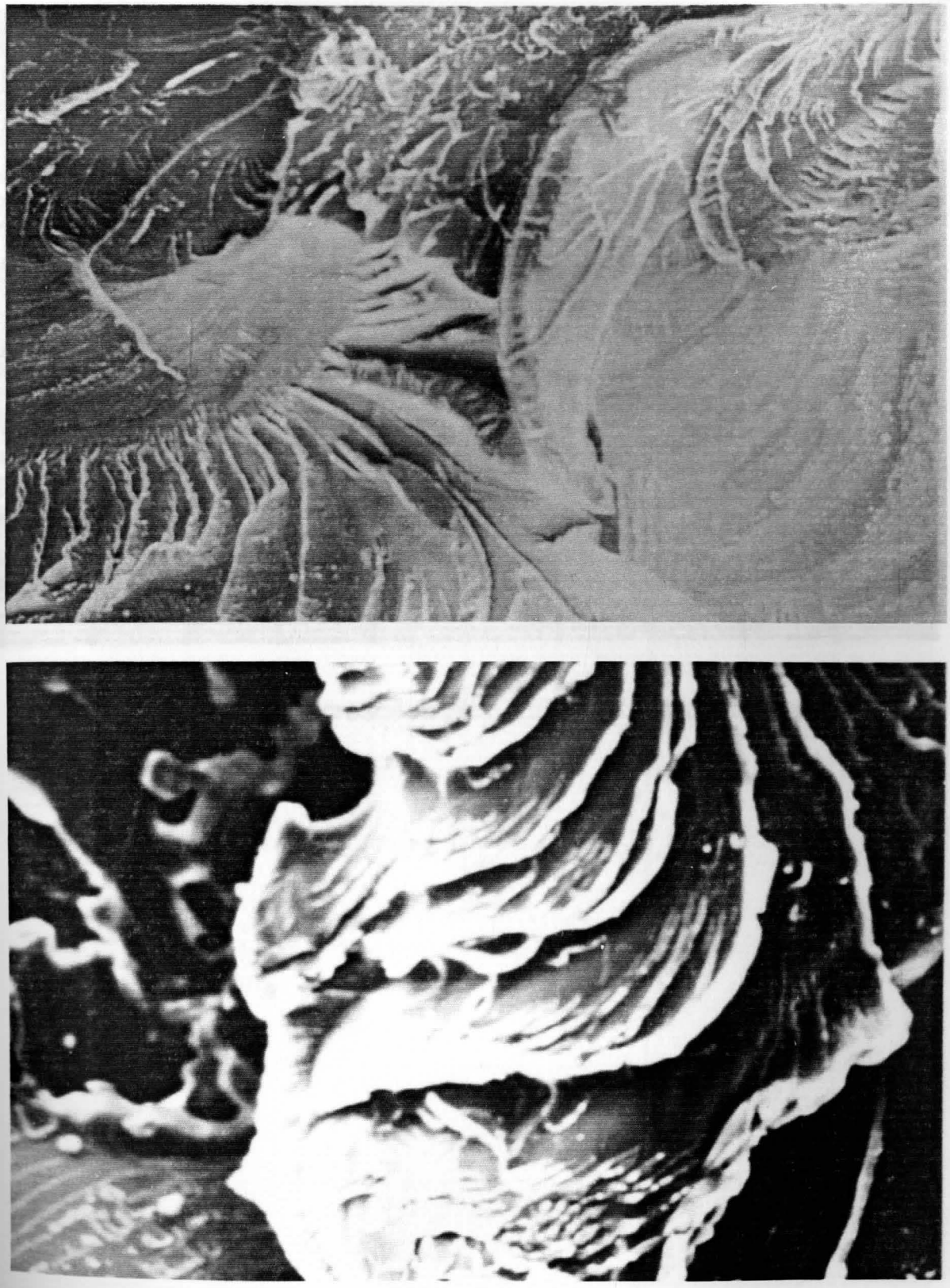

FIGURE 21. (M = 142 top, M = 380 bottom) SEM photographs of fracture surface of Charpy impact test showing swirling concave areas and enlargement of these features.

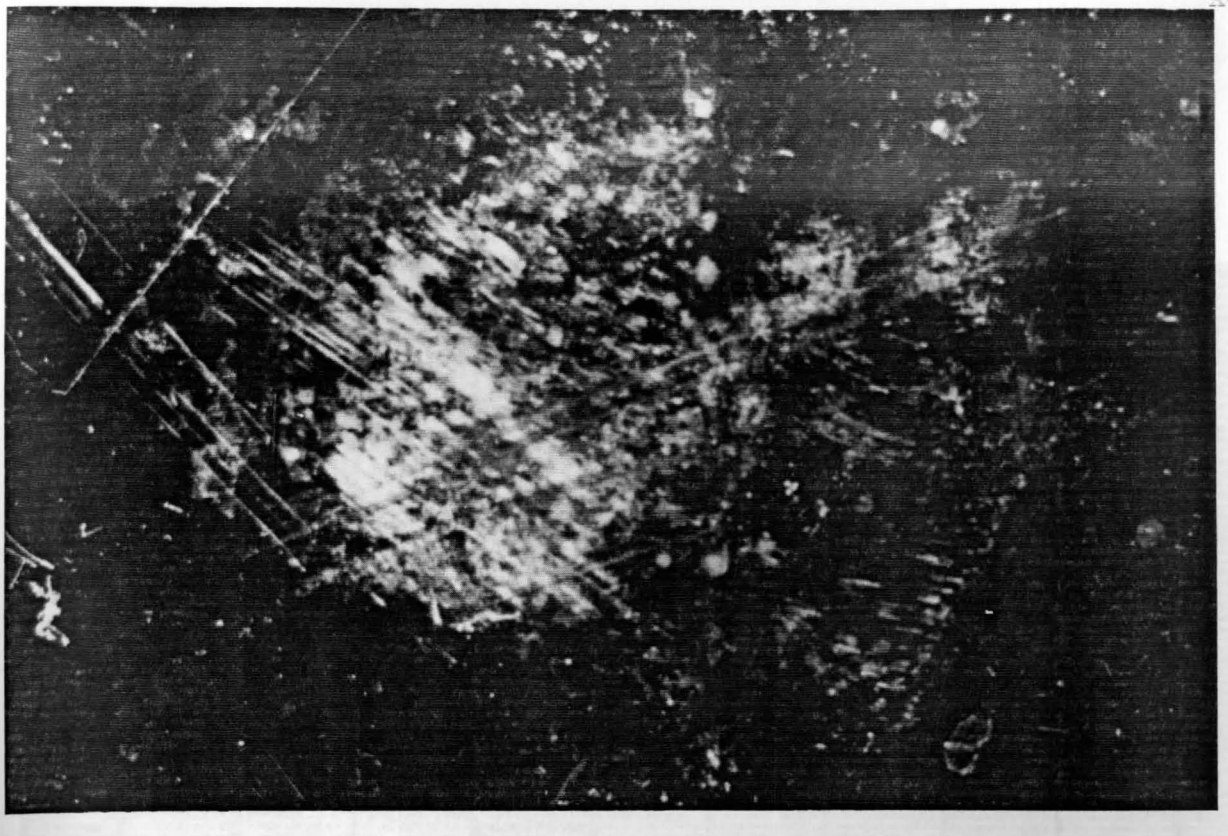

FIGURE 22. Stereomicroscope photograph of impacted surface with "dart-drop" tester.

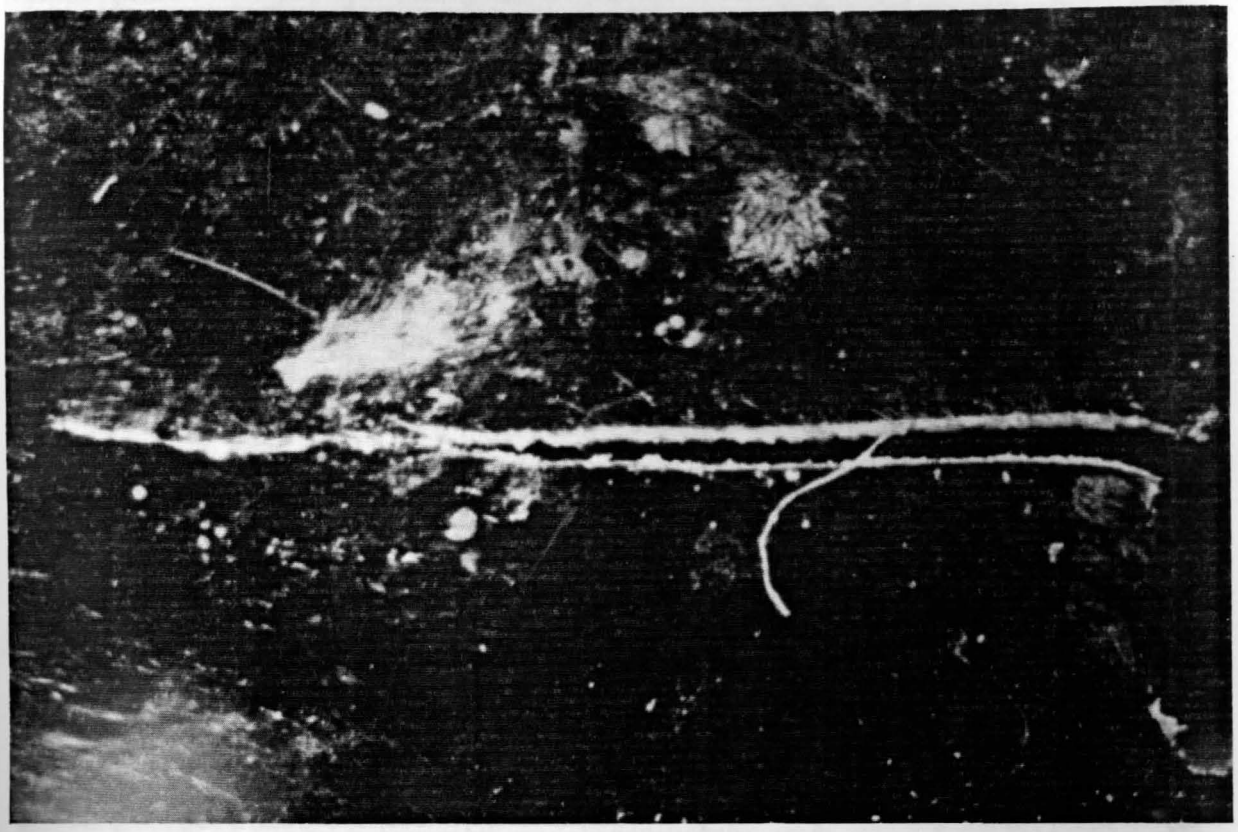

FIGURE 23. Stereomicroscope photograph of impacted surface with "dart-drop" tester. Feature to be noted is the crack propagating from the notch (right to left).

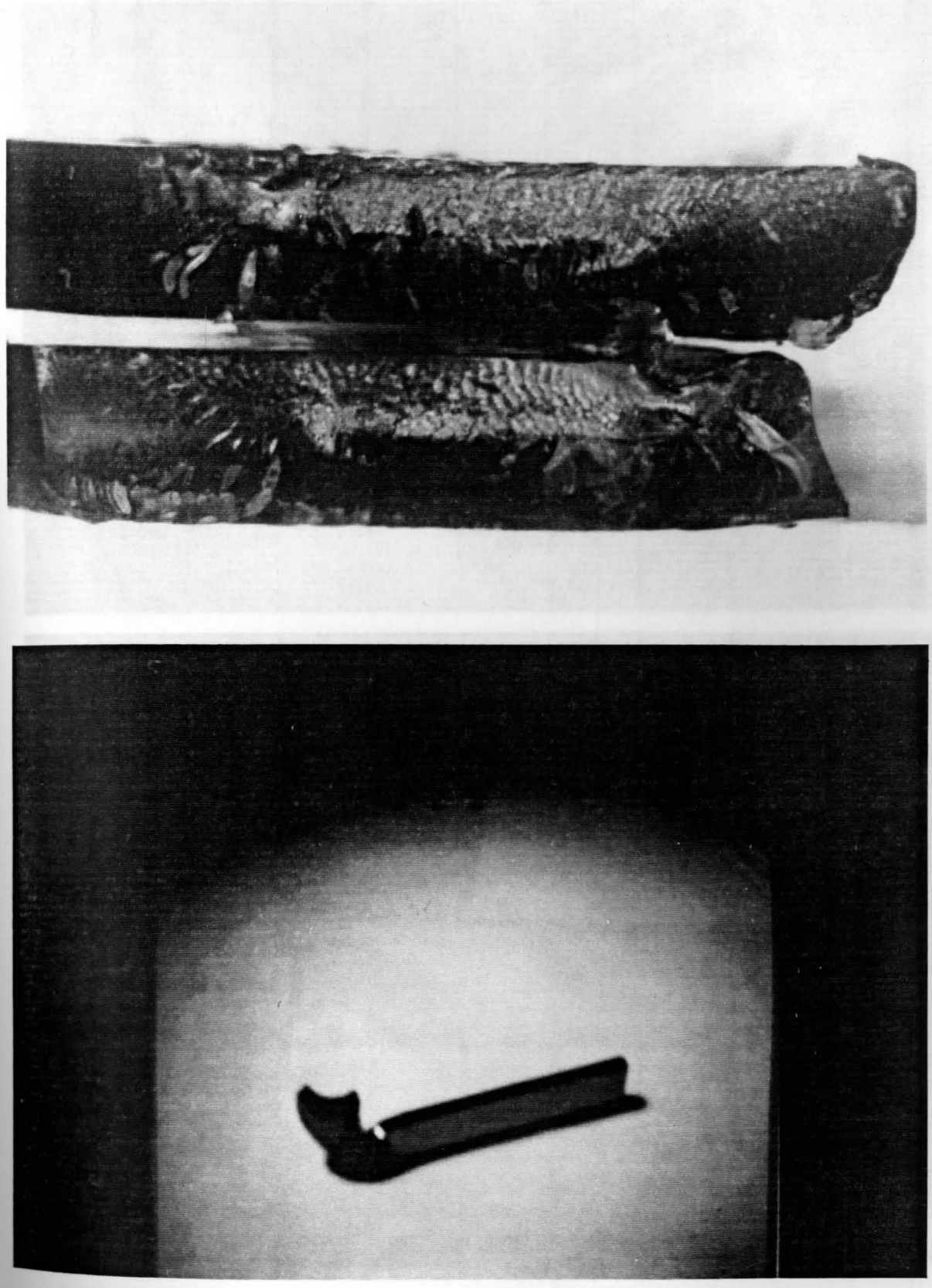

FIGURE 24. Stereomicroscope photograph of the fracture surface in torsion. Photograph of the sample in torsion.

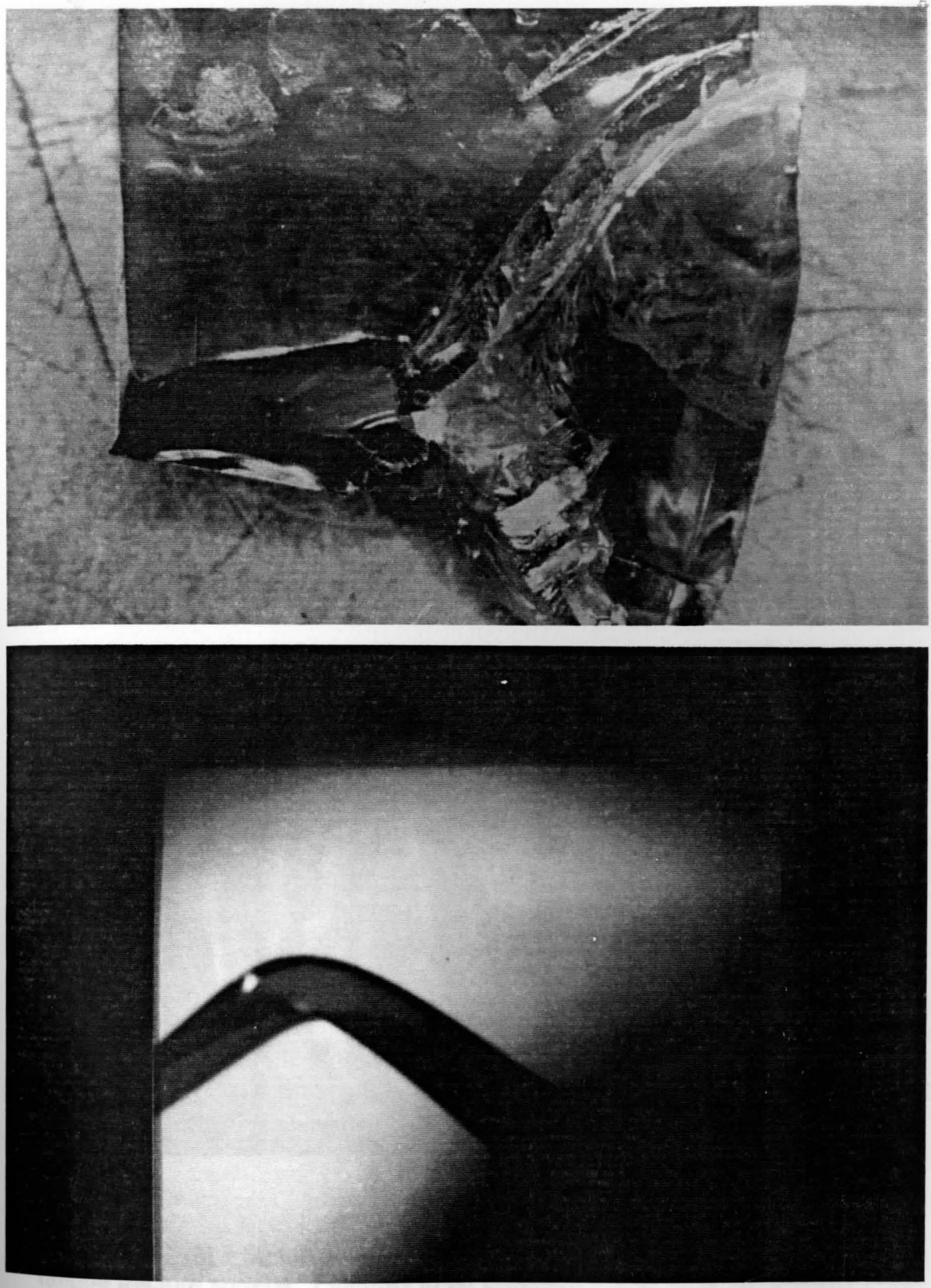

FIGURE 25. Stereomicroscope photograph of fracture surface in torsion with bending.

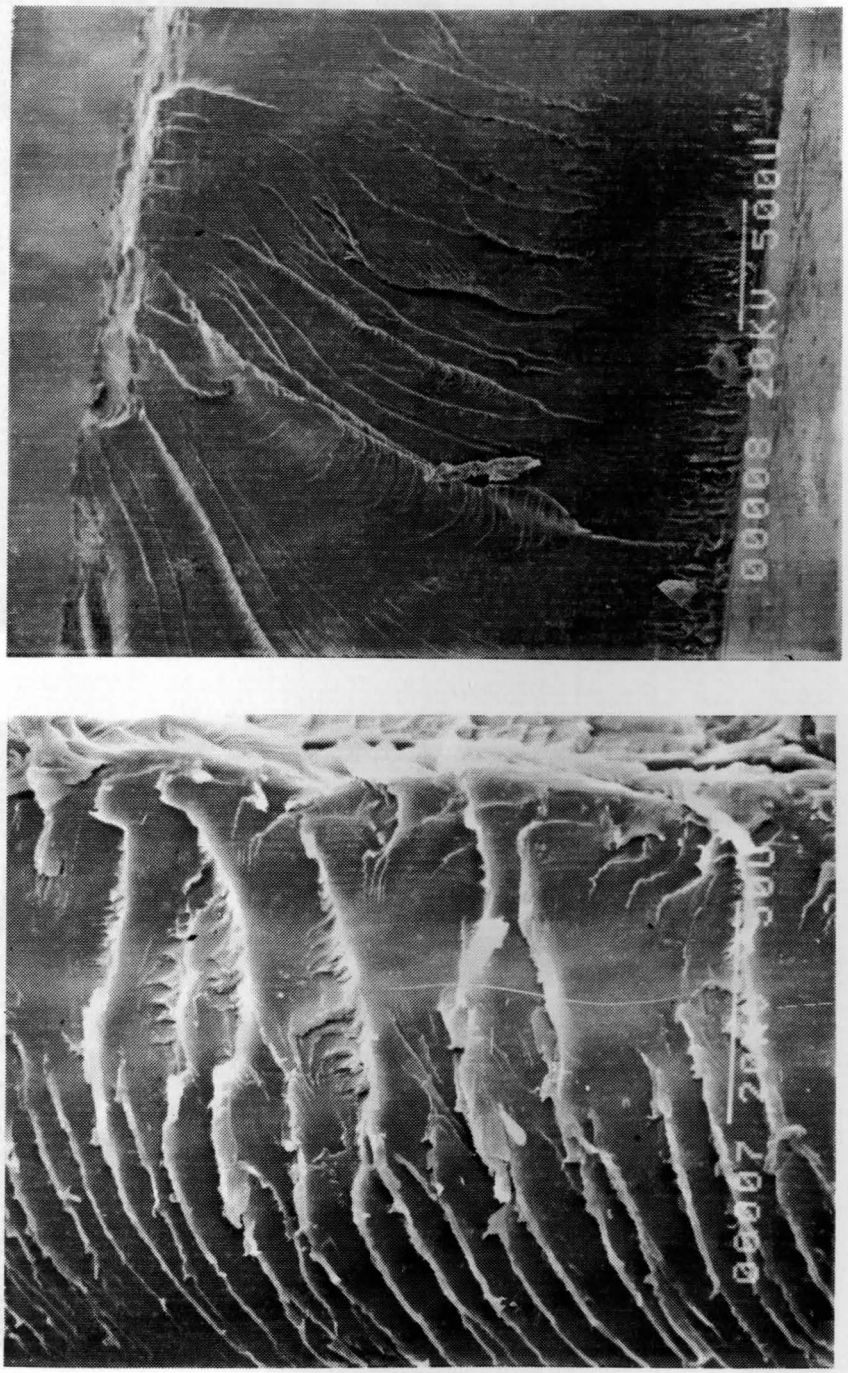

FIGURE 26. (M = 39 top and M = 670 bottom). SEM photographs of fatigue fracture surface. Features to be observed are white lines, crazes, showing the direction of crack propagation and smaller parallel lines called fatigue striations.

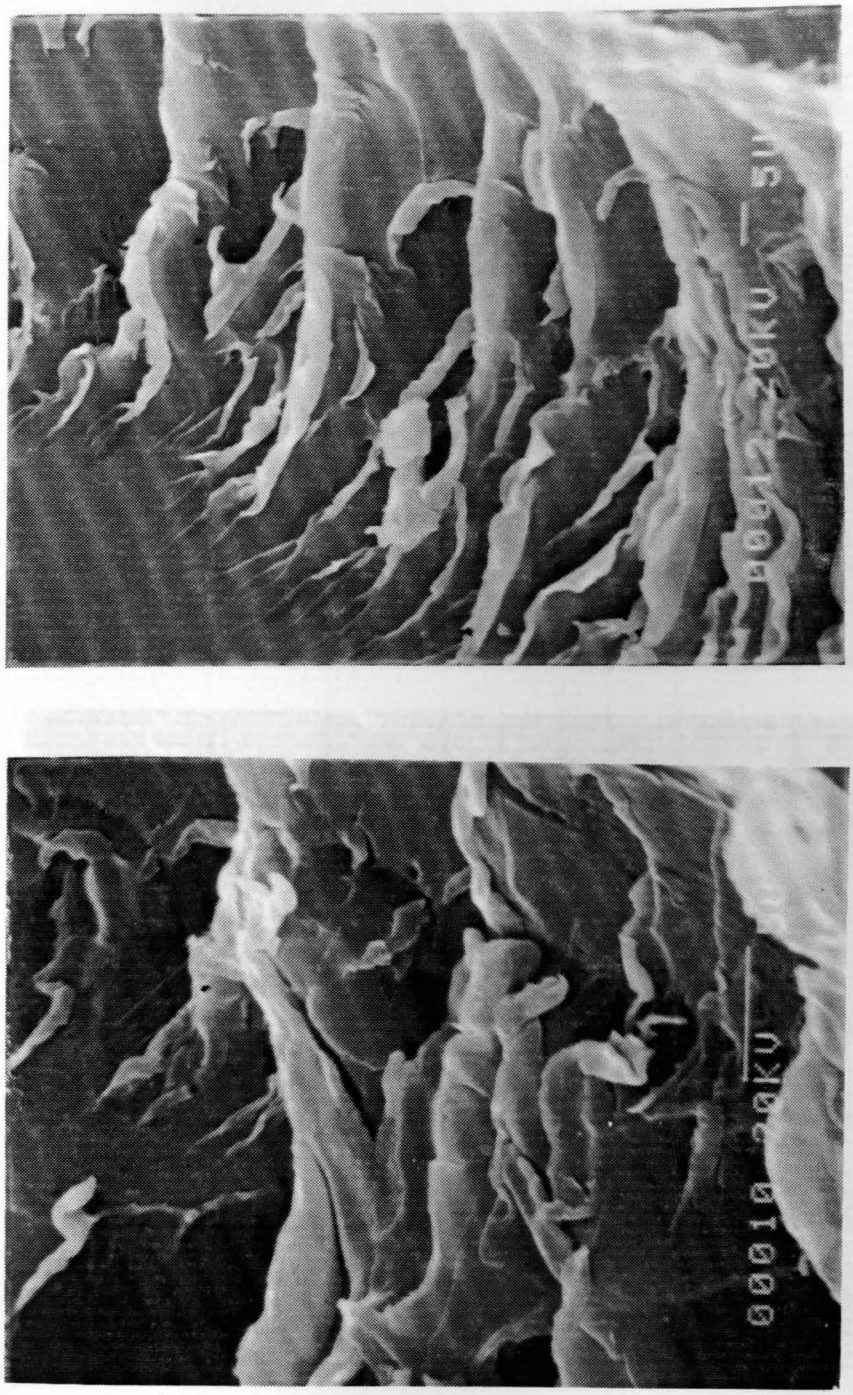

FIGURE 27. (M - 1200 top and M = 4100 bottom). SEM photograph of fatigue striations. Features to be observed are crease-like, rounded, and flap-like. Dimples and voids can also be noted.

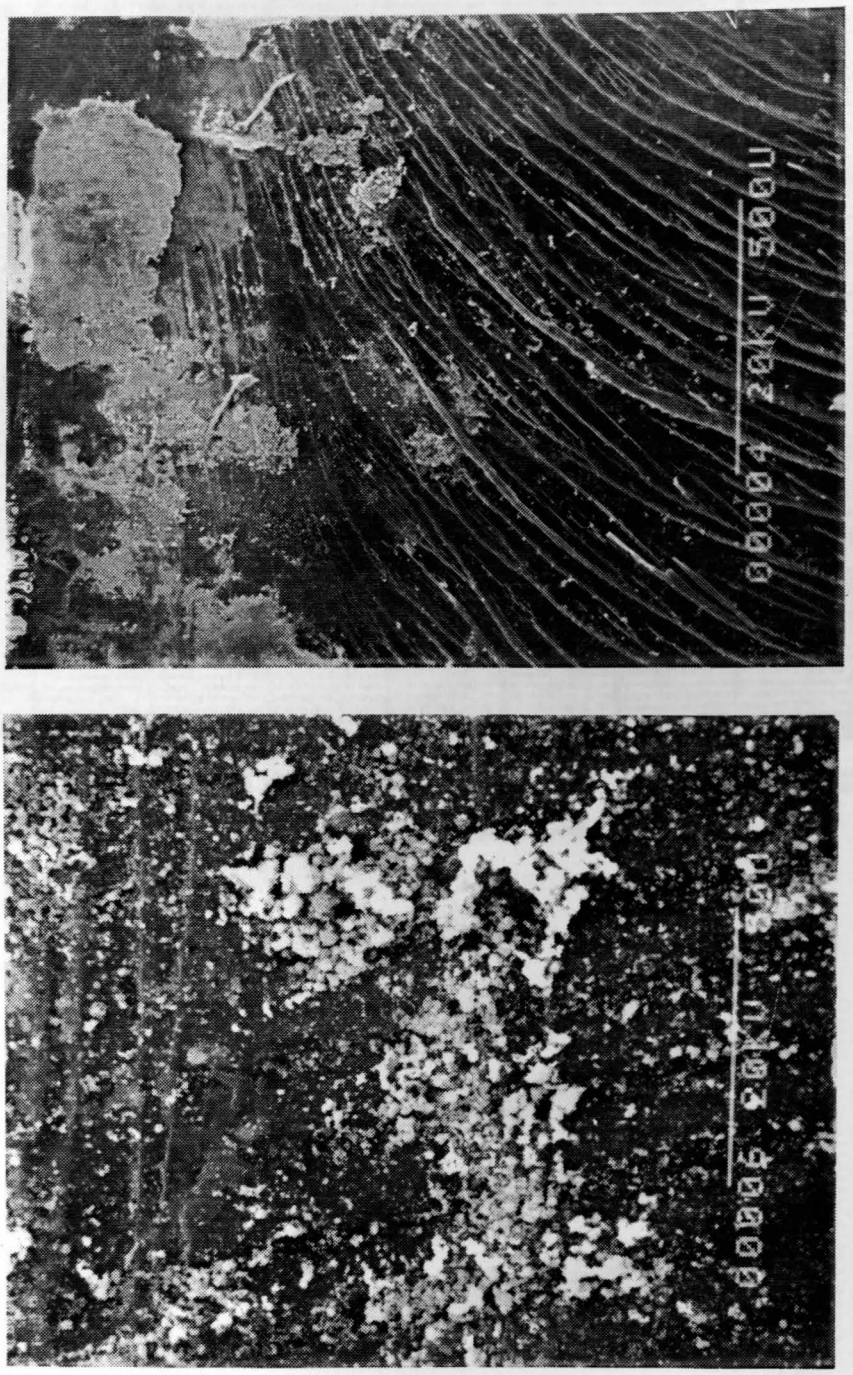

FIGURE 28. (M = 82 top and M = 850 bottom). SEM photographs of sample showing rough region and white spheres of chain breakage.

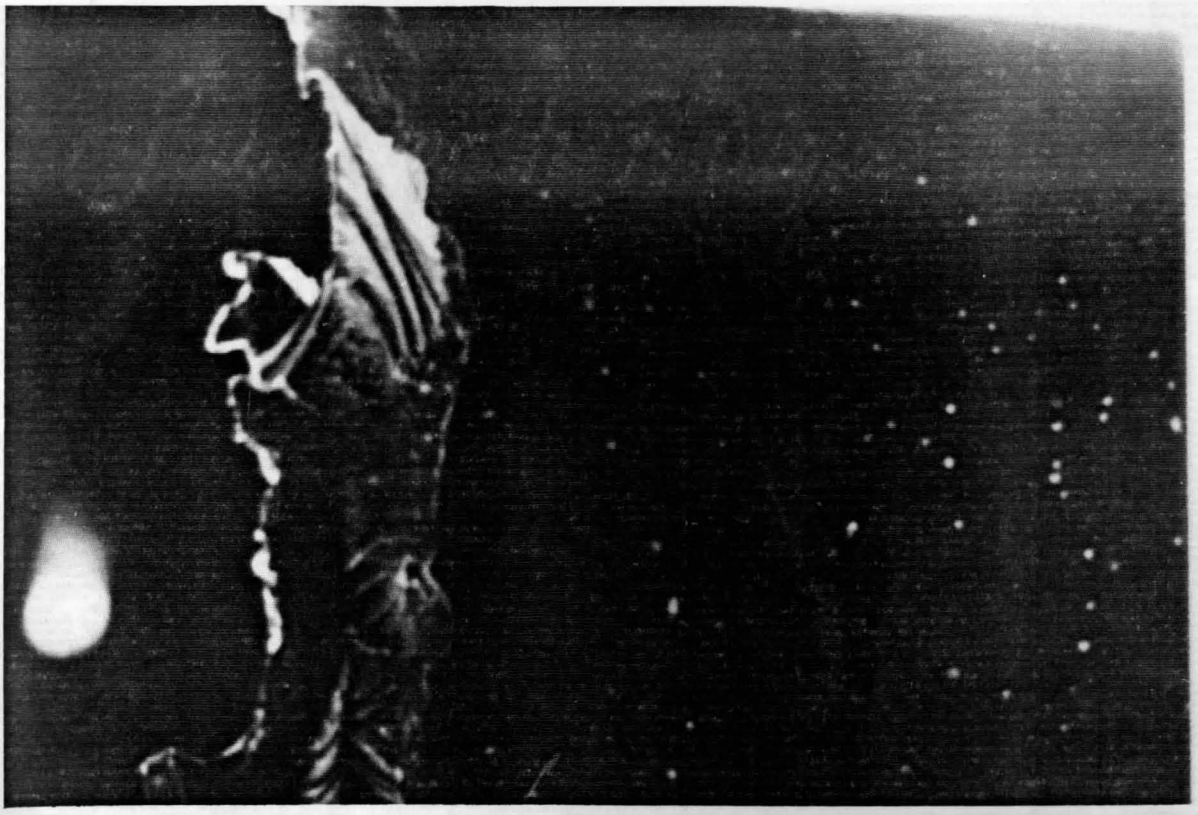

FIGURE 29. (M = 46) SEM photograph of the tear fracture that was caused by cutting the sample.

FIGURE 30. Stereomicroscope photograph of the specimen surface showing stress corrosion cracking.

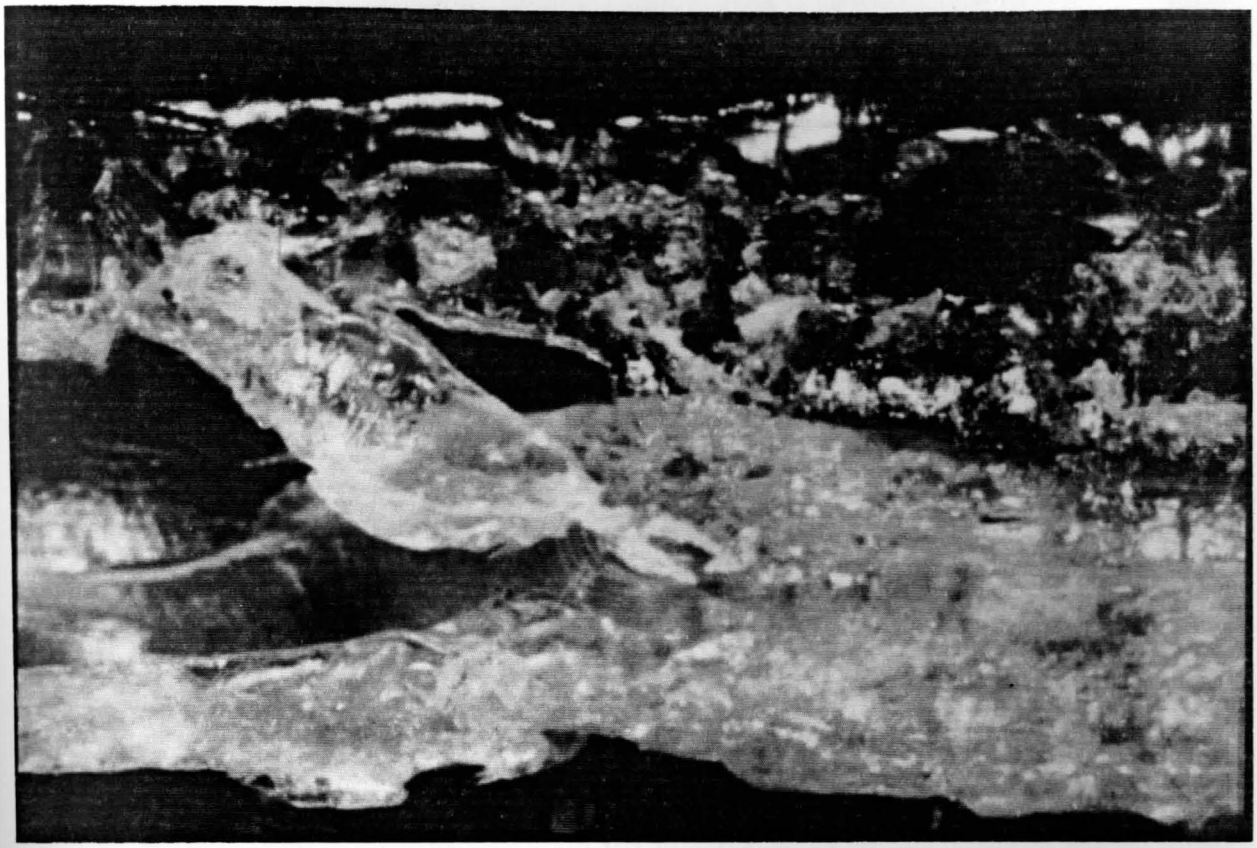

FIGURE 31. Stereomicroscope photograph of the specimen surface upon dissolving in trichloroethane.

Appendix 2

ULTEM® resin Standard Grades

Typical Property Values

English Units (SI Units)

ULTEM 1000: Low viscosity unmodified resin
ULTEM 1010: Unmodified resin

PROPERTY	ASTM TEST METHOD	UNITS	ULTEM 1000 resin
PHYSICAL			
Specific Gravity	D792	—	1.27
Mold Shrinkage, 1/8" (3.2 mm)	D955	in/in(m/m)	0.007
Water Absorption	D570	%	
24 hours, 73°F(23°C)			0.25
Equilibrium, 73°F(23°C)			1.25
MECHANICAL			
Tensile Strength	D638	psi(MPa)	15,200(105) [Y]
Tensile Modulus, 1% Secant	D638	psi(MPa)	430,000(3,000)
Tensile Elongation, Yield	D638	%	7–8
Tensile Elongation, Ultimate	D638	%	60
Flexural Strength	D790	psi(MPa)	22,000(150)
Flexural Modulus, Tangent	D790	psi(MPa)	480,000(3,300)
Compressive Strength	D695	psi(MPa)	21,900(150)
Compressive Modulus	D695	psi(MPa)	480,000(3,300)
Shear Strength, Ultimate	—	psi(MPa)	15,000(100)
Gardner Impact Strength	—	in-lb(N-m)	320(36)
Izod Impact Strength	D256	ft-lbs/in(J/m)	
Notched, 1/8" (3.2 mm)			1.0(50)
Unnotched, 1/8" (3.2 mm)			25(1,300)
Rockwell Hardness	D785	—	M109
Taber Abrasion (CS 17, 1 kg)	D1044	mg. wt. loss/ 1000 cycles	10
Poisson's Ratio	E132	—	0.44
THERMAL			
Deflection Temperature, Unannealed	D648	°F(°C)	
@ 66 psi, 1/4" (0.45 MPa, 6.4 mm)			410(210)
@ 264 psi, 1/4" (1.82 MPa, 6.4 mm)			392(200)
Vicat Softening Point, Method B	D1525	°F(°C)	426(219)
Thermal Index, UL Bulletin 746B	UL746B	°F(°C)	338(170)
Coefficient of Thermal Expansion,	D696	in/in-°F(m/m-°C)	3.1×10^{-5}
			(5.6×10^{-5})
0 to 300°F (−18 to 150°C), Mold Direction			
Thermal Conductivity	D2214	Btu-in/hr-ft²-°F(W/m-°C)	0.85(0.12)
FLAMMABILITY			
Vertical Burn @ 0.010" (0.25 mm)	UL94	—	
UL Bulletin 94**			—
@ 0.016" (0.41 mm)			V-0
@0.075" (1.9 mm)			5V
NBS Smoke, Flaming	E662	—	
Mode, 0.060"(1.5 mm)			
D_s @ 4 min			0.7
D_{max} @ 20 min			30
Oxygen Index	D2863	%	47
ELECTRICAL			
Dielectric Strength, 1/16" (1.6 mm)	D149	V/mil(kV/mm)	
in oil			710(28)
in air			830(33)
Dielectric Constant 1 kHz, 50% RH	D150	—	3.15
Dissipation Factor	D150	—	
1 kHz, 50% RH, 73°F(23°C)			0.0013
2450 MHz, 50% RH, 73°F(23°C)			0.0025
Volume Resistivity, 1/16" (1.6 mm)	D257	ohm-cm(ohm-m)	6.7×10^{17}
			(6.7×10^{15})
Arc Resistance	D495	seconds	126

* Applies to electrical and mechanical properties without impact.
** This rating is not intended to reflect hazards presented by this or any other material under actual fire conditions.
n.a. Not applicable.
[Y] Yield
[B] Break

Mechanical Properties

Strength

At room temperature ULTEM resin exhibits strength far beyond that of most engineering thermoplastics, with a tensile strength at yield of over 15,000 psi (100 MPa) and a flexural strength at 5% deflection of 21,000 psi (145 MPa).

Even more impressive is the retention of strength at elevated temperatures. At 375°F (190°C), a temperature well beyond the useful range of most other engineering thermoplastics, ULTEM resin retains approximately 6,000 psi (41 MPa) tensile strength, as illustrated in Figure 1.

Figure 2 demonstrates the superior tensile strength of ULTEM 1000 compared to other high performance engineering materials. This outstanding inherent strength of ULTEM resin is further enhanced through reinforcement with glass fibers. ULTEM 2400 resin, for example, exhibits a tensile strength at ultimate of 27,000 psi (186 MPa). Figure 3 compares ULTEM 2200 and 2300 resins with other glass reinforced engineering thermoplastics.

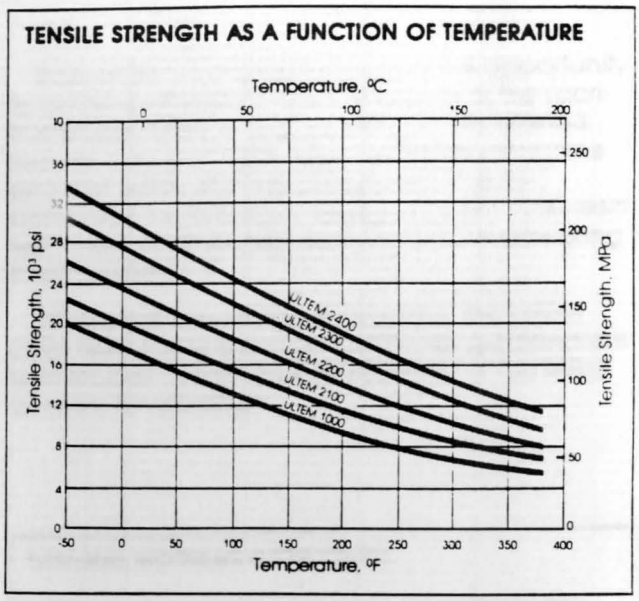

FIG. 1

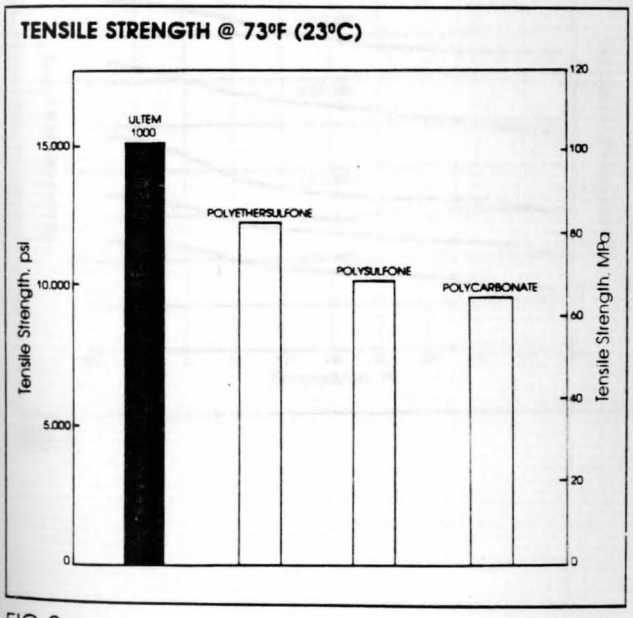

FIG. 2

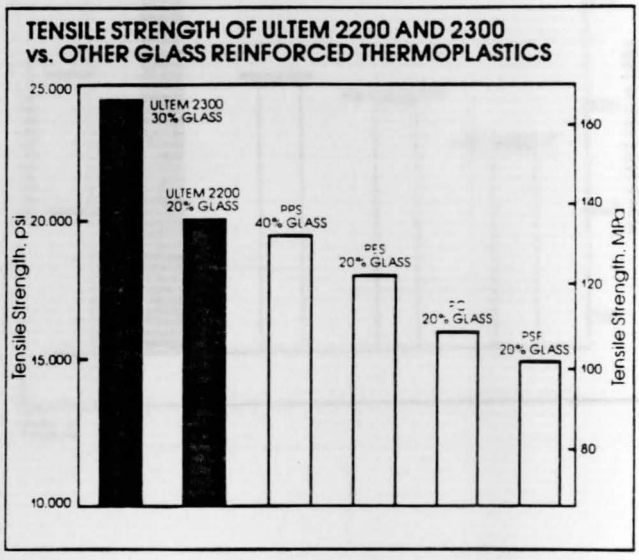

FIG. 3

Mechanical Properties

Modulus

Another outstanding mechanical property of ULTEM resin is its high modulus. The 480,000 psi (3,300 MPa) flexural modulus of ULTEM 1000 resin is one of the highest room temperature moduli of any high performance engineering plastic. In load-bearing applications where deflection is a primary consideration, unreinforced ULTEM resin provides structural rigidity approaching that of many glass reinforced resins.

In addition, the flexural modulus of ULTEM resin remains exceptionally high at elevated temperatures, as shown in Figure 4. For example, at 350°F (175°C) the modulus of ULTEM 1000 resin is higher than that of most engineering plastics at room temperature.

Thus, ULTEM resin offers designers the opportunity to achieve desired stiffness with none of the sacrifices associated with glass reinforced materials, such as loss of transparency, increased machine and tool wear, and decreased flow. Figure 5 compares the flexural modulus of ULTEM 1000 resin with those of other high performance engineering thermoplastics.

Where greater stiffness is required, the ULTEM 2000 resin series provides additional performance with moduli as high as 1,700,000 psi (11,700 MPa) at room temperature.

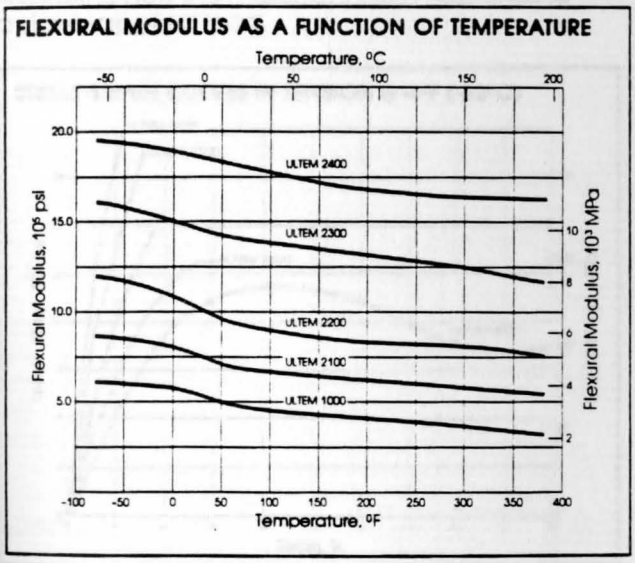

FIG. 4

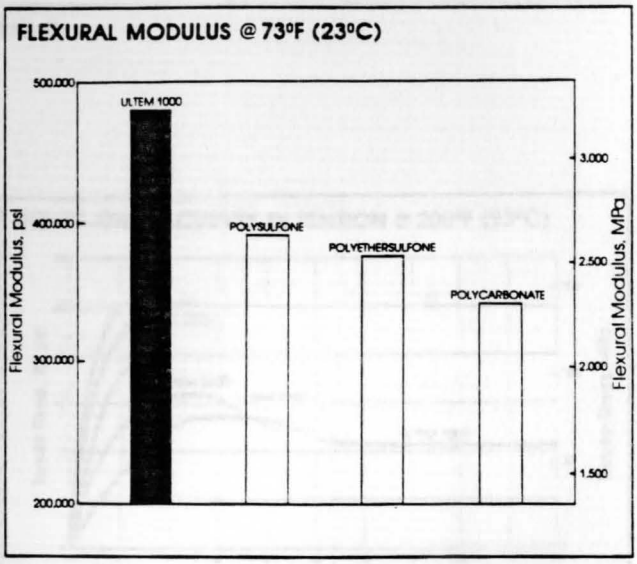

FIG. 5

Stress-Strain Relationship

ULTEM resin exhibits classical stress-strain relationships at varying temperatures, as shown in Figures 6 through 10. In addition to its unique combination of high strength and modulus derived from the stress-strain curves, ULTEM resin exhibits outstanding ductility. This ductility is shown by its tensile elongation at yield of 6% and at fracture of 60%.

The standard stress-strain properties derived from Figures 6-10 are produced from short-term testing at low strain rates. These properties are useful for designing parts subjected to momentary or intermittent, slowly-applied loads, where the time frame and the strain rate are the same as that in the testing (ASTM D638). They are also useful for comparing materials, quality control, and illustrating how the material initially responds to a slowly-applied load.

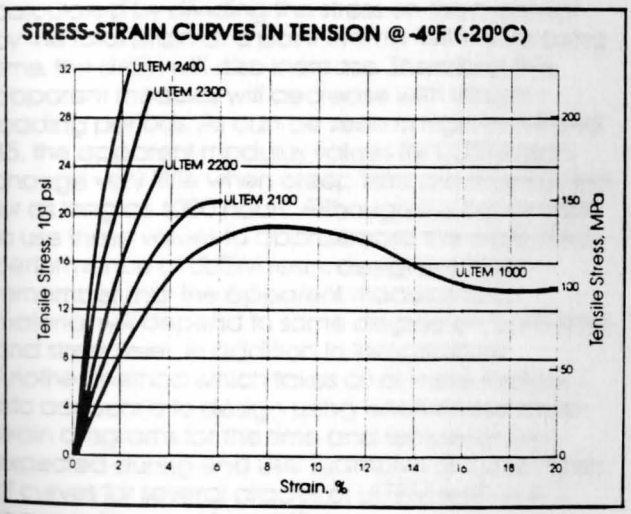

FIG. 6

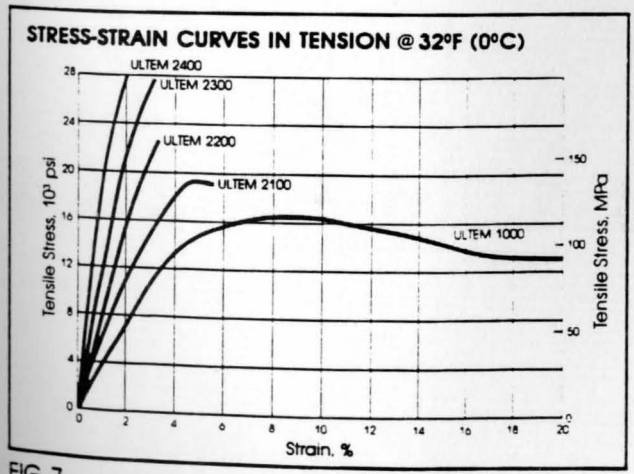

FIG. 7

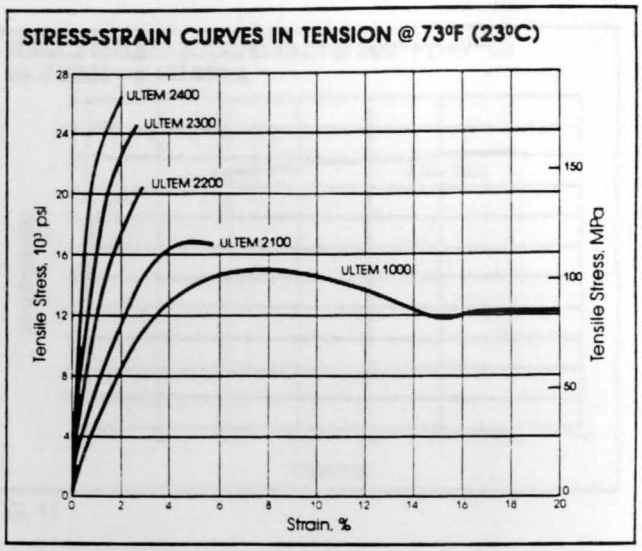

FIG. 8

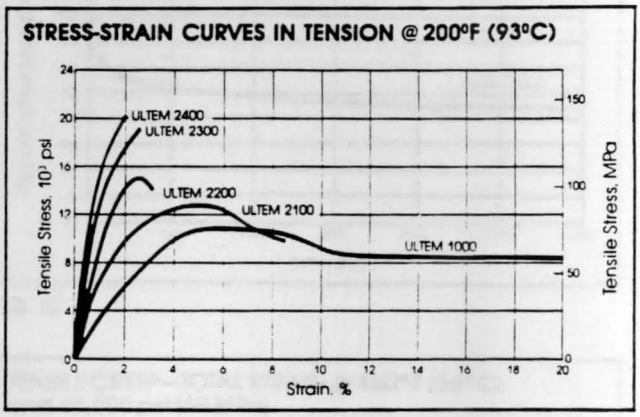

FIG. 9

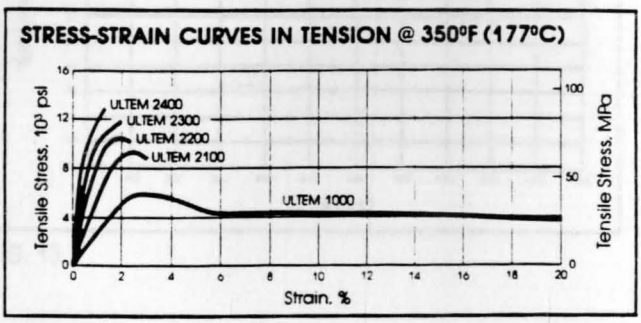

FIG. 10

Mechanical Properties

Creep Behavior

When considering the mechanical properties of any thermoplastic material, designers must recognize the effects of temperature, stress level and load duration on material performance. ULTEM resin, like other thermoplastics, will behave differently depending on these variables. However, ULTEM resin displays excellent creep resistance even at temperatures and stress levels which would prohibit the use of many other thermoplastics. This behavior can be seen in Figures 11 and 12, which respectively show the total strain and apparent modulus vs. time for ULTEM 2300 resin when tested at 300°F and 3000 psi. In addition, as can be seen in Figure 13, under similar conditions, ULTEM 2400 resin provides even greater creep resistance than ULTEM 2300 resin.

When tested under conditions of constant stress, the apparent modulus of a material can be calculated by dividing the stress on the material by the total strain at a point in time. With increasing time, the strain will also increase. Therefore, the apparent modulus will decrease with longer loading periods. As can be seen in Figures 14 and 15, the apparent modulus values for ULTEM resin change very little when creep tests are maintained for as long as 1000 hours. Although it is convenient to use these values to approximate the expected performance of ULTEM resin, designers must remember that the apparent modulus of a material will depend to some degree on both time and stress level, in addition to temperature. Another method which takes all of these factors into account is to design using isochronous stress-strain diagrams for the time and temperatures expected during end use. Examples of these types of curves for several grades of ULTEM resin are shown in Figures 16 and 17.

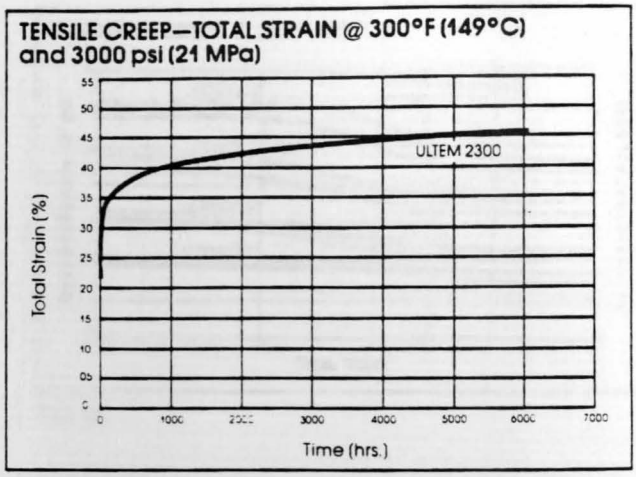

FIG. 11

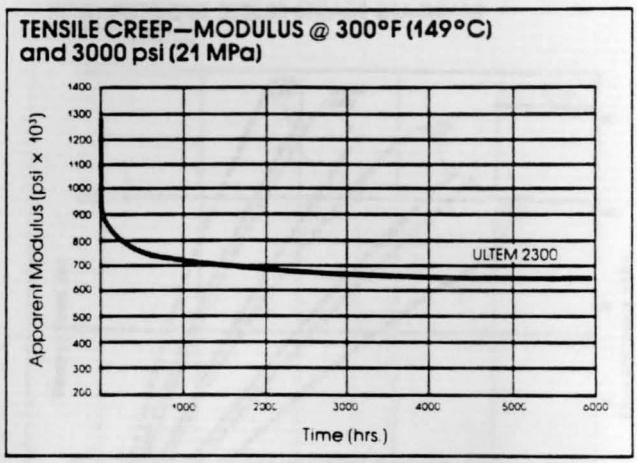

FIG. 12

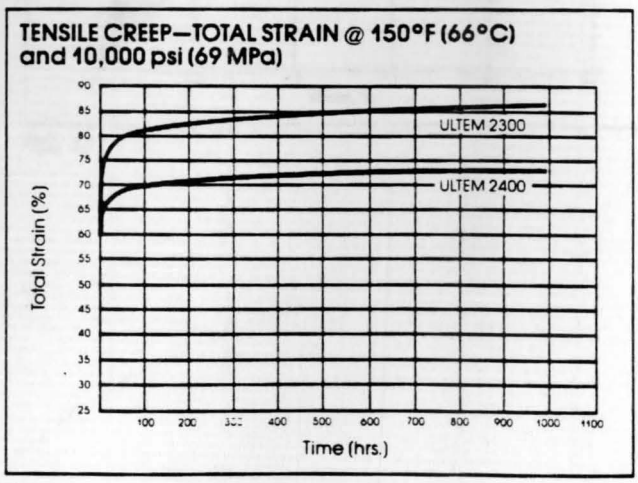

FIG. 13

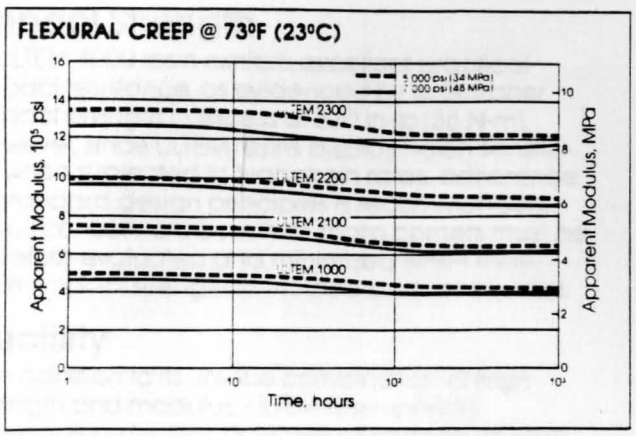

FIG. 14

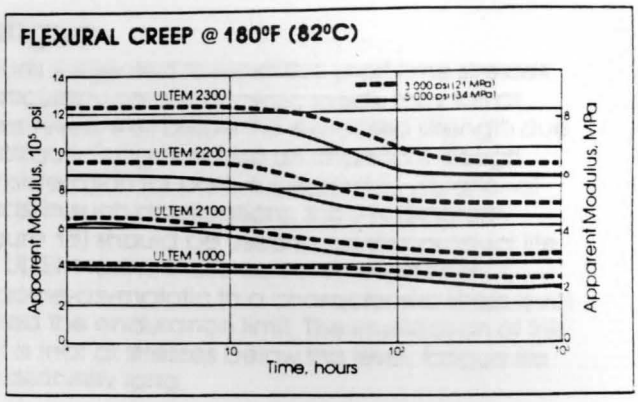

FIG. 15

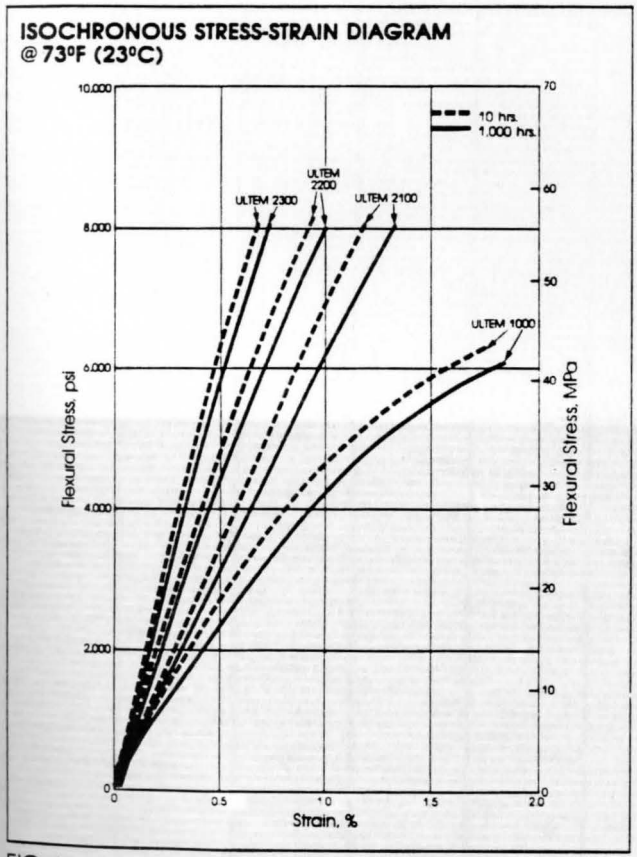

FIG. 16

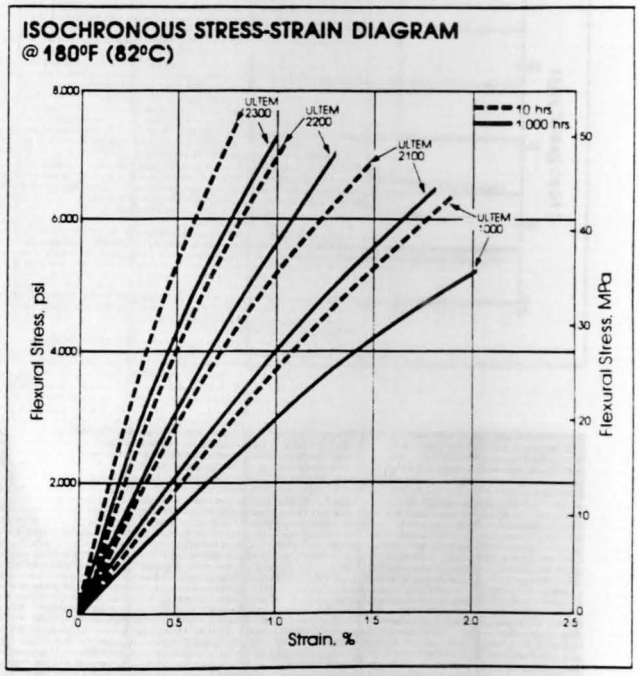

FIG. 17

Mechanical Properties

Impact Strength

ULTEM 1000 resin exhibits excellent practical impact resistance, as evidenced by its Gardner impact strength in excess of 320 in-lb (36 N-m). However, since ULTEM resins display notch sensitivity when subjected to high strain rates, adherence to standard design principles is recommended. Stress concentrators such as sharp corners must be carefully evaluated and minimized when maximum impact strength in molded parts is required.

Ductility

In addition to its unique combination of high strength and modulus, ULTEM resin exhibits outstanding ductility. Its tensile elongation at yield affords the freedom to incorporate snap-fit designs for ease of assembly.

Fatigue

Parts subjected to repetitive short-time stresses, particularly continual cyclic loads, may fail at stress levels well below the expected strength due to fatigue. Fatigue is also an important design consideration for parts subjected to vibrational loads. In such applications, the S-N diagram (Figure 18) should be used to predict product life. For ULTEM resins, these curves level off and become asymptotic to a characteristic stress level called the endurance limit. The implication of this limit is that at stresses below this level, fatigue life is indefinitely long.

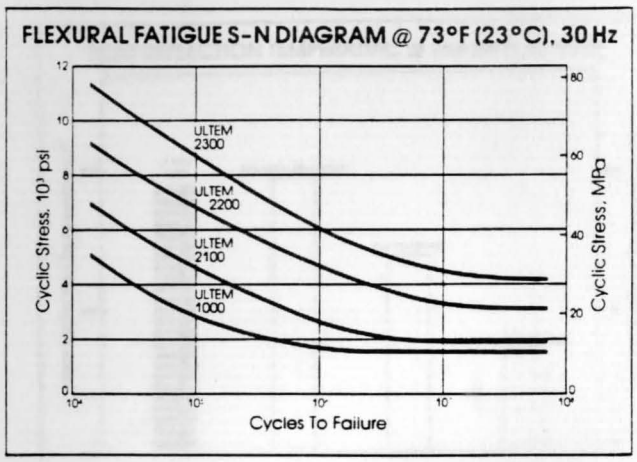

FIG. 18

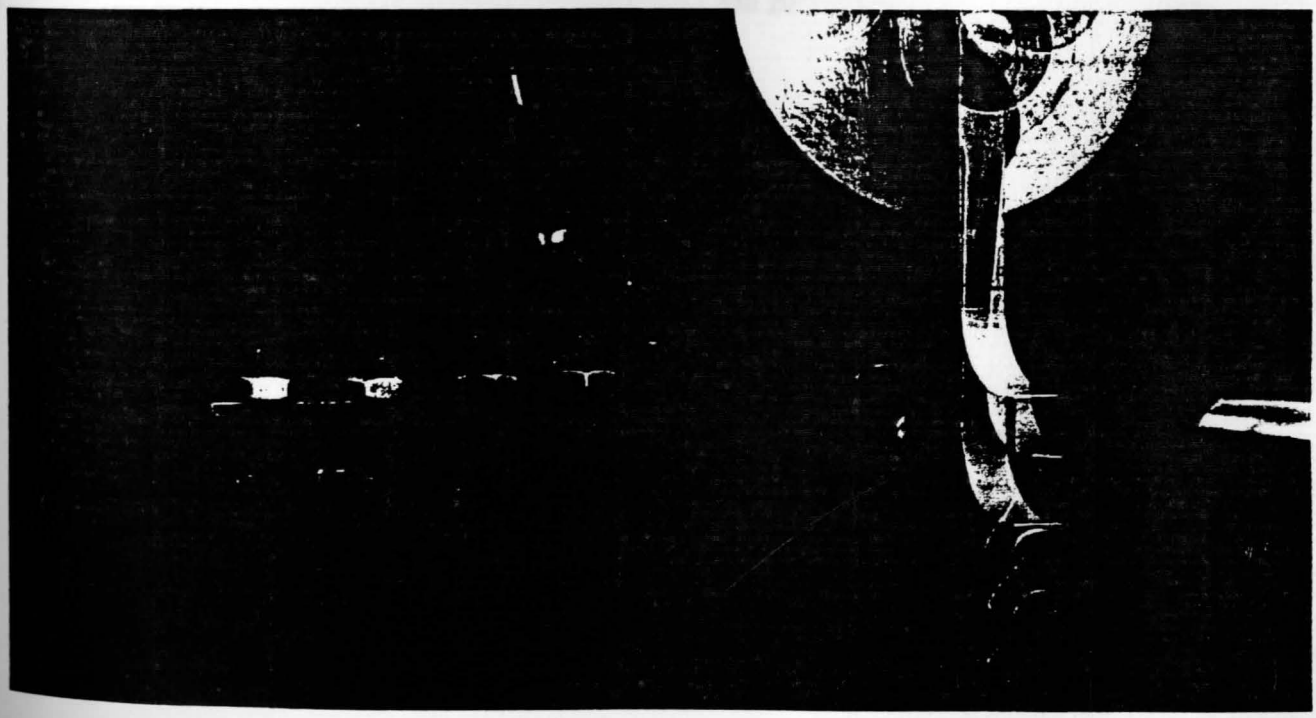

Thermal Properties

An outstanding property of ULTEM resin is its ability to withstand long-term exposure to elevated temperatures. ULTEM resin provides the excellent thermal stability commonly associated with exotic specialty resins, but without sacrificing processability. This high heat performance, combined with excellent flammability ratings and UL recognition, qualifies ULTEM resin for demanding high temperature applications.

Heat Deflection Temperature and Continuous Use Ratings

ULTEM 1000 resin's UL continuous use temperature rating of 170°C reflects its inherent thermal stability.

The resin's high glass transition temperature, Tg, of 419°F (215°C), coupled with its high heat deflection temperature of 392°F (200°C) at 264 psi (1.82 MPa), contributes to its excellent retention of physical properties at elevated temperatures. Figure 19 shows the ability of ULTEM resin to maintain this high heat deflection temperature with increased stress, an important consideration to the design engineer. Figure 20 compares the high heat deflection temperature of ULTEM 1000 resin with those of other high performance engineering thermoplastics.

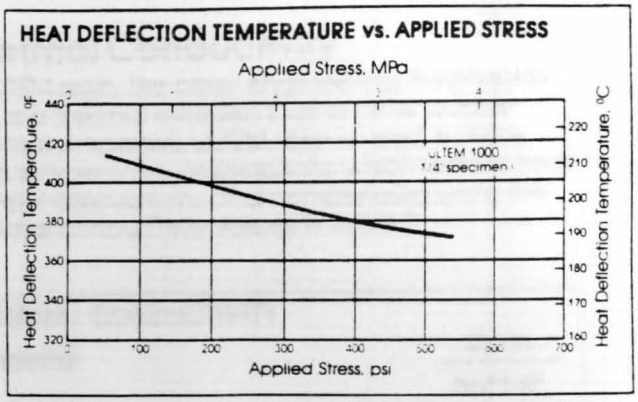

FIG. 19

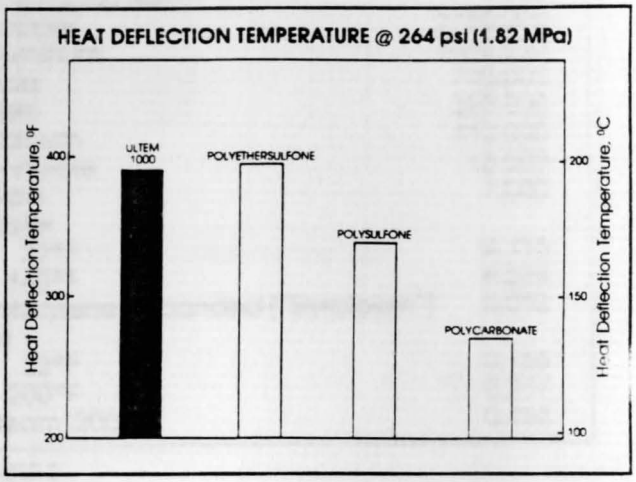

FIG. 20

Thermal Properties

Coefficient of Thermal Expansion

Another important design consideration is the thermal expansion of a material, particularly in applications where plastic parts are mated with metal parts, or have metal inserts. Table 1 lists the coefficients of thermal expansion for five ULTEM resin grades along with values of other materials.

COEFFICIENT OF LINEAR THERMAL EXPANSION

Material	10^{-5} in/in-°F
ULTEM 1000 resin	3.10
ULTEM 2100 resin	1.80
ULTEM 2200 resin	1.40
ULTEM 2300 resin	1.10
ULTEM 2400 resin	0.80
NORYL® resin, unreinforced	4.00
LEXAN® resin, unreinforced	3.75
Polyphenylene Sulfide, 40% GR	1.60
Polyethersulfone, 30% GR	1.27
Zinc	1.52
Magnesium Alloys	1.40-1.50
Aluminum Alloys	1.17-1.37
Copper Alloys	0.90-1.15
Brass	0.93-0.97
Brass, cast	1.04
Bronze	1.00
Steel	0.60-0.90
Iron, cast	0.59
Concrete	0.80
Glass	0.40-0.50

Average values for ULTEM grades between 0°F and 300°F in mold flow direction. Cross flow values will be greater.

TABLE 1

Thermal Conductivity

ULTEM resin, like other engineering thermoplastics, is a thermal insulator. Due to other unique thermal properties, ULTEM resin is used in many high temperature applications which require heat transfer calculations and comparisons using the thermal conductivity values in Table 2.

THERMAL CONDUCTIVITY

Material	Btu-in / hr-°F-ft²
ULTEM 1000 resin	0.850
ULTEM 2300 resin	1.560
Copper	2780.000
Aluminum	1560.000
Brass	730.000
Steel	320.000
Titanium	110.000
Concrete	13.000
Glass	7.000
Water	
32°F	4.116
140°F	4.524
Polystyrene, expanded ("Styrofoam")	0.252
Air	
32°F	0.168
200°F	0.217
Steam (200°F)	0.158

TABLE 2

Flammability Properties

Flame Resistance

ULTEM resin exhibits exceptionally high flame resistance without the use of additives. For example, ULTEM 1000 resin is rated V-0 at 0.016 inch (0.41mm) under UL Bulletin 94, and 5V at 0.075 inch (1.9mm). In addition, as seen in Figure 21, it has a limiting oxygen index of 47, the highest of any commonly used engineering thermoplastic.

Heat Release

The Ohio State University Heat Release Rate Calorimeter (OSUHRRC) procedure has been established by the FAA as the test which will be used to qualify polymeric materials for use in commercial aircraft. As with other flammability tests, ULTEM polyetherimide resin also displays excellent performance in this type of analysis. For example, ULTEM 1000 resin displays a two-minute heat release of 40 kW-min/m² and a maximum heat release rate of 55 kW/m².

Combustion Characteristics

A key factor in determining the relative safety of a polymeric material is its smoke generation under actual fire conditions. Measured against other engineering thermoplastics, ULTEM resin exhibits extremely low levels of smoke generation as demonstrated by the NBS smoke evolution test results shown in Figure 22. Furthermore, the products of combustion of ULTEM resin have been shown to be no more toxic than those of wood, with CO, CO_2 and H_2O being the primary gases evolved.*

* These tests are small-scale tests and may not reflect the behavior of the material during fire.

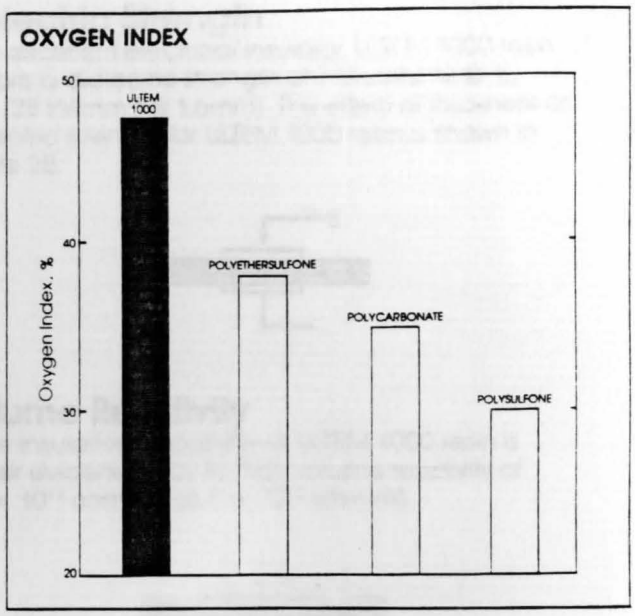

FIG. 21

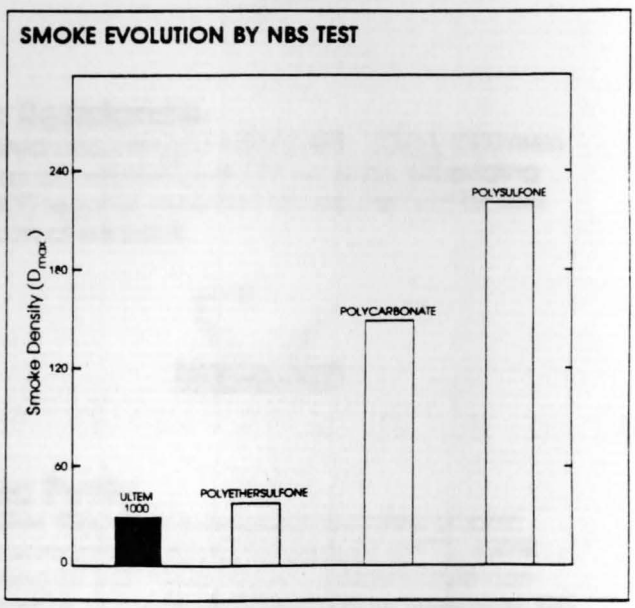

FIG. 22

Electrical Properties

ULTEM resins exhibit excellent electrical properties which remain stable over a wide range of environmental conditions. This stability, together with outstanding thermal and mechanical properties, makes ULTEM resins ideal for highly demanding electrical and electronic applications.

Dielectric Constant

Although either low or high absolute values of the dielectric constant may be desirable depending upon the application, it is more important that the values remain stable over the entire service temperature and/or frequency range. Figures 23 and 24 demonstrate the stability of ULTEM 1000 resin over varying temperatures and frequencies.

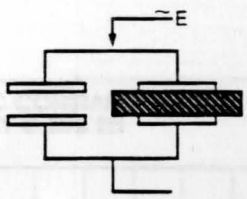

Dissipation Factor

As shown in Figure 25, ULTEM 1000 resin exhibits an exceptionally low dissipation factor over a wide range of frequencies, particularly in the kilohertz (10^3 Hz) and gigahertz (10^9 Hz) ranges. In addition, this low dissipation factor remains constant over the resin's entire useful temperature range. This behavior is of prime importance in applications such as computer circuitry, radomes and microwave cooking components where the resin provides a minimum loss of electrical energy in the form of heat.

Figures 26 and 27 demonstrate the superior performance of ULTEM resin over other thermoplastic resins traditionally considered for these applications.

Dielectric Strength

An excellent electrical insulator, ULTEM 1000 resin exhibits a dielectric strength of 710 volts/mil @ 1/16 inch (28 kV/mm ° @ 1.6mm). The effect of thickness on dielectric strength for ULTEM 1000 resin is shown in Figure 28.

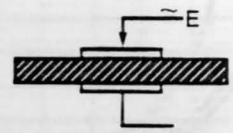

Volume Resistivity

The insulative capability of ULTEM 1000 resin is further evidenced by its high volume resistivity of 6.7×10^{17} ohm-cm (6.7×10^{15} ohm-m).

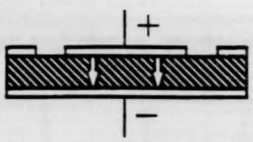

Arc Resistance

Tested according to ASTM D495, ULTEM 1000 resin has an arc resistance of 128 seconds, exceeding the 120 seconds minimum UL requirement for sole support of live parts.

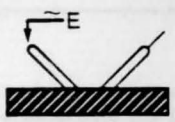

Ionic Purity

ULTEM 1000 resin is extraordinarily free of ionic contaminants. Ion extraction tests at 121°C, 100% R.H. and 30 psig have shown no observable contamination of a water/alcohol mixture. Even after 120 hours, the electrical resistance of the fluid extract has been found to remain above 20 megohms.

DIELECTRIC CONSTANT OF ULTEM 1000 vs. TEMPERATURE @ 50% RH

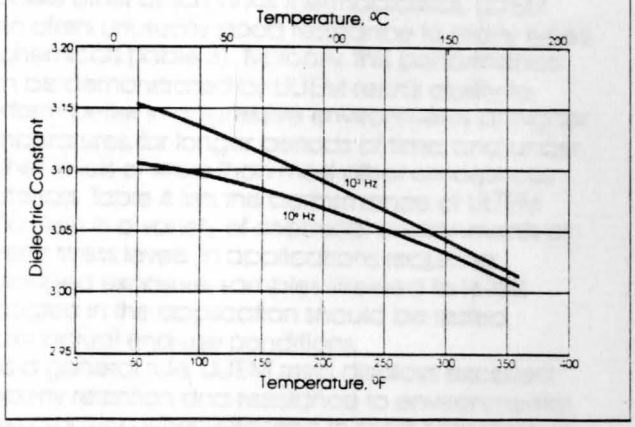

FIG. 23

DISSIPATION FACTOR vs. FREQUENCY @ 73°F (23°C), 50% RH

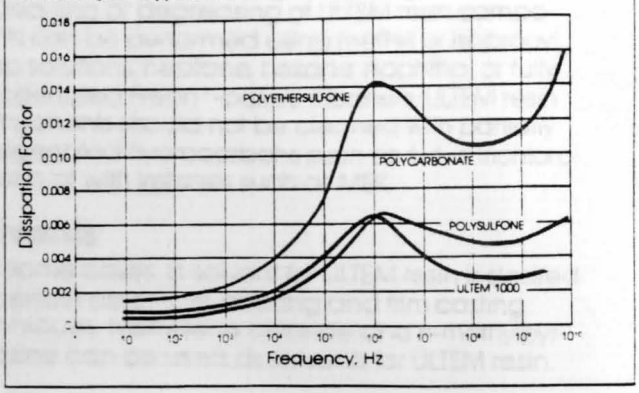

FIG. 26

DIELECTRIC CONSTANT OF ULTEM 1000 vs. FREQUENCY @ 50% RH

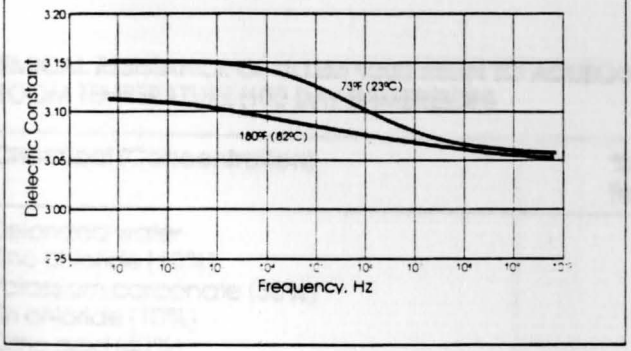

FIG. 24

DISSIPATION FACTOR vs. TEMPERATURE @ 2.45 x 10⁹ Hz

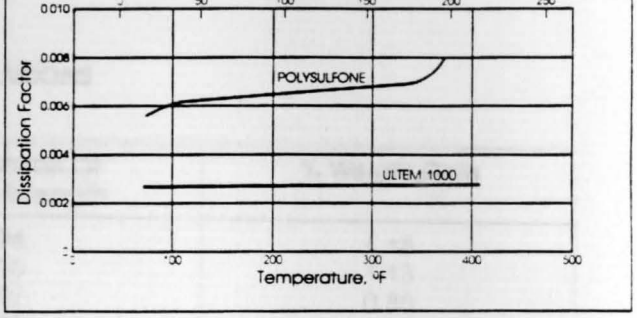

FIG. 27

DISSIPATION FACTOR OF ULTEM 1000 vs. FREQUENCY @ 50% RH

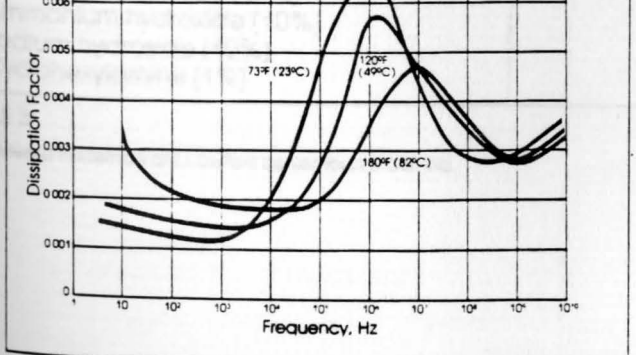

FIG. 25

DIELECTRIC STRENGTH OF ULTEM 1000 AS A FUNCTION OF THICKNESS

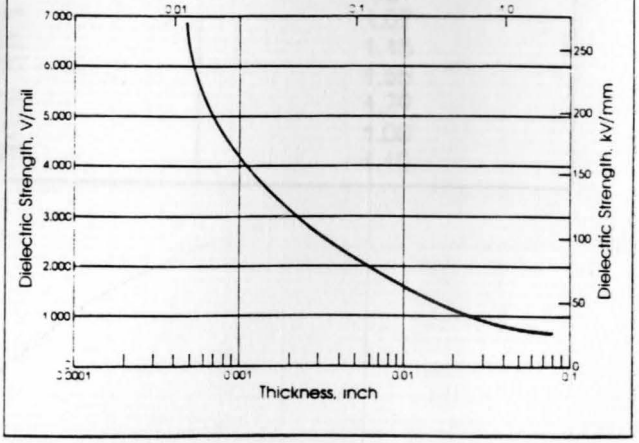

FIG. 28

Environmental Resistance

Chemical Resistance

Unlike other amorphous thermoplastics, ULTEM resin offers unusually good resistance to many types of chemicals (Table 3). Typically, this performance can be demonstrated by ULTEM resin's ability to perform better in aggressive environments at higher temperatures, for longer periods of time, and under higher levels of stress than most other amorphous materials. Table 4 lists the performance of ULTEM 1000 resin in a variety of chemical environments at several stress levels. In applications requiring prolonged exposure, samples stressed to levels expected in the application should be tested under actual end-use conditions.

As a general rule, ULTEM resin displays excellent property retention and resistance to environmental stress cracking when exposed to most commercial automotive and aircraft fluids, fully halogenated hydrocarbons, alcohols, and weak aqueous solutions. Exposure to partially halogenated hydrocarbons and strong alkaline environments should be avoided.

Cleaning and Degreasing

Cleaning or degreasing of ULTEM resin components can be performed using methyl or isopropyl, soap solutions, heptane, hexane, naphtha, or fully halogenated Freon*-based cleaners. ULTEM resin components should not be cleaned with partially halogenated hydrocarbons such as 1, 1, 1 trichloroethane or with ketones such as MEK.

Solvents

In some cases, a solvent for ULTEM resin is desired for certain assembly, coating and film casting techniques. Methylene chloride and n-methylpyrrolidone can be used as solvents for ULTEM resin.

CHEMICAL RESISTANCE OF ULTEM 1000 RESIN TO AQUEOUS SOLUTIONS @ ROOM TEMPERATURE (100 DAY IMMERSION)

Chemical (Concentration)	% Retention Of Tensile Strength	% Weight Gain
Deionized water	94	1.18
Zinc chloride (10%)	96	1.13
Potassium carbonate (30%)	97	0.85
Tin chloride (10%)	97	1.05
Citric acid (40%)	96	1.06
Hydrochloric acid (20%)	99	0.61
Phosphoric acid (20%)	97	0.99
Sulfuric acid (20%)	97	0.89
Chromic acid (15%)	94	0.73
Formic acid (10%)	94	1.29
Nitric acid (20%)	96	1.07
Acetic acid (20%)	95	1.15
Potassium hydroxide (10%)	97	1.55
Ammonium hydroxide (10%)	68	1.79
Sodium hydroxide (10%)	97	1.00
Cyclohexylamine (1%)	97	1.10

TABLE 3

* Registered Trademark of E.I. DuPont deNemours & Co., Inc.

Environmental Stress Resistance of ULTEM 1000 Resin

AIRCRAFT AND AUTOMOTIVE FLUIDS	Time, Hours	Temp., °F	FLEXURAL STRESS LEVELS			
			600 psi (4 MPa)	1,200 psi (8 MPa)	1,800 psi (12 MPa)	2,500 psi (17 MPa)
Antifreeze (Prestone II) 75%	336	72	NC	NC	NC	NC
100%	336	72	NC	NC	NC	NC
75%	168	250	NC	NC	NC	NC
100%	168	250	NC	NC	NC	NC
75%	336	300	NC	<24C	<24C	<24C
100%	336	300	NC	NC	<24C	<24C
Brake Fluid (Wagner 21-8 Ford)	336	72	NC	NC	NC	NC
Brake Fluid (NAPA HD 5-2)	120	72	NC	96C	<24C	<24C
Diesel Fuel (AMOCO)	120	72	NC	NC	NC	NC
Gasoline (AMOCO, Regular)	336	72	NC	NC	NC	NC
Gasoline (AMOCO, Unleaded)	336	72	NC	NC	NC	NC
Gasohol (AMOCO)	700	72	NC	NC	NC	NC
Hydraulic Fluid (Keystone KLC-5)	336	72/140	NC	NC	NC	NC
Jet Fuel (JP-4)	120	72	NC	NC	NC	NC
Kerosene	120	72	NC	NC	NC	NC
Motor Oil (Valvoline XLO 10W-40)	120	72	NC	NC	NC	NC
Skydrol (500B)	336	72	NC	NC	NC	336C
Transmission Fluid (NAPA-GM Dextron II)	120	72	NC	NC	NC	NC
Transmission Fluid (NAPA-GM Dextron II)	168	250	NC	NC	NC	NC
ORGANIC CHEMICALS						
Acetone	336	72	NC	NC	24C	1C
Butyl Alcohol	336	72	NC	NC	NC	NC
Carbon Tetrachloride	336	72	NC	NC	NC	NC
Chloroform	336	72	<1C	<1C	<1C	<1C
Cyclohexane	336	72	NC	NC	NC	NC
Ethanol	120	72	NC	NC	NC	NC
2-Ethoxyethanol (Cellosolve)	336	72	NC	NC	NC	NC
Ethyl Acetate	336	72	NC	NC	<24C	<24C
Ethyl Ether	336	72	NC	NC	NC	NC
Freon TF	120	72	NC	NC	NC	NC
Hexane	336	72	NC	NC	NC	NC
Isopropanol	336	72	NC	NC	NC	NC
Methanol	336	72	NC	NC	NC	NC
Methylene Dichloride	336	72	<24C	<24C	<24C	<24C
Methylethylketone	336	72	NC	24C	<1C	<1C
Naphtha	120	72	NC	NC	NC	NC
Phenol (Saturated Solution)	336	72	NC	16C	<16C	<16C
Propylene Glycol	120	72	NC	NC	NC	NC
Tetrachloroethylene	120	72	NC	NC	NC	NC
Toluene	336	72	NC	NC	2C	2C
1, 1, 2-Trichloroethane	336	72	<1C	<1C	<1C	<1C
Triethylphosphate	336	72	NC	NC	96C	16C
Xylene	336	72	NC	NC	24C	24C
AQUEOUS DETERGENTS, CLEANERS						
Alconox 10%	336	72/140	NC	NC	NC	NC
Clorox	336	72	NC	NC	NC	NC
Hexcel FO 465	360	72	NC	NC	NC	NC
Joy Detergent (10% Concentration)	336	72/140	NC	NC	NC	NC
Lestoil 1	336	72/140	NC	NC	NC	NC

TABLE 4

NC = No cracking or crazing for duration of test.
C = Cracking at number of hours shown.

These results are intended to show short-term resistance to environmental stress cracking, and do not necessarily imply long-term compatibility. Each user of the material should make his own tests with actual parts in end-use conditions to determine the material's suitability for his own particular use.

Environmental Resistance

Hydrolytic Stability

ULTEM resin displays excellent retention of tensile properties following long-term exposure to hot water. This performance is shown in Figure 29 which displays retention of tensile strength following 10,000 hours of exposure to water at room temperature and at 212°F.

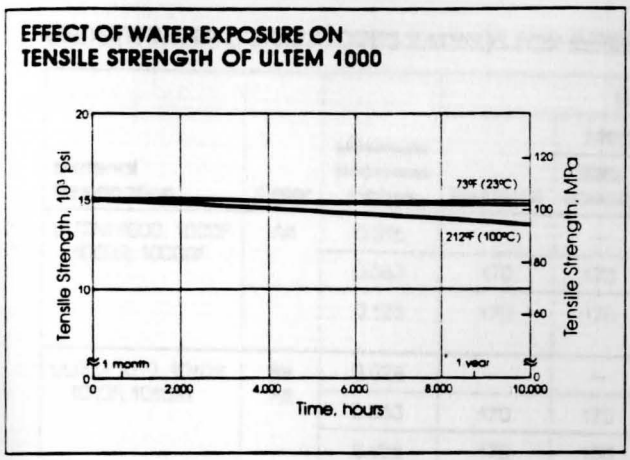

FIG. 29

Autoclavability

The ability to undergo repeated steam sterilization can be among the most important aspects of performance when selecting a material for medical applications. As shown in Figure 30, ULTEM resin has been found to display excellent retention of tensile properties following steam sterilization cycling.

Ultraviolet Exposure

ULTEM resin is inherently resistant to UV radiation without the addition of stabilizers. Exposure to 1,000 hours of xenon arc weatherometer irradiation (0.35 W/m² irradiance at 340 nm, 63°C) produces a negligible change in the tensile strength of the resin as shown in Figure 31.

Radiation Resistance

Parts molded of ULTEM resin have demonstrated excellent resistance to gamma radiation as shown in Figure 32. A loss of less than 6% tensile strength was observed after cumulative exposure to 500 megarads at the rate of one megarad per hour using Cobalt 60.

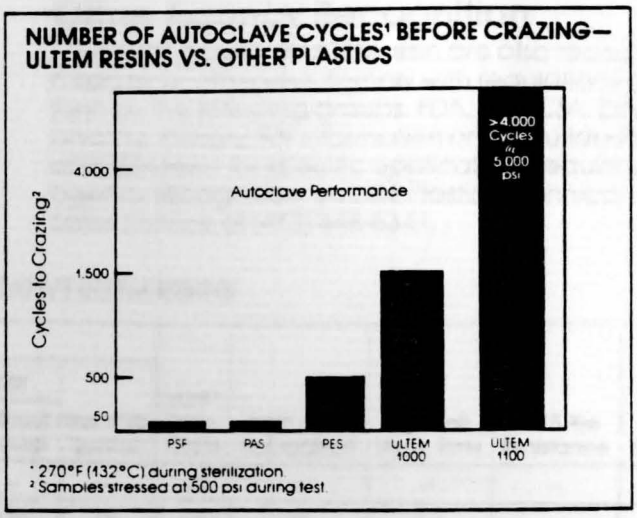

FIG. 30

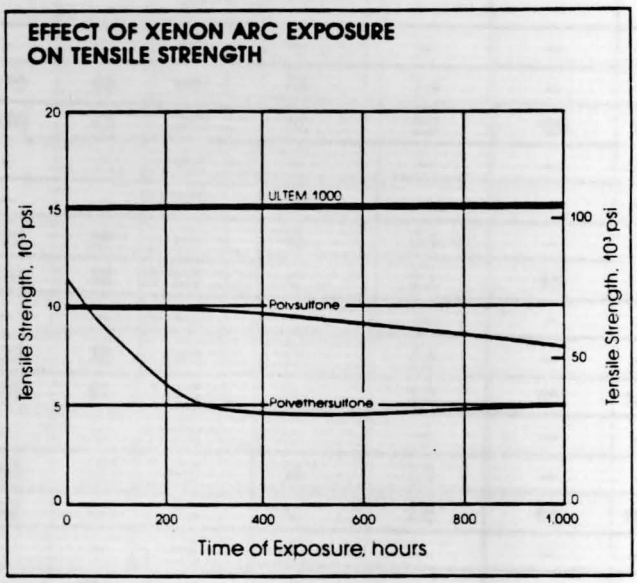

FIG. 31

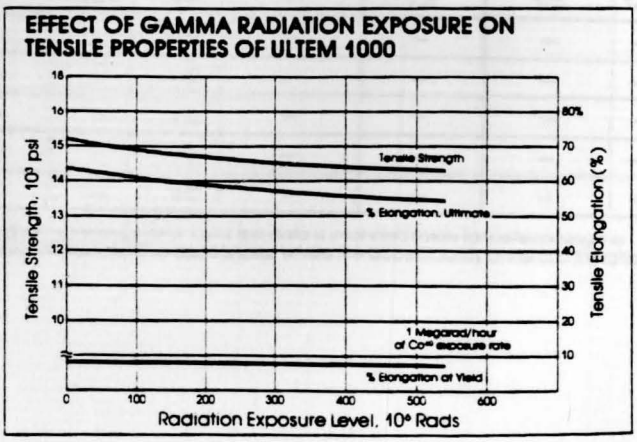

FIG. 32

Agency Recognition

Underwriters Laboratories

ULTEM resins have been tested and comply with a number of agency regulations and specifications. As can be seen in Table 5, ULTEM resin's heat stability and flammability characteristics make it an excellent choice for numerous applications which require UL approval.

Other Agency Recognition

Several grades of ULTEM resin are also recognized by or otherwise comply with regulations put forth by the following groups: FDA, NSF, CSA, DIN, and the military. For information on the suitability of ULTEM resin for specific applications requiring agency recognition, call GE Plastics Technical Sales Service at (413) 448-6341.

UNDERWRITERS LABORATORIES RATINGS FOR REPRESENTATIVE ULTEM RESINS

Material Designation	Color	Minimum Thickness Inches	C.U.T.				UL94* Flam. Class	High Amp Arc Ignition	High Volt. Track. Rate	D495 Arc Resistance	CTI
			Electrical	Mechanical		Hot Wire Ignition					
				With Impact	Without Impact						
ULTEM 1000, 1000F 1000R, 1000RF	All	0.016	—	—	—	—	V-0	—	—	—	—
		0.063	170	170	170	58	V-0	13	2.4	—	—
		0.125	170	170	170	82	V-0/ 5V	15	2.2	126	140
ULTEM 1010, 1010R 1010F, 1010RF	Blk All	0.028	—	—	—	—	V-0	—	—	—	—
		0.063	170	170	170	58	V-0	13	2.4	—	—
		0.125	170	170	170	82	V-0	15	2.2	126	140
ULTEM 1100, 1100F	All	0.029	—	—	—	—	V-0	—	—	—	—
ULTEM 2100, 2100R 2110,2110R	All	0.016	—	—	—	—	V-0	—	—	—	—
		0.063	170	170	170	58	V-0	13	2.4	—	—
		0.126	170	170	170	82	V-0	6	2.2	85	
ULTEM 2200, 2200R 2210, 2210R	All	0.016	—	—	—	—	V-0	—	—	—	—
		0.063	170	170	170	58	V-0	13	2.4	—	—
		0.126	170	170	170	82	V-0	6	2.2	85	140
ULTEM 2300, 2300R 2310, 2310R	All	0.010	—	—	—	—	V-0	—	—	—	—
		0.063	180	170	180	107	V-0	16	3.3	—	—
		0.125	180	170	180	110	V-0	6	3.6	85	155
ULTEM 2400, 2400R 2410, 2410R	All	0.010	—	—	—	—	V-0	—	—	—	—
		0.062	—	—	—	120+	V-0	4	—	—	—
		0.124	—	—	—	120+	V-0	7	7.8	125	145
ULTEM 6000	Nat.	0.062	—	—	—	—	V-0	—	—	—	—
ULTEM 6100	Nat.	0.062	—	—	—	—	V-0	—	—	—	—
ULTEM 6200	Nat.	0.062	—	—	—	—	V-0	—	—	—	—
ULTEM 6300	Nat.	0.062	—	—	—	—	V-0	—	—	—	—
ULTEM 6202	Nat.	0.062	—	—	—	—	V-0	—	—	—	—

* UL94 small-scale test data does not pertain to building materials, furnishings and related contents. UL94 test data is intended solely for determining the flammability of plastic materials used in components and parts of the end-product devices and appliances, where the acceptability of the combination is determined by UL.

R = Release grade
F = FDA grade

TABLE 5

Thermoplastic Considerations

Part Geometry

After functional, stress and deflection characteristics have been determined, the next major consideration in the design of an ULTEM resin part is part geometry. Structural configuration will directly affect the way in which the resin fills the mold and will influence cycle time, dimensional stability, flatness, impact resistance and appearance of the finished part. The following are the most common geometric considerations for ULTEM resin.

Variable Wall Thickness

While uniform wall sections (Figure 41) are the most desirable, structural appearance and draft considerations sometimes dictate the necessity for varying wall sections in a given part. In such cases, gating should be designed so that the resin flows from the heaviest section into progressively thinner sections (Figure 42). Flow in the opposite direction (from thin to thick) can result in sink marks, voids, non-fills, high molded-in stresses and other molding problems.

It is also important that the transition from thick to thin wall sections be gradual rather than abrupt. A sharp transition may cause turbulent flow, resulting in poor appearance of the finished part. Also, from a structural standpoint, a sharp transition risks stress concentration. This sudden change in section thickness may adversely affect part performance under loading or impact. Figure 42 shows recommended transition design for ULTEM resin.

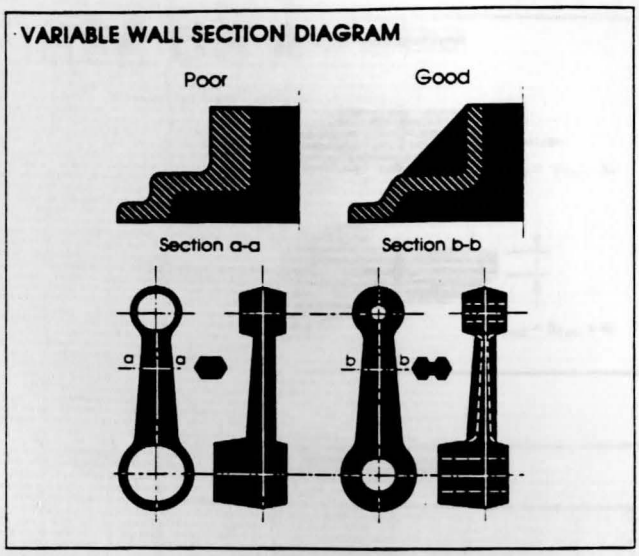

FIG. 41

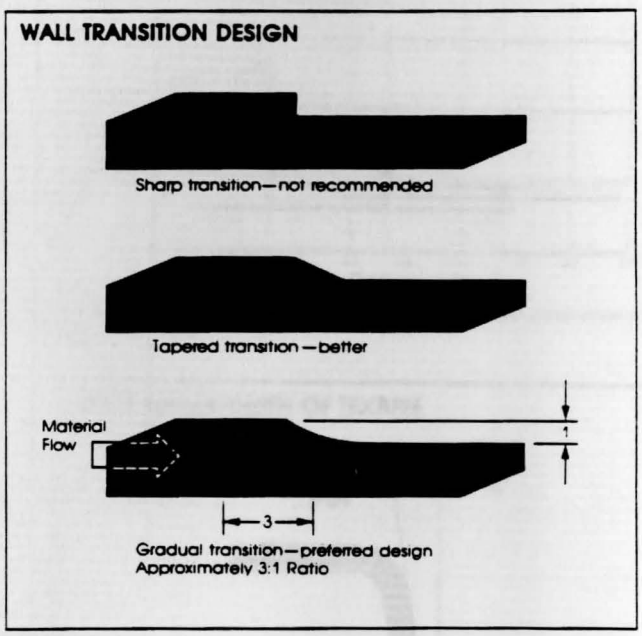

FIG. 42

Corners, Fillets and Radii

Sharp inner corners should be avoided when designing parts with ULTEM resin because of potential stress concentrations which could lead to premature failure, particularly under fatigue or impact. The use of fillets on internal corners will reduce stress levels, aid flow during molding, and facilitate part ejection.

To maintain molded-in stress levels within acceptable limits, a radius equal to half the adjacent section wall thickness is recommended for an inside corner, and 1.5 times the adjacent wall thickness for an outside corner. A fillet radius of 0.015 inch (0.4mm) should be considered a minimum. Figures 43 and 44 show how to calculate stresses for unreinforced ULTEM resin parts under tensile and flexural loading.

Draft Angle

To insure easy part removal, the designer should allow a draft angle of ½ to 2° per side for both inside and outside walls. More draft should be used when the shape of the part is complex or the draw is relatively deep. Designs utilizing cores also require additional draft, due to the tendency of the resin to shrink tightly onto cores.

Although draft as low as ⅛ to ¼° has been used successfully with parts molded of ULTEM resin, small draft angles require individual analysis.

When dealing with a textured finish, draft angles should be at least 1° per side for every 0.001 inch (0.025mm) of texture depth (Figure 45).

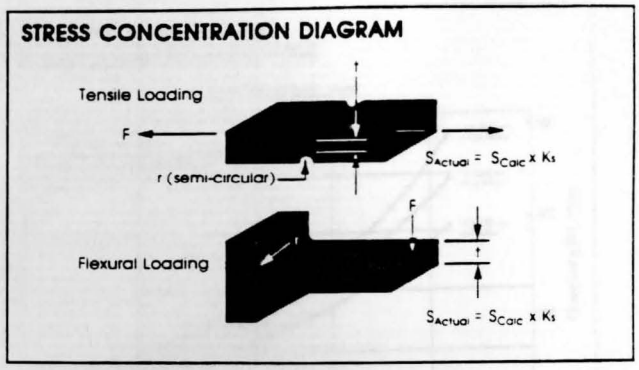

FIG. 43

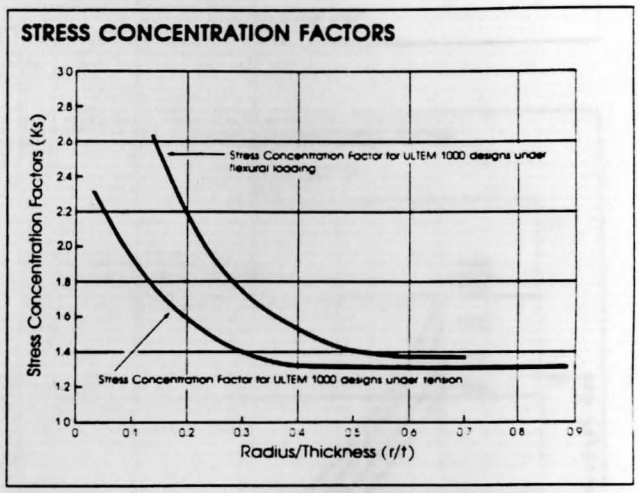

FIG. 44

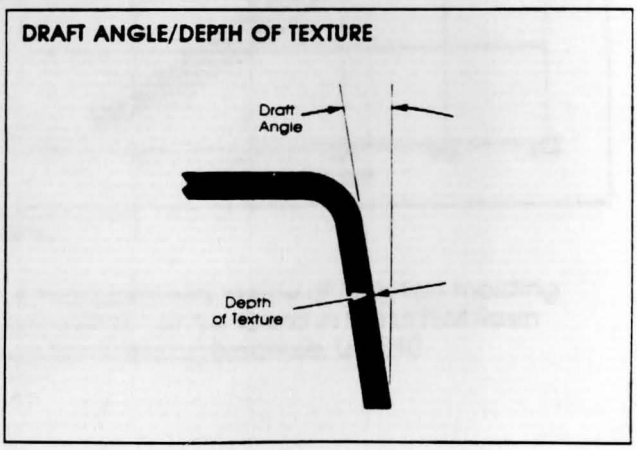

FIG. 45

Injection Molding Considerations

Wall Thickness

Parts molded of ULTEM resin should be designed with the appropriate wall thickness to simultaneously meet these criteria:

1. Engineering (e.g. sufficient stiffness)
2. Thermoplastic (e.g. uniform wall thickness when possible)
3. Adequate wall thickness for proper flow.

Many times this third constraint on wall thickness is overlooked.

Adequate wall thickness for injection molded ULTEM resin parts can be determined by hand or by computer analysis. In brief, a hand analysis requires determination of the maximum flow length to the most distant point on the part. This length is used with Figures 51 and 52 to determine an adequate wall thickness.

Practical wall sections of injection molded ULTEM resin parts generally range from 0.03 to 0.20 inch (0.75 to 5.00mm). However, parts have been successfully molded with sections as thin as 0.01 inch (0.25mm) for short flow lengths, and as thick as 0.50 inch (12.5mm) in special applications. For optimum moldability the designer should attempt to achieve uniform wall sections in ULTEM resin.

Shrinkage

ULTEM resins, being amorphous, exhibit very predictable, repeatable shrink rates. ULTEM 1000 resin shrinks isotropically; shrinkage becomes anisotropic as the resin is reinforced (Table 10).

Although shrink rate is an inherent characteristic of any plastic material, it is affected by wall thickness and molding conditions.

ULTEM GRADE	NOMINAL SHRINK RATE, in/in @ .125" WALL THICKNESS	
	Parallel to Flow	Perpendicular to Flow
1000	0.007	0.007
2100	0.005	0.006
2200	0.003	0.005
2300	0.002	0.004
2400	0.001	0.003

TABLE 10

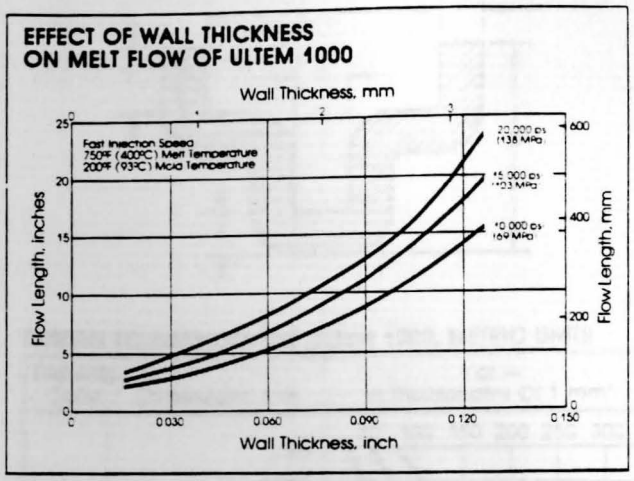

FIG. 51

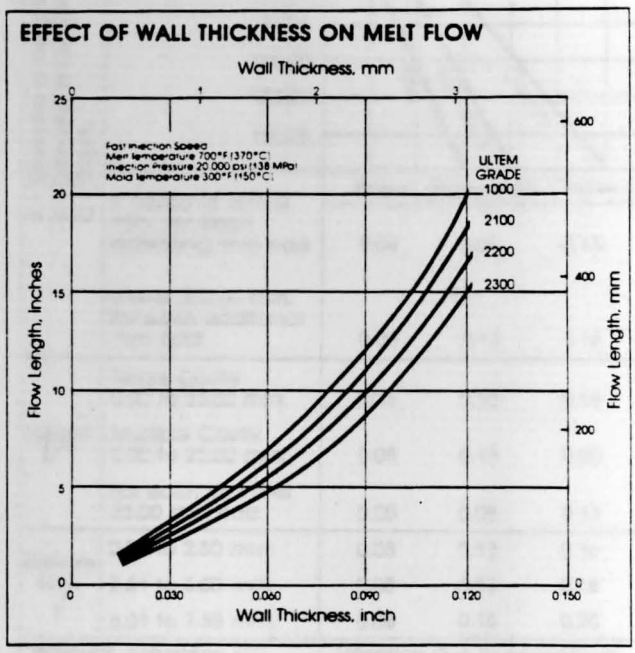

FIG. 52

A more detailed review of injection molding parameters can be found in the ULTEM Resin Injection Molding Brochure, ULT-210.

Tolerances

Every critical measurement should show the nominal dimension plus acceptable high and low limits. Excessively tight tolerances increase the cost of both mold construction and parts. Typical tolerances for parts molded of ULTEM 1000 resin are shown in Tables 11A and 11B.

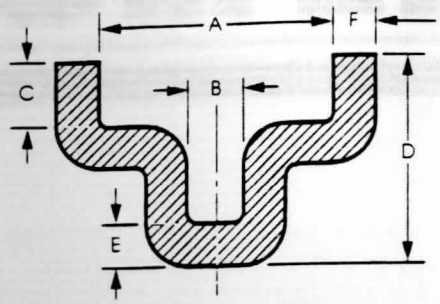

DESIGN TOLERANCES FOR ULTEM 1000, ENGLISH UNITS

Drawing Code / Dimensions, inches		+ or − In Thousandths Of An Inch*		
A = Diameter or Length B = Diameter or Length C = Depth	0.000 to 6.000	1 2 3 4 5 6 7 8 9 10 11 12 (Fine, Standard, Coarse)		
		Fine±	Standard±	Coarse±
	If 6.000 to 12.000 inches, for each additional inch add:	0.0015	0.0035	0.005
	If over 12.000 inches, for each additional inch add:	0.003	0.005	0.007
Height D**	Single Cavity 0.000 to 1.000 inch:	0.003	0.004	0.007
	Multiple Cavity 0.000 to 1.000 inch:	0.003	0.005	0.008
	For each inch over 1.000 inch add:	0.002	0.003	0.005
Bottom Wall E	0.000 to 0.100 inch:	0.003	0.005	0.006
	0.101 to 0.200 inch:	0.003	0.005	0.007
	0.201 to 0.300 inch:	0.004	0.006	0.008
Sidewall dimension F*** Section thickness held relatively uniform		Variation due to eccentricity 0.005 to 0.007 inch Interlocking reduces this.		
Draft Allowance—per side****		¼°	½°	1 to 2°
Flatness in/in	0.000 to 6.000 inches:	0.002	0.004	0.006
	For each inch over 6.000 inches add:	0.003	0.005	0.007
	For each inch over 12.000 inches add:	0.004	0.006	0.008

TABLE 11A

DESIGN TOLERANCES FOR ULTEM 1000, METRIC UNITS

Drawing Code / Dimensions, mm		+ or − In Thousandths Of 1 mm*		
A = Diameter or Length B = Diameter or Length C = Depth	0.00 to 150.00	50 100 150 200 250 300 (Fine, Standard, Coarse)		
		Fine±	Standard±	Coarse±
	If 150.00 to 300.00 mm, for each additional mm add:	0.04	0.09	0.13
	If over 300.00 mm, for each additional mm add:	0.08	0.13	0.18
Height D**	Single Cavity 0.00 to 25.00 mm:	0.08	0.10	0.18
	Multiple Cavity 0.00 to 25.00 mm:	0.08	0.13	0.20
	For each mm over 25.00 mm add:	0.05	0.08	0.13
Bottom Wall E	0.00 to 2.50 mm:	0.08	0.13	0.16
	2.51 to 5.00 mm:	0.08	0.13	0.18
	5.01 to 7.50 mm:	0.08	0.16	0.20
Sidewall dimension F*** Section thickness held relatively uniform		Variation due to eccentricity 0.10 to 0.20 mm. Interlocking reduces this.		
Draft Allowance—per side****		0.25°	0.5°	1 to 2°
Flatness mm/mm	0.00 to 150.00 mm:	0.05	0.10	0.15
	For each mm over 150.00 mm add:	0.08	0.13	0.18
	For each mm over 300.00 mm add:	0.10	0.15	0.20

TABLE 11B

*These tolerances do not apply to screw threads, gear teeth or match fits. Provisions can usually be made to hold this type of dimension to close limits.

**Parting line must be taken into consideration (English-±0.002, Metric-±0.05).

***This dimension is a function of mold design and construction.

****These values should be considered minimum. The designer should allow as much draft as is compatible with his design. Liberal use of draft will minimize ejection problems, and reduce distortion due to ejection.

TECHNICAL MARKETING BULLETIN

ULTEM® resin

TMB 83-5
October, 1983

DETERMINING MOLDED-IN STRESS LEVELS IN ULTEM® RESIN PARTS

Dwane A. Daley

INTRODUCTION

This paper describes a method for determining the stresses that can be induced upon the molding of parts made of ULTEM® 1000 resin.

The method involves the use of a solvent aggressive to polyetherimide (PEI) resin, and the development of curves that relate time to cracking and crazing as a function of stress levels. The part is immersed into the solvent. The time it takes for the part to crack or craze is "read" off the appropriate curve. This provides an estimate of the stress in the part.

The molded-in stresses on the specimens used for this study were reduced to a minimum. To achieve this, certain molding parameters were monitored. Runner, sprue, and gate design in the tool, as well as wall thickness, and overall size of the part were carefully controlled. Most importantly, specimens were annealed prior to testing. Annealing involves placing specimens inside a 212°C air circulating oven for four to six hours (length of time varies on the size and complexity of the part), followed by gradual cooling.

® A registered Trademark of General Electric Company

GENERAL ELECTRIC COMPANY
Plastics Group
ULTEM Products Section
One Plastics Avenue, Pittsfield, MA 01201

GENERAL ELECTRIC

PROCEDURE

Solvents* used for the study were selected on the basis of their availability, cost, safety, and aggressiveness towards ULTEM resin. Halogenated alkanes were used for low stress levels, and an aromatic alcohol for higher stresses.

The annealed samples molded of ULTEM 1000 resin were mounted on specially designed stainless steel stress jigs. The specimens (2 1/2" x 1/2" x 1/8") were thus subjected to static loads of 400, 800, 1000, 1200, and 1400 psi. The load is called induced stress since it results from clamping the specimens to a jig with a fixed curvature.

Jigs showing 1400 psi stress

Jig showing 1400 psi stress and cracks, caused by benzyl alcohol

Figure 1 Fixed curvature stress jigs, showing induced stresses.

* As with all chemicals, these solvents should be handled by trained personnel cognizant of the potential hazards and using appropriate protective measures per the manufacturer's recommendations.

1,2-Dichloroethane, 1,1,2-trichloroethane, and benzyl alcohol were selected because of their rapid effects on ULTEM resin. Immediately after mounting the specimens on the jigs, the samples were immersed in the solvents. A stop watch was used to record the time to crack at each stress level. A crack was considered to be a craze line across the width of the specimen. Room conditions (73°F, 55% RH, 1 atm) were used throughout.

Solvents from more than one supplier were used, to ensure the reliability of the data.

Each of the stress levels generated a series of dependent variables. These consisted of seven data points, of which the highest and lowest were discarded.

Upon developing a series of data points for each stress level, a method of statistical analysis was employed to obtain the mean and the standard deviation for each time point. The high and low times values corresponding to each stress level were then computer plotted.

CONCLUSION

The plots shown depict the time to crack of ULTEM 1000 specimens as a function of stress level. Confidence limits (upper and lower curves) are shown. In addition, a crack is 1/2 inch long across the sample; therefore any comparison between experimental specimens and actual parts should be carefully analyzed.

Time to craze as a function of stress level is also shown. From these curves one can estimate the values of the molded-in stresses, then confirm by checking them against the values obtained from the crack vs time curves. Confirmation may, however, depend upon part geometry. A large, complex part may craze easily but may not crack. In this case, one should rely on the results obtained from the craze curves. In addition, a magnifying glass may be needed to detect any crazing, especially when using 1,1,2-trichloroethane as the stress crazing solvent.

Table I summarizes some of the properties of the three solvents used in this study.

TABLE I

Solvent*	Specific Gravity	MP,°C	BP,°C	Stress Level Range, psi
1,2-Dichloroethane	1.2350	-35.36	83.47	400-1400
1,1,2-Trichloroethane	1.4397	-36.50	113.77	400-1400
Benzyl Alcohol	1.0460	-15.00	205.00	1200-5000

*CRC Handbook of Chemistry and Physics, 53rd Edition, 1972-1973.

STRESS LEVELS VS. TIME TO CRAZE, ULTEM-1000 IN BENZYL ALCOHOL @ RT

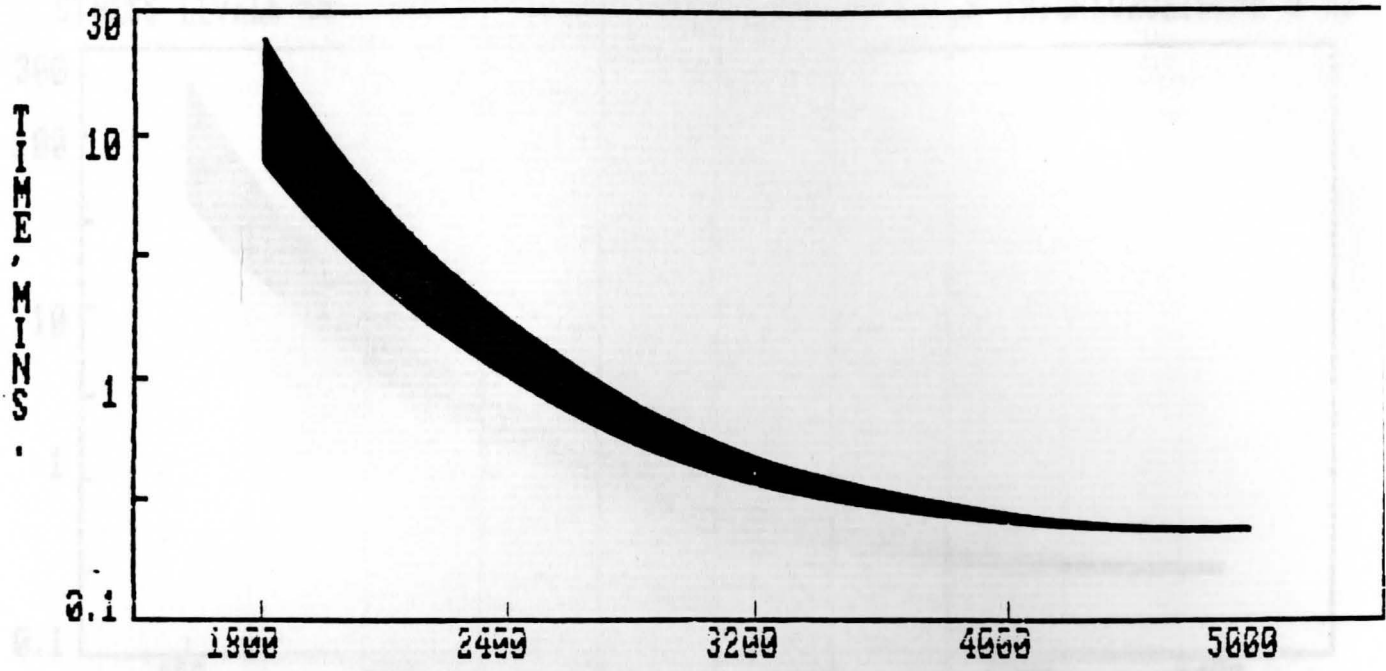

STRESS LEVELS VS. TIME TO CRACK, ULTEM-1000 IN BENZYL ALCOHOL @ RT

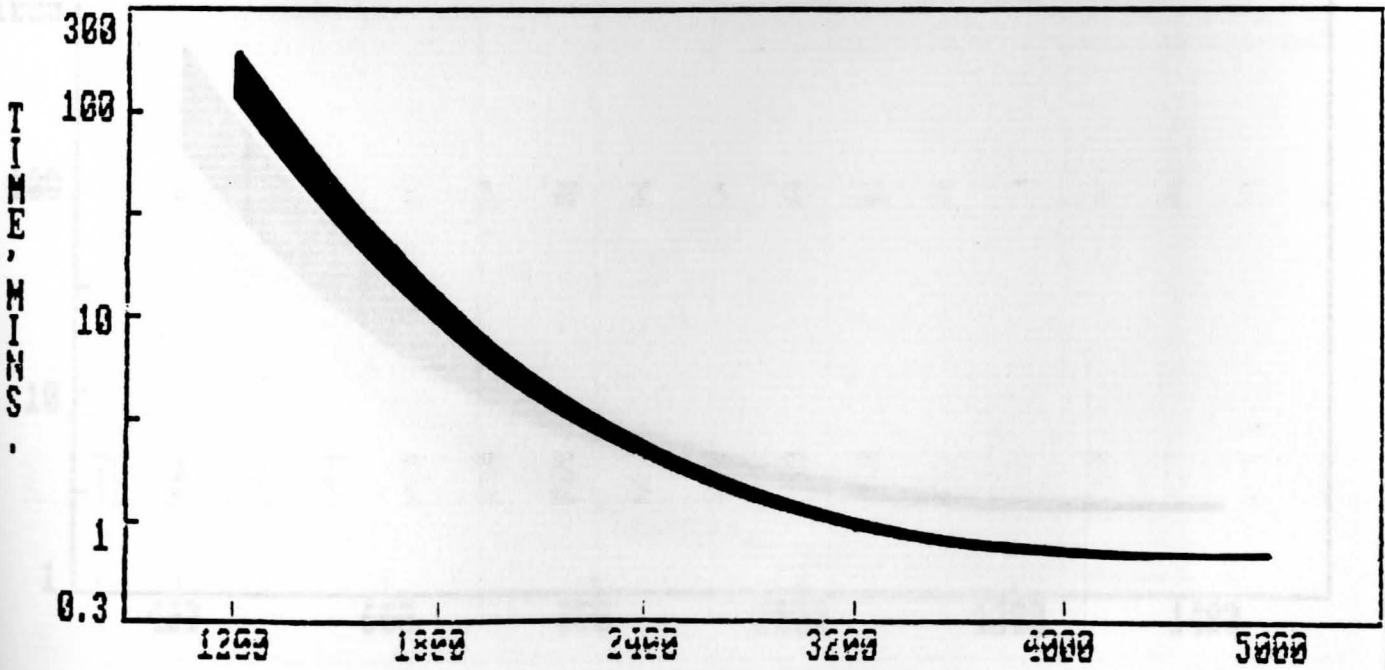

STRESS LEVELS VS. TIME TO CRAZE, ULTEM-1000 IN 1,1,2-TRICHLOROETHANE @ RT

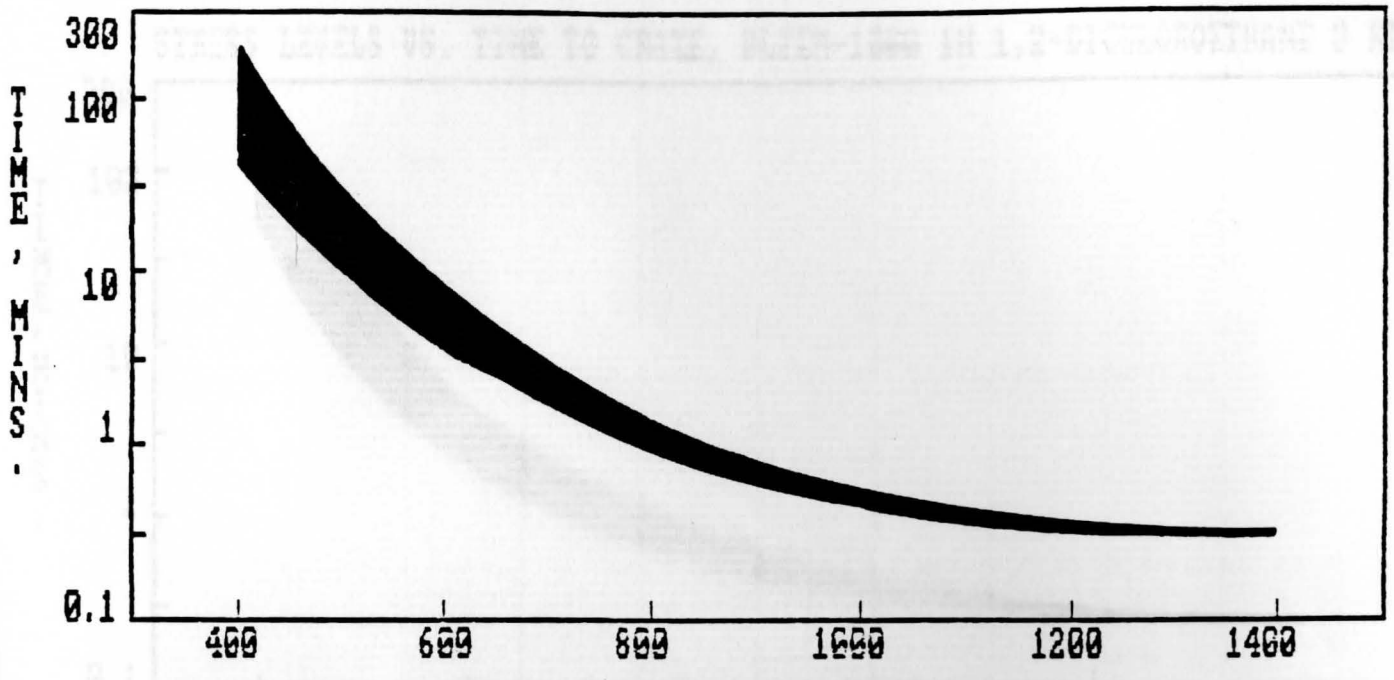

STRESS LEVELS VS. TIME TO CRACK, ULTEM-1000 IN 1,1,2-TRICHLOROETHANE @ RT

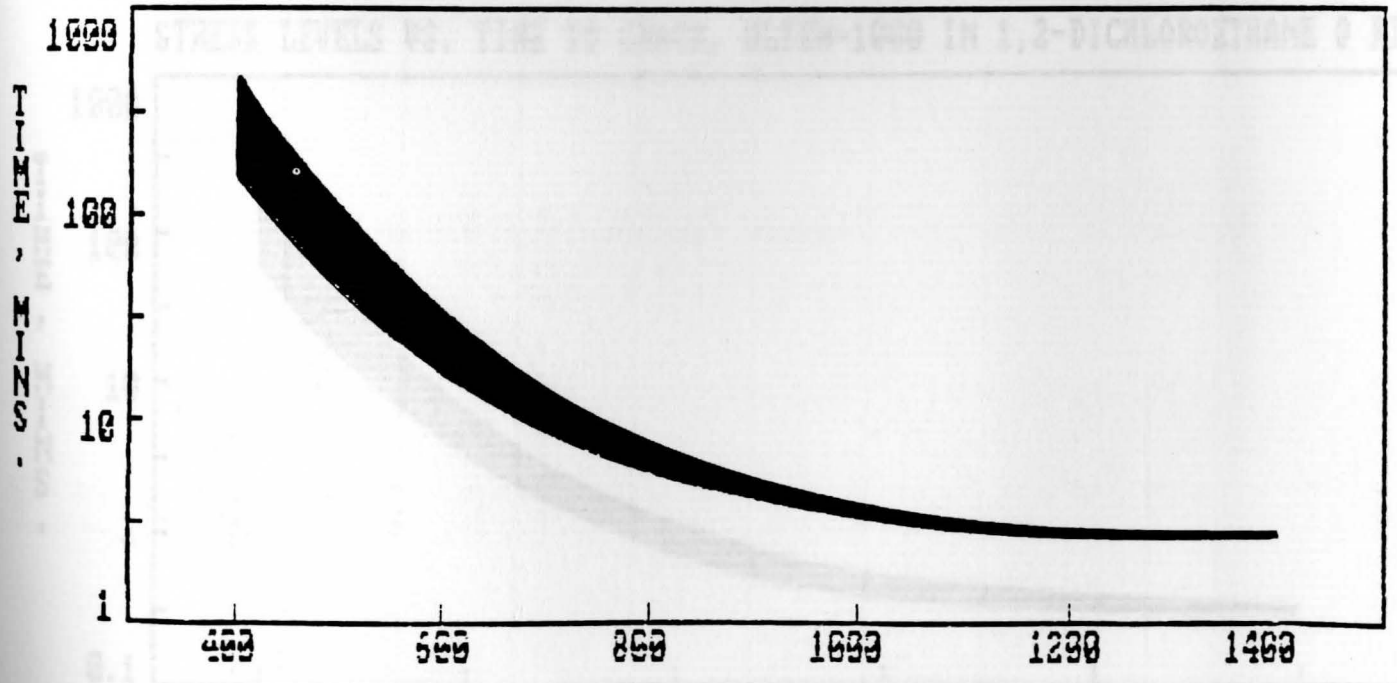

STRESS LEVELS VS. TIME TO CRAZE, ULTEM-1000 IN 1,2-DICHLOROETHANE @ RT

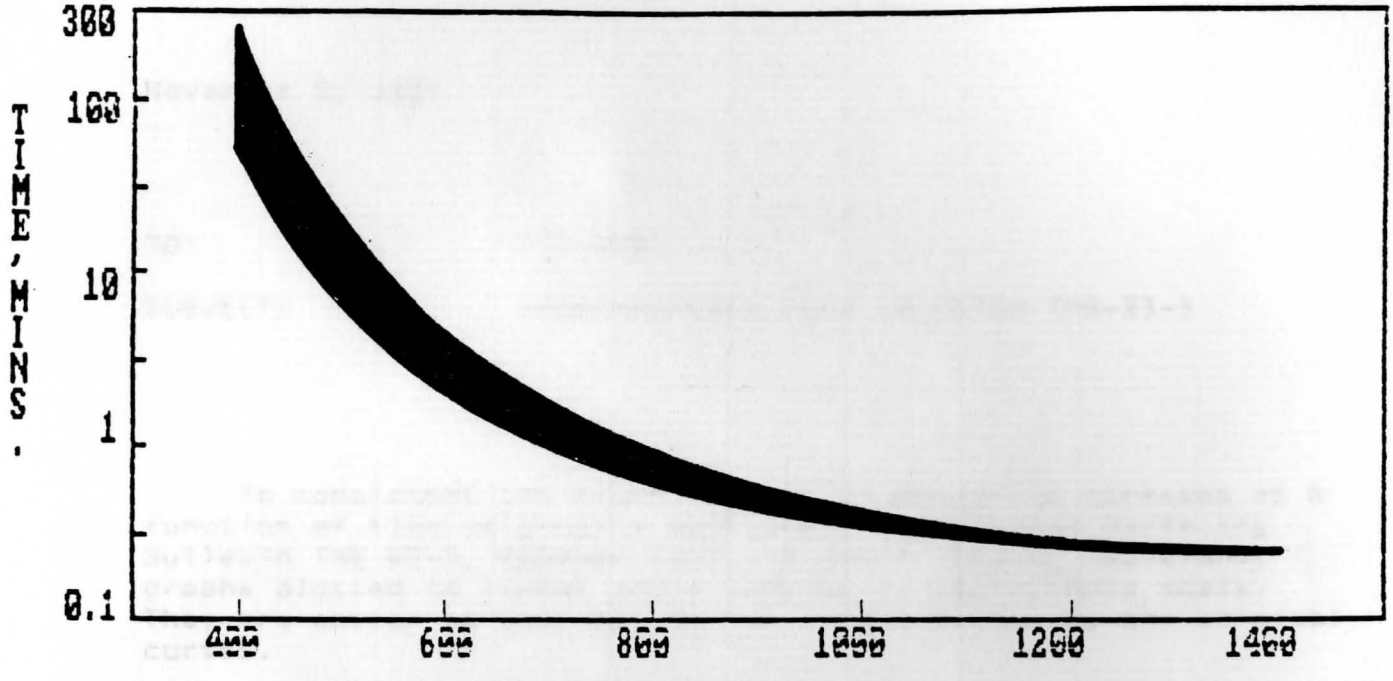

STRESS LEVELS VS. TIME TO CRACK, ULTEM-1000 IN 1,2-DICHLOROETHANE @ RT

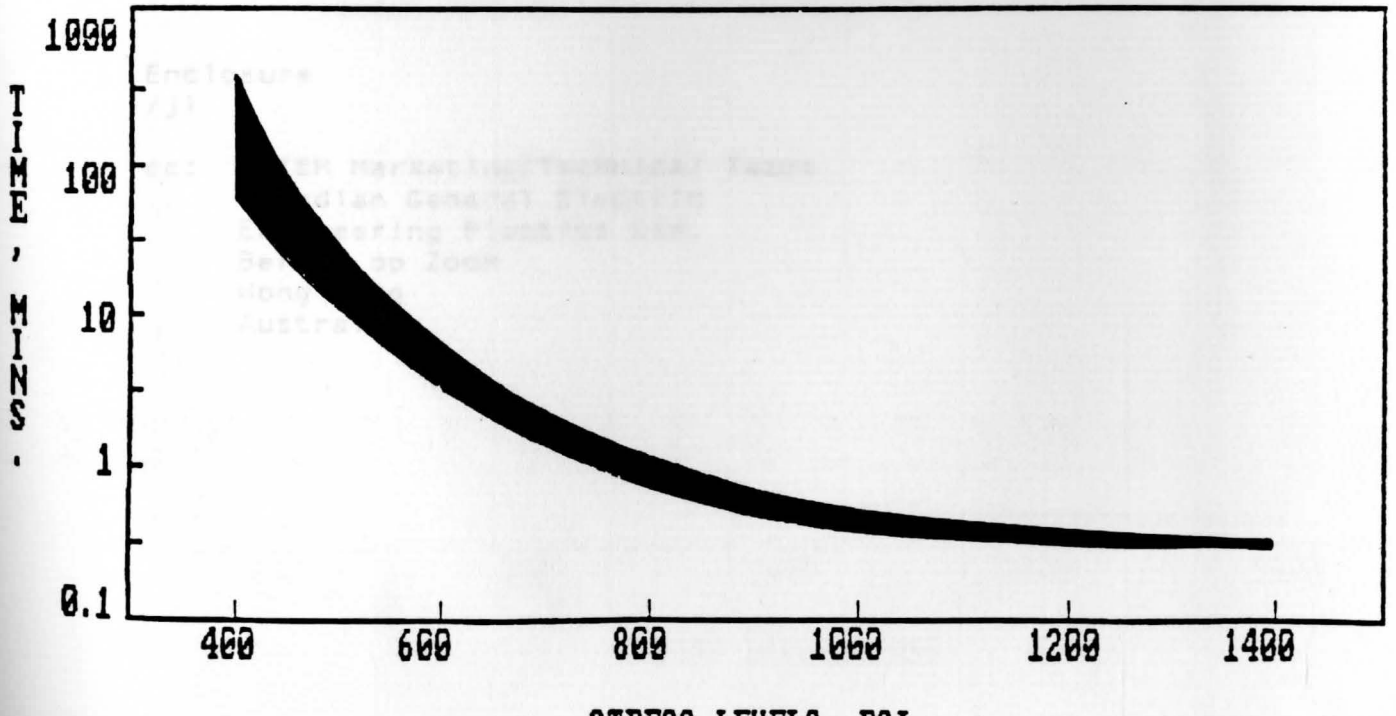

ULTE

November 9, 1983

TO: All PSD

SUBJECT: Supplementary Data to ULTEM TMB-83-5

To complement the curves depicting molded-in stresses as a function of time originally published in Technical Marketing Bulletin TMB 83-5, October 1983, we are enclosing additional graphs plotted in linear scale instead of logarithmic scale. They are easier to use, but do not extend as far as the original curves.

Regards,

I. William Serfaty
Manager, Technical Marketing

Enclosure
/jl

cc: ULTEM Marketing/Technical Teams
Canadian General Electric
Engineering Plastics Ltd.
Bergen op Zoom
Hong Kong
Australia

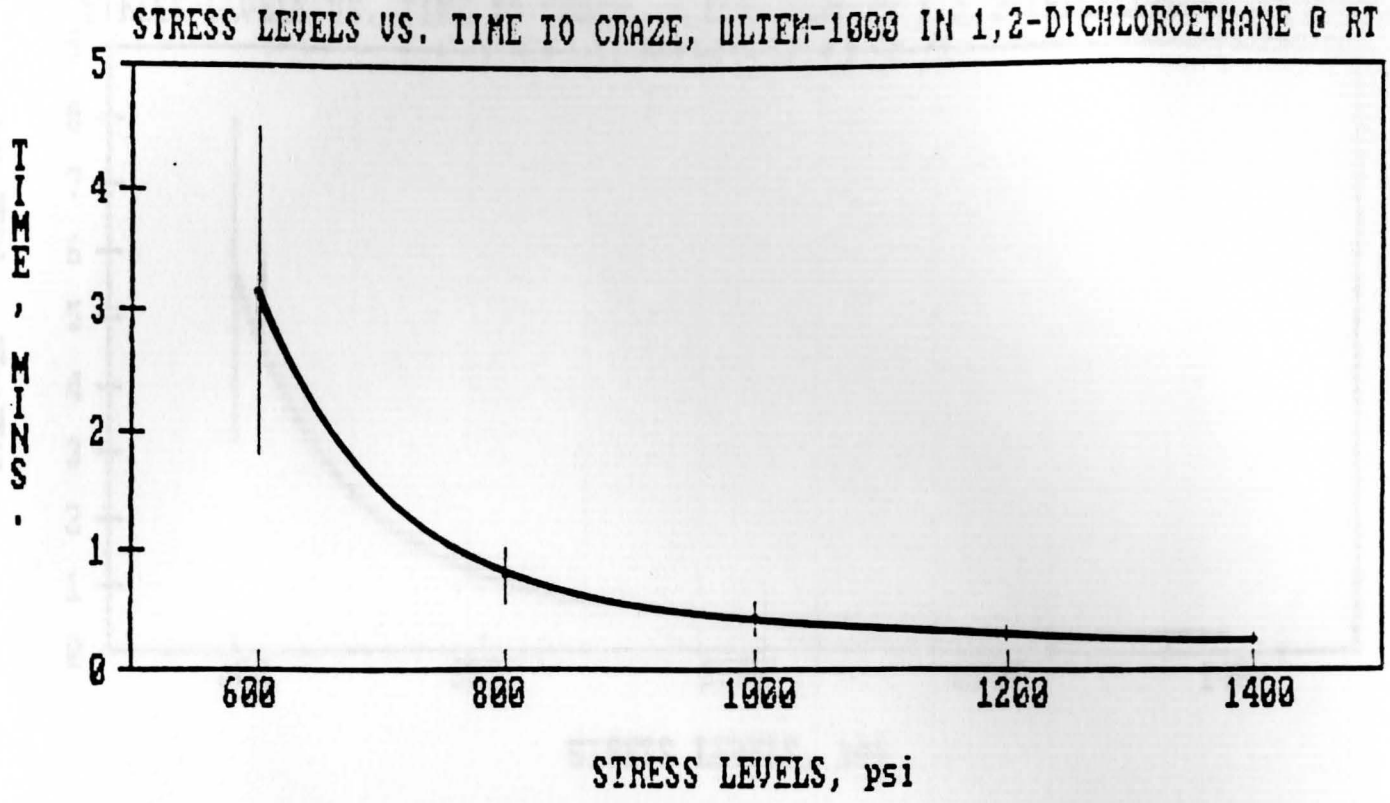
STRESS LEVELS VS. TIME TO CRAZE, ULTEM-1000 IN 1,2-DICHLOROETHANE @ RT
TIME, MINS.
0
1
2
3
4
5
600
800
1000
1200
1400
STRESS LEVELS, psi

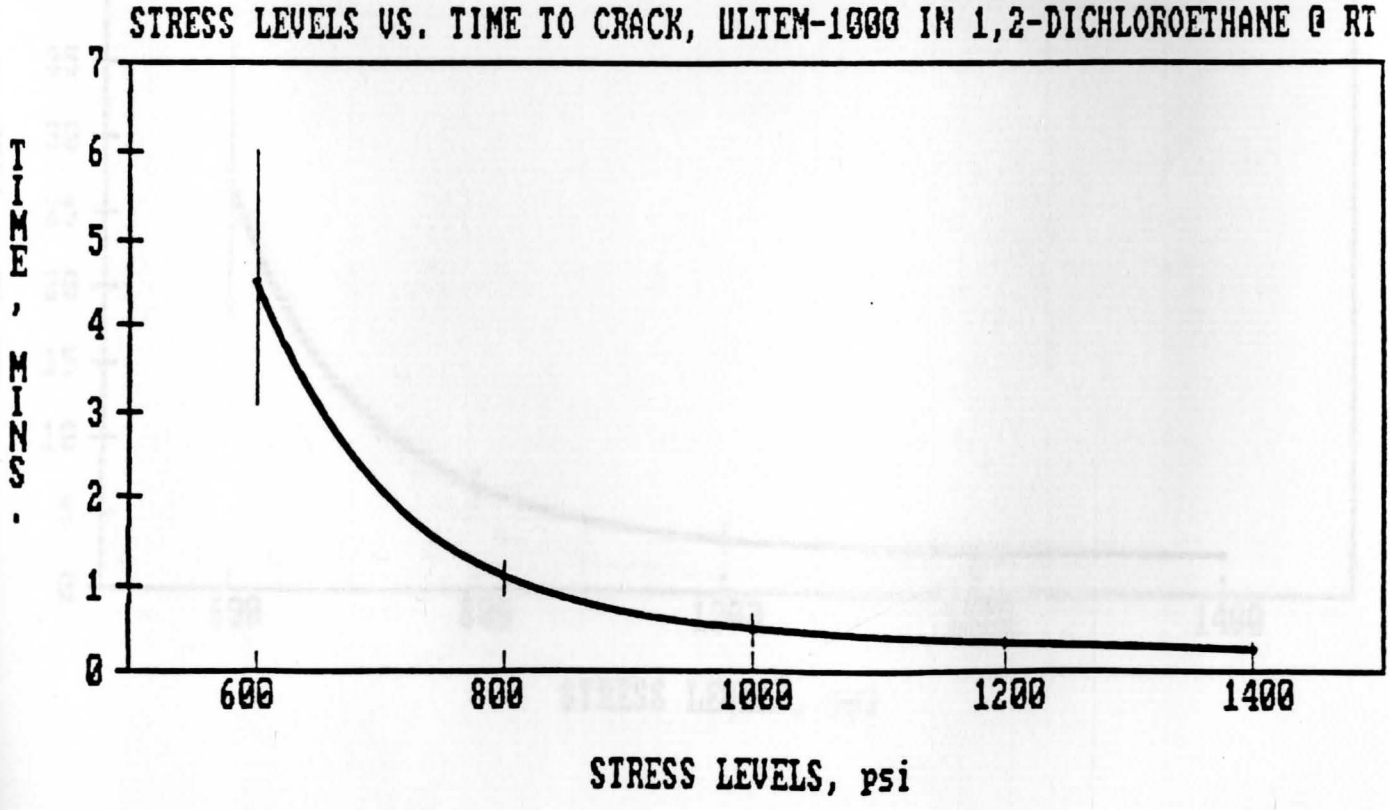
STRESS LEVELS VS. TIME TO CRACK, ULTEM-1000 IN 1,2-DICHLOROETHANE @ RT
TIME, MINS.
0
1
2
3
4
5
6
7
600
800
1000
1200
1400
STRESS LEVELS, psi

STRESS LEVELS VS. TIME TO CRAZE, ULTEM-1000 IN 1,1,2-TRICHLOROETHANE @ RT

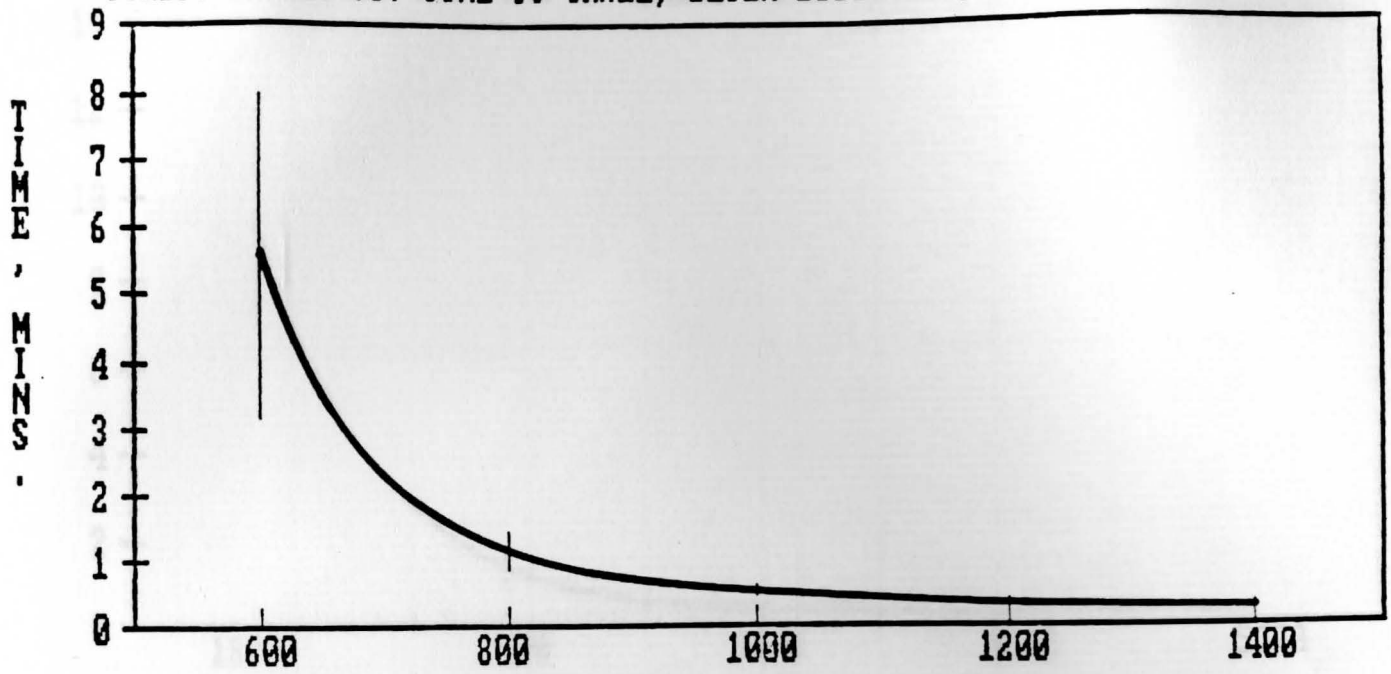

STRESS LEVELS VS. TIME TO CRACK, ULTEM-1000 IN 1,1,2-TRICHLOROETHANE @ RT

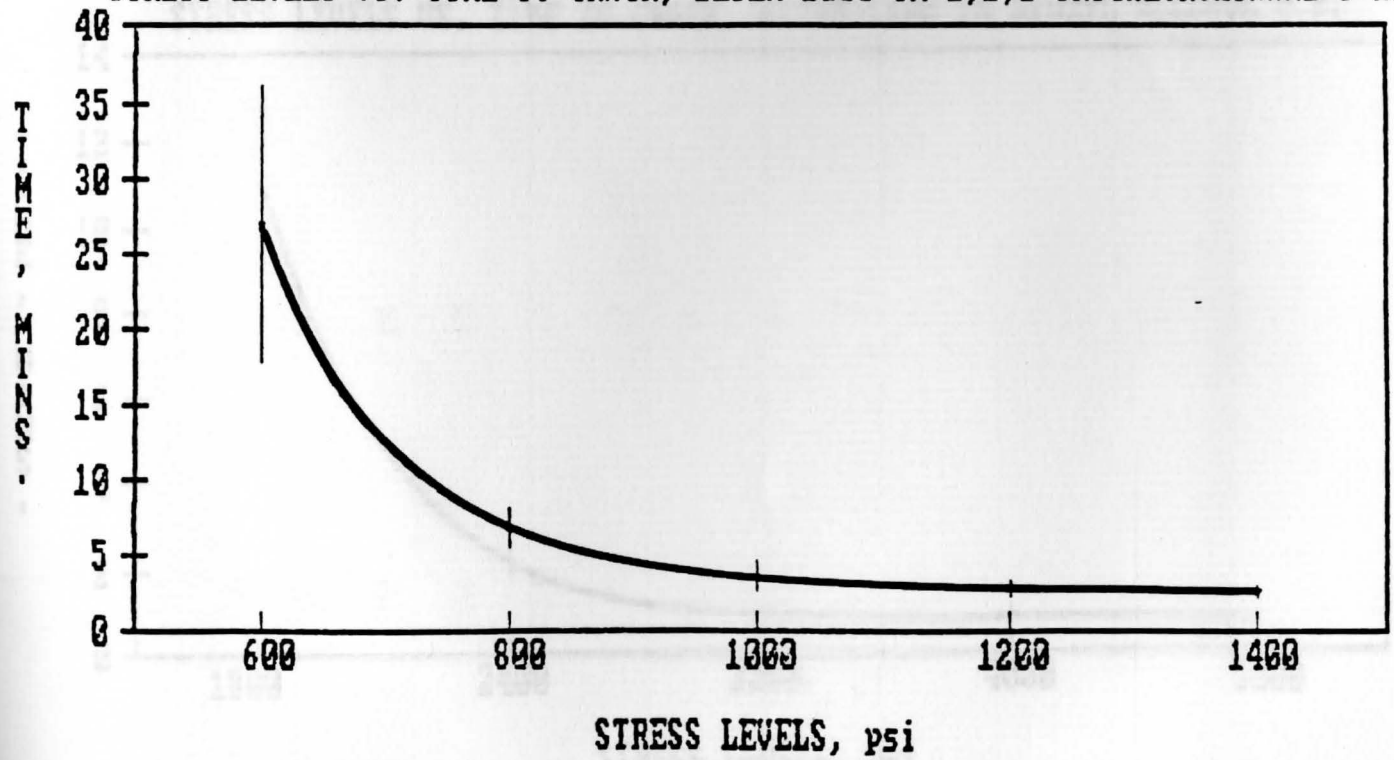

ULTEM

STRESS LEVELS VS. TIME TO CRAZE, ULTEM-1000 IN BENZYL ALCOHOL @ RT

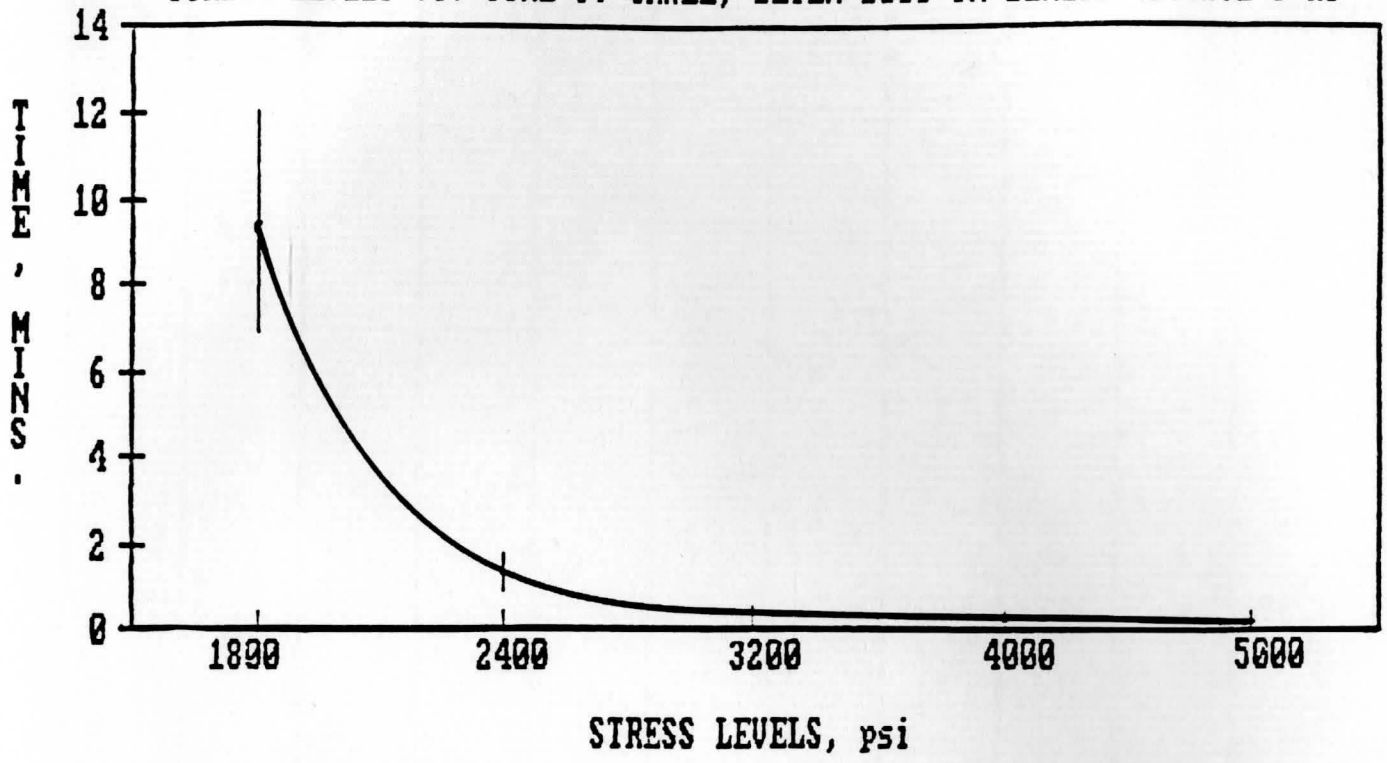

STRESS LEVELS VS. TIME TO CRACK, ULTEM-1000 IN BENZYL ALCOHOL @ RT